# PARTIALLY COHERENT PULSE PROPAGATION IN RESONANT LINEAR AND NONLINEAR MEDIA

by

Laleh Mokhtarpour

Submitted in partial fulfillment of the requirements
for the degree of Doctor of Philosophy

at

Dalhousie University
Halifax, Nova Scotia
January 2016

*I dedicate this thesis to my loving parents Fatemeh and Morteza for their endless love and support even being thousands of miles apart. This work is also dedicated to my best friend, Behzad, for his continuous encouragement, support and company in all of these years.*

## Table of Contents

**List of Figures** . . . . . **viii**

**Abstract** . . . . . **ix**

**List of Abbreviations and Symbols Used** . . . . . **x**

**Acknowledgements** . . . . . **xii**

**Chapter 1 Introduction** . . . . . **1**

1.1 Preface . . . . . 1

1.2 Thesis Theme . . . . . 1

1.3 Thesis Objectives . . . . . 3

1.4 Thesis Contributions . . . . . 4

1.5 Thesis Organization . . . . . 5

**Bibliography** . . . . . **7**

**Chapter 2 Optical Coherence Theory** . . . . . **13**

2.1 Random Processes, Stationarity and Ergodicity . . . . . 13

2.2 Correlation Functions . . . . . 14

2.3 Representation of Partially Coherent Fields . . . . . 16

2.4 Coherent-Mode Representation . . . . . 18

**Bibliography** . . . . . **20**

**Chapter 3 Near Resonance Pulse Propagation Theory** . . . . . **22**

3.1 Two-Level Atom Model . . . . . 22

3.2 Homogenous and Inhomogeneous Broadening and Damping Times . . . . 25

**Bibliography** . . . . . **28**

**Chapter 4 Partially Coherent Self-similar Pulses in Resonant Linear Absorbers 29**

4.1 Abstract . . . . . 29

4.2 Introduction . . . . . 29

4.3 Partially Coherent Self-similar Pulses in Coherent Linear Absorbers . . . . 30

4.4 Conclusion . . . . . 36

**Bibliography** . . . . . **37**

**Chapter 5 Complex Area Correlation Theorem for Statistical Pulses in Coherent Linear Absorbers** . . . . . **39**

5.1 Abstract . . . . . 39

5.2 Introduction . . . . . 39

5.3 Conclusion . . . . . 45

**Bibliography** . . . . . **46**

**Chapter 6 Ultrashort Pulse Coherence Properties in Coherent Linear Amplifiers** . . . . . **47**

6.1 Abstract . . . . . 47

6.2 Introduction . . . . . 47

6.3 Statistical Pulse Propagation in Coherent Linear Amplifiers . . . . . 48

6.4 Intensity and Complex Degree of Coherence Evolution for Intrinsically Statistically Stationary Pulses in Coherent Linear Amplifiers . . . . . 50

6.5 Discussion . . . . . 53

6.6 Conclusion . . . . . 54

**Bibliography** . . . . . **55**

**Chapter 7 Fluctuating Pulse Propagation in Resonant Nonlinear Media: Self-induced Transparency Random Phase Soliton Formation** . . . . **57**

7.1 Abstract . . . . . 57

7.2 Introduction . . . . . 57

7.3 Pulse Propagation in Resonant Nonlinear Media . . . . . 59

7.4 Statistical Properties of Fluctuating Pulses and Statistical Ensemble Generation . . . . . 60

7.5 Physical Model of the Source and Host Medium . . . . . 64
7.6 Numerical Simulation Results . . . . . 66
7.7 Conclusion . . . . . 71

**Bibliography** . . . . . **72**

**Chapter 8 Discussion** . . . . . **75**

8.1 Conclusion . . . . . 75
8.2 Future work . . . . . 78

**Appendix A Simulation Codes for Simulating Propagation of Partially Coherent Self-similar Pulses in Resonant Linear Absorbers** . . . . . **79**

**Appendix B Numerical Codes for Simulating Propagation of Partially Coherent Pulses in Resonant Linear Absorbers and Amplifers** . . . . **84**

**Appendix C Numerical Codes for Simulating Propagation of Fluctuating Pulses in Resonant Nonlinear Media** . . . . . **87**

**Appendix D Copyright Permissions** . . . . . **94**

**Bibliography** . . . . . **96**

## List of Figures


2.1 Michelson interferometer composed of source, beam splitter, two mirrors and observation plane [6] . . . . . 17

3.1 Diagram of a two-level atom model . . . . . 22

3.2 Illustation of homogenous and inhomogenous broadenings [1] . . . 26

4.1 Spectral amplitude of the pulse with the power-law modal weight distribution in arbitrary units. The parameters are (a) $\lambda = 0.1$, $Z_0 = 5$; (b) $\lambda = 0.3$, $Z_0 = 3$, and (c) $\lambda = 10$, $Z_0 = 0.1$. . . . . 32

4.2 Modulus of the spectral degree of coherence. The parameters are (a) $\lambda = 0.1$, $Z_0 = 5$ and (b) $\lambda = 10$, $Z_0 = 0.1$. . . . . 32

4.3 Modulus of the spectral degree of coherence as a function of $\Omega_1$ for a fixed $\Omega_2$: (a) $\Omega_2 = -15$, (b) $\Omega_2 = 0$. . . . . 33

4.4 Spectral amplitude of the pulse with $\lambda_n \propto \lambda^{2n}/(n!)^2$ in arbitrary units. The parameters are (a) $\lambda = 0.9$, $Z_0 = 0.1$; (b) $\lambda = 0.9$, $Z_0 = 15$; (c) $\lambda = 2$, $Z_0 = 0.1$, and (d) $\lambda = 2$, $Z_0 = 15$. . . . . 34

4.5 Modulus of the spectral degree of coherence. The parameters are (a) $\lambda = 0.9$, $Z_0 = 15$ and (b) $\lambda = 2$, $Z_0 = 15$. . . . . 35

4.6 Modulus of the spectral degree of coherence as a function of $\Omega_1$ for a fixed $\Omega_2$: (a) $\Omega_2 = -15$, (b) $\Omega_2 = 0$. . . . . 35

5.1 GSM pulse intensity profile. The pulse parameters are (a) $t_c = T_{eff} = 5t_p$ and (b) $t_c = T_{eff} = t_p/5$. . . . . 44

5.2 Magnitude of the temporal degree of coherence of a relatively long GSM pulse at (a) $Z = 1$ and (b) $Z = 50$. The pulse parameters are $t_c = T_{eff} = t_p/5$. . . . . 44

5.3 Magnitude of the temporal degree of coherence of a rather short GSM pulse at (a) $Z = 1$ and (b) $Z = 50$. The pulse parameters are $t_c = T_{eff} = 5t_p$. . . . . 45

6.1 Pulse intensity profile in arbitrary units (a.u) as a function of the dimensionless propagation distance $Z$ for two partially coherent pulses: (a) $t_c = 5t_p$ and (b) $t_c = t_p/5$. . . . . 51

6.2 Energy gain factor as a function of the dimensionless propagation distance $Z$ for two partially coherent pulses: (a) $t_c = 5t_p$ and (b) $t_c = t_p/5$. . . . . 52

6.3 Magnitude of the complex degree of coherence of a short GSM pulse with $t_c = 5t_p$ for (a) $Z = 1$ and (b) $Z = 5$. Insets: the corresponding pulse intensity profiles. . . . . 52

6.4 Magnitude of the temporal degree of coherence of a short GSM pulse with $t_c = t_p/5$ for (a) $Z = 1$ and (b) $Z = 5$. Insets: the corresponding pulse intensity profiles. . . . . 53

7.1 Magnitude of 10 random field realizations of the GSM pulse at the source $Z = 0$ as a function of dimensionless time $T = t/t_p$ in three cases (a) $t_c = 10t_p$, (b) $t_c = 2t_p$ and (c) $t_c = t_p$. Black thick line: ensemble average amplitude. . . . . 64

7.2 Profile of the mutual coherence function at the source, $Z = 0$ as a function of dimensionless time $T_1$ and $T_2$ in three cases : (a) $t_c = 10t_p$, (b) $t_c = 2t_p$ and (c) $t_c = t_p$. . . . . 65

7.3 Average intensity evolution of relatively coherent pulses as a function of the propagation distance $Z$. The cases $(a)$ and $(b)$ correspond to the average input pulse areas $\mathscr{A}_0 = 0.8\pi$ and $\mathscr{A}_0 = 1.5\pi$, respectively. . . . . 66

7.4 Evolution of the average pulse area as a function of the propagation distance $Z$ for relatively coherent pulses with $\mathscr{A}_0 = 0.8\pi$ (dashed ) and, $\mathscr{A}_0 = 1.5\pi$ (solid), respectively. . . . . 67

7.5 Average intensity evolution as a function of propagation distance $Z$ for input pulses with (a) $t_c = 2t_p$ and (b) $t_c = t_p$. The average pulse area at the source is $\mathscr{A}_0 = 1.5\pi$. . . . . 67

7.6 Evolution of the averaged pulse area as a function of propagation distance $Z$, corresponding to $t_c = 2t_p$ (dashed line) and, $t_c = t_p$ (solid line) with the initial area $\mathscr{A}_0 = 1.5\pi$. The red dotted-dashed line represents the $\mathscr{A} = 2\pi$ limit. . . . . 68

7.7 Intensity of five relatively coherent, $t_c = 10t_p$, pulse realizations with $\mathscr{A}_0 = 1.5\pi$ at three sample points in $Z$: $Z = 0$ (a), $Z = 5$ (b), and $Z = 10$ (c), respectively. . . . . 69

7.8 Intensity of five rather incoherent, $t_c = t_p$ pulse realizations with $\mathscr{A}_0 = 1.5\pi$ at three sample points in $Z$: $Z = 0$ (a), $Z = 5$ (b), and $Z = 10$ (c), respectively. . . . . 69

7.9 Magnitude of the mutual coherence function at $Z = 0$, (top row) and $Z = 10$, (bottom row); $t_c = 10t_p$,(a,d); $t_c = 2t_p$, (b,e); $t_c = t_p$, (c,f). . . 70

7.10 Magnitude of the complex degree of coherence function at $Z = 0$, (top row) and $Z = 10$, (bottom row); $t_c = 10t_p$,(a,d); $t_c = 2t_p$, (b,e); $t_c = t_p$, (c,f). . . . . 70

## Abstract

Optical experiments reveal the fact that real laser pulses have random fluctuations in their amplitude and phase that crucially affect pulse evolution. Statistical optics considers the random nature of light to give a more realistic description of laser pulses behavior.

Generation of ultrashort pulses, operating at frequencies close to internal transition frequencies of medium atoms, motivated the growing interest in studying on-resonance light-matter interactions. Moreover, there exist optical phenomena that only occur at optical resonance. Thus, near resonance light-matter interactions are of great importance.

In this dissertation, statistical properties of ultrashort pulses propagating in different linear and nonlinear media near optical resonance is studied. Various partially coherent pulses are simulated and effects of initial statistical properties of pulses on their propagation in resonant absorbing and amplifying media are explored. The research performed throughout this thesis leads to following results.

1- Various classes of ultrashort self-similar partially coherent pulses are explored along with closed form expressions for their correlation functions. Also, the evolution of coherence properties of pulses upon their short-distance and long-distance propagation is investigated.

2- Generic partially coherent pulses are simulated and their global and local correlation properties upon propagation in resonant linear absorber media are studied. The evolution of the coherence functions of pulses shows that partially coherent pulses are strongly affected by the medium regarding to their coherence levels. A correlation area theorem is also derived to describe global correlation properties of stochastic pulses propagating in such media.

3- Evolution of small-area pulse coherence properties, propagating in linear amplifiers near optical resonance, is studied. Our simulation results reveal that more coherent pulses are amplified more effectively by the medium than are their less coherent counterparts.

4- Propagation of partially coherent pulses in resonant, inhomogenously broadened nonlinear media is simulated. Stochastic pulses of different coherence levels are generated to investigate effects of initial properties of pulses on their long-term evolution. We also provide evidence of self-induced transparency phenomena and soliton formation for relatively coherent pulses. Also, evolution of the coherence functions reveal that low-coherence pulses lose their coherence level upon propagation faster than do highly coherent pulses.

## List of Abbreviations and Symbols Used

| | |
|---|---|
| $I$ | Field intensity |
| $L_B$ | Beer's absorption length |
| $N$ | Atom density |
| $P$ | Probability density function |
| $S$ | Pulse spectrum |
| $T_\perp$ | Transverse relaxation time |
| $T_{\text{eff}}$ | Effective relaxation time |
| $T_\parallel$ | Energy relaxation time |
| $U$ | Random process |
| $U$ | Stochastic field |
| $W$ | Cross-spectral density |
| $\Delta$ | Frequency detuning |
| $\Gamma$ | Mutual coherence function |
| $\Omega$ | Rabi frequency |
| $\alpha$ | Absorption coefficient |
| $\delta$ | inhomogenous broadening width |
| $\varepsilon_0$ | Free space permitivity |
| $\gamma$ | Temporal degree of coherence |
| $\gamma_\perp$ | Transverse relaxation rate |
| $\gamma_\parallel$ | Energy relaxation rate |
| $\kappa$ | Coupling constant |
| $\lambda_n$ | Modal weight |
| $\mathscr{A}$ | Pulse area |
| $\mathscr{C}_{\mathscr{R}}$ | Area correlation function |
| $\mathscr{E}$ | Field envelope |
| $\mathscr{R}$ | Spectral response function of the medium |
| $\mu$ | Spectral degree of coherence |
| $\omega$ | Optical frequency |

| | |
|---|---|
| $\omega_0$ | Resonace frequency |
| $\sigma$ | Atomic dipole moment |
| $\tilde{\mathscr{E}}$ | Spectral field profile |
| $\varphi_n$ | Random phase |
| $d_{eg}$ | Dipole matrix element |
| $e$ | Excited state |
| $g$ | Ground state |
| $t_{\text{eff}}$ | Effective pulse width |
| $t_c$ | Coherence time |
| $t_p$ | Pulse width |
| $u$ | In-phase component of dipole moment |
| $v$ | In-quadrataure component of dipole moment |
| $w$ | Single atom inversion |

| | |
|---|---|
| **GSM** | Gaussian-Schell model pulses |

| | |
|---|---|
| **PCP** | Partially coherent pulses |

| | |
|---|---|
| **SIT** | Self-induced transparency |

## Acknowledgements

I would like to express my deepest appreciation to my supervisor Dr. Sergey Ponomarenko for his excellent scientific guidance, continuous support and motivations during my Ph.D program. I would also like to thank my committee members, Dr. Olga Korotkova, Dr. Zhizhang (David) Chen and Dr. William Philips for their support and recommendations.

# Chapter 1

# Introduction

## 1.1 Preface

In this thesis, we focus on resonant interactions of partially coherent pulses and matter. This chapter starts with an introduction to the general theme of our thesis. Then, thesis objectives, contributions, and organization are presented.

## 1.2 Thesis Theme

The invention of lasers in the late 1950s led to a revolution in the field of optics and its applications [1]. Improvements in the generation of short and high intensity laser pulses resulted in the development of nonlinear optics. Short pulses are being increasingly used in various aspects of science and technology due to their special characteristics such as broad bandwidth, low absorption rate, high peak power, and short duration [2, 3].

The laser technology, initiated by the invention of ruby lasers [4] and continued by the development of semiconductor lasers, led to the formation of short and high intensity pulses in the optical regime [5]. Laser technology has improved to the point that short pulse generation with time duration at femto or even atto-second is now possible. Femtosecond pulses can be generated by the method of passive mode-locking of semiconductor lasers, as with Titanium:Sapphire (Ti:Sa) Lasers [6, 7]. Such ultrashort pulses have a wide range of applications to the optical communication technology [8]. The invention of attosecond pulses is also expected to lead to new insights in describing the electron-scale responses of the medium [9, 10].

The generation of ultrashort pulses, able to operate at optical frequencies, has led to growing interest in the investigation of resonant light-matter interactions. Resonance occurs when a pulse carrier frequency coincides with a particular optical resonance frequency of the medium. The importance of resonance phenomena arises from the fact that there are many significant optical phenomena that occur only near optical resonance, for instance,

enhanced absorption, amplification and self-induced transparency effects. The latter leads to self-similar pulse propagation and soliton formation [11]. Examples of resonant media include dilute atomic vapors, filling the cells of hollow-core photonic crystal fibers, solids with doped impurity atoms, and semiconductor quantum dots [12]. Throughout this thesis, our research focuses on resonant and near resonant regimes of pulse propagation in the medium, and the two-level atom approximation is used to describe the characteristics of light-matter interactions [11, 13].

In most applications of light-matter interactions, optical pulses are generally assumed to be fully deterministic (coherent). However, experimental evidence reveals that pulses are intrinsically stochastic (partially coherent) objects and often cannot be accurately described in purely deterministic terms [14, 15]. In fact, realistic lasers generate pulses that have random fluctuations in their time duration amplitude and phase. These fluctuations are of great importance and should be taken into account in simulation of realistic optical systems. The importance of investigating statistical properties of ultrashort pulses arises from the crucial impact of noise on the efficiency of optical communication systems [16]. Optical coherence theory studies optical phenomena as stochastic processes and considers pulses to be partially coherent. Although accurate simulation and prediction of noisy pulse characteristics is not achievable, their averages and correlations can be described by statistical functions. These mathematical tools also enable us to simulate random pulses with various noise levels or different coherence levels.

In optical systems, partially coherent pulses have a wide range of applications such as image processing [17], optical biopsy [18], optical coherence tomography [19, 20], and production of light pulses with controlled coherence [14, 21–23]. In contrast to the common belief that fully coherent pulses are more applicable, there exist applications in which partially coherent pulses are preferable. For instance, in optical lithography [24–27], the randomness of light improves the resolution of an imaging system. This improvement confirms the importance of having a tool for measuring, characterizing, and generating partially coherent pulses.

The description of optical fields with the help of coherence theory was initiated by Wolf for stationary [1, 14, 15] fields and then extended to non-stationanry [28–33] cases in both space time and space frequency domains. To date, extensive studies have been done on modeling and characterizing various realistic partially coherent sources [34–44],

along with the stochastic pulses produced by such sources [45–50]. Moreover, different representations of partially coherent pulses [51–57] have been advanced, together with measuring and defining their coherence properties [58–64]. Additionally, various theoretical approaches have been presented to simulate the coherence functions upon propagation in optical fibers [65–69], different linear [70–74] and nonlinear [75–81] dispersive media far away from any internal resonances.

Even though the propagation of partially coherent pulses in various linear and nonlinear media has been explored, no study has yet, to the best of our knowledge, investigated the coherence properties of stochastic pulses on propagation near optical resonances. Therefore, explorations into the near resonance behavior of stochastic pulses are of great importance.

### 1.3 Thesis Objectives

Our overarching goal throughout this thesis is to explore statistical properties of ultrashort pulses propagating in different linear and nonlinear media in the vicinity of an optical resonance. More specifically, the objectives of this study are summarized as follows:

1. We aim to explore the possibility of observing self-similar evolution of partially coherent pulses in resonant absorber media.

2. We propose to investigate temporal evolution of generic partially coherent pulses in resonant linear absorbers.

3. We intend to examine coherence properties of small-area, intrinsically stationary pulses upon their propagation in amplifying media in the vicinity of an optical resonance.

4. We plan to explore possible effect of the initial coherence level of pulses on their reshaping and amplifying ratio as the pulses propagate into the amplifying medium.

5. Our aim is to numerically study the evolution of an ensemble of short stochastic pulses in inhomogenously broadened resonant nonlinear media.

6. We plan to investigate influence of the initial coherence state of pulses on variations of their mutual intensities and degree of coherence upon propagation in resonant nonlinear media.

7. We intend to study the possibility of observing self-induced transparency phenomena and random phase soliton formation for partially coherent pulses.

## 1.4 Thesis Contributions

This thesis explores resonant interactions of partially coherent short pulses with matter. Gaussian-Schell model pulses are employed as a generic model to simulate realistic partially coherent pulses in both space-time and space-frequency domains. Resonant absorbers and amplifiers are utilized as the host media, and the evolution of coherence properties of stochastic pulses with respect to their initial coherence level is investigated upon propagation. Quantum mechanical Bloch equations together, with the classical Maxwell wave equations, are employed to explore the response of near resonant atoms to the applied stochastic field. Also, characteristics of the propagated partially coherent pulses through various resonant media are studied and discussed using statistical functions.

The research performed throughout this thesis is divided into four distinct phases which are published as journal papers [82–85]. Contributions of each research phase is summarized as follows:

1. Various classes of ultrashort self-similar partially coherent pulses are explored. Closed form expressions for correlation functions are found to describe second-order statistical properties of such pulses. Also, the evolution of coherence properties of pulses upon their short-distance and long-distance propagation is investigated.

2. Generic partially coherent pulses are simulated and their global and local correlation properties upon propagation in resonant absorber media are studied. The evolution of the intensity and degree of coherence of pulses shows that partially coherent pulses are strongly affected by the medium with regard to their coherence level. A correlation area theorem is also derived to describe global correlation properties of generic partially coherent pulses propagating in such media.

3. The evolution of small-area pulse coherence properties, propagating in coherent linear amplifiers in the vicinity of optical resonance, is studied. Our simulation results reveal that the coherence level of pules increases upon propagation in resonant amplifying media. Calculating the energy gain factor of output pulses shows that more

coherent pulses are amplified more effectively by the medium than are their less coherent counterparts.

4. A Monte Carlo method is applied to simulate propagation of partially coherent pulses in resonant, inhomogenously broadened nonlinear media. Stochastic sample pulses of different coherence levels and initial areas are generated at the source to investigate effects of initial properties of pulses on their long-term evolution. We also provide evidence of self-induced transparency phenomena and soliton formation for relatively coherent, large-area pulses. Also, examining the evolution of the averaged intensity and degree of coherence reveal that low-coherence pulses lose their coherence level upon propagation faster than do highly coherent pulses.

## 1.5 Thesis Organization

This dissertation is in a paper-based format and is composed of a brief introduction to the physical concepts of the theories used throughout the thesis along with the results of our research as published journal papers.

Chapter 1 presents the introduction to a general theme of this research, along with the objectives and contributions. The remainder of this thesis is organized as follows.

Chapter 2 briefly reviews the theory of optical coherence and its basic concepts. Fundamental stochastic pulse models, along with their mathematical correlation functions used throughout this thesis, are also presented in this chapter.

Chapter 3 discusses some background theories on the physics of resonant light-matter interactions. In this chapter, the two-level atom theory and its governing equations are concisely reviewed.

In Chapter 4, propagation of partially coherent ultrashort pulses through homogeneously broadened absorber media under exact resonance conditions is explored. Furthermore, several classes of ultrashort partially coherent pulses with self-similar evolution in resonant media are presented.

In Chapter 5, partially coherent pulses are simulated and the evolution of their intensity profile and degree of coherence passing through resonant absorbers is explored. Moreover, a pulse area correlation theorem is derived.

In chapter 6 we explore the second-order statistical properties of partially coherent small-area pulses propagating in linear amplifying media close to optical resonance. Evolution of coherence properties of the stochastic pulses over their propagation in the amplifying medium are also investigated in this chapter.

Chapter 7 presents a numerical study of ultrashort partially coherent pulse propagation in nonlinear media near optical resonance. This novel approach investigates the role of the initial coherence level of the source pulses in transformation of their correlation functions. Moreover, the evolution of partially coherent pulses, having rather small and large areas in inhomogenously broadened resonant nonlinear media, is simulated. The possibility of observing self-induced transparency phenomena and soliton formation is also explored.

Chapter 8 provides a brief summary of the main results of this thesis along with suggestions for future work.

## Bibliography


[1] M. Born and E. Wolf, *Principles of Optics*, 7th ed. (Cambridge University Press, 1999).

[2] M. E. Fermann, A. Galvanauskas, and G. Sucha, *Ultrafast Lasers. Technology and Applications*, (Marcel Dekker, New York, 2003).

[3] T. Brabec and F. Krausz, "Intense few-cycle laser fields: Frontiers of nonlinear optics," Rev. Mod. Phys. **72**, 545–591 (2000).

[4] T. H. Maimann, "Stimulated optical radiation in ruby," Nature **187**, 493–494 (1960).

[5] F. P. Schfer, F. P. W. Schmidt, and J. Volze, "Organic dye solution laser", Appl. Phys. Lett. **9**, 306–309 (1966).

[6] R. Ell, U. Morgner, F. X. Kartner, J. G. Fujimoto, E. P. Ippen, V. Scheuer, G. Angelow, and T. Tschudi, "Generation of 5-fs pulses and octave-spanning spectra directly from a Ti:sapphire laser", Opt. Lett. **26**, 373–375 (2001).

[7] G. Steinmeyer, D. H. Sutter, L. Gallmann, N. Matuschek, and U. Keller, "Frontiers in ultrashort pulse generation: pushing the limits in linear and nonlinear optics," Science **286**, 1507–1512 (1999).

[8] H. G. Weber and M. Nakazawa, *Ultra High Speed Optical Transmission Technology*, (Springer Verlag, New York, 2007).

[9] H. Hentschel, R. Kienberger, Ch. Spielmann, G. A. Reider, N. Milosevic, T. Brabec, P. Corkum, U. Heinzmann, M. Drescher, and F. Krausz, "Attosecond metrology," Nature **414**, 509–513 (2001).

[10] P. H. Bucksbaum, "The future of attosecond spectroscopy," Science **317**, 766–769 (2007).

[11] L. Allen and J. H. Eberly, *Optical Resonance and Two-level Atoms,* (Dover Publications Inc., New York, 1975).

[12] J. C. Diels and W. Rudolph, *Ultrashort Laser Pulse Phenomena*, 2nd ed. (Academic Press, 2006).

[13] P. W. Milonni and J. H. Eberly, *Lasers*, (Wiley, New York, 1985).

[14] L. Mandel and E. Wolf, *Optical Coherence and Quantum Optics*, (Cambridge University Press, 1995).

[15] J. W. Goodman , *Statistical Optics*, (John Willy and Sons INC, 2000).

[16] G. P. Agrawal, *Fiber-Optic Communication Systems,* 3rd., (Wiley, New York, NY 2002).

[17] W. H. Carter and B. E. A. Saleh, "Applications of coherence and statistical optics, J.Opt.Soc.Am.A 7, 934–1012 (1984).

[18] V. V. Tuchin, *Handbook of Coherent Domain Optical methods: Biomedical Diagnostics, Environmental and Material Science* V2, Kluver Academic Publishers (2004).

[19] A. F. Fercher, W. Drexler, C. K. Hitzenberger, and T. Lasser, "Optical coherence tomography - principles and applications," Rep. Prog. Phys. 66, 239303 (2003).

[20] V. Torres Company, "Coherence in ultrashort pulses and applications in temporal optics", Universitat de Valncia, Department d'ptica (2009).

[21] J. Tervo, T. Setala and A. T. Friberg, "Theory of partially coherent electromagnetic fields in the space-frequency domain," J. Opt. Soc. Am. A **21**, 1084–7529 (2004).

[22] J. Tervo, T. Setala and A. T. Friberg, "Degree of coherence for electromagnetic fields," Opt. Express **11**, 1137–1143 (2003).

[23] W. H. Carter and B. E. A. Saleh, "Applications of coherence and statistical optics," J. Opt. Soc. Am. A **7**, 934–1012 (1984).

[24] C. Rydberg, "Statistical optics and optical elements for micro-technologies: partial coherence, lithography and micro-lenses", Chalmers University of Technology Department of Micro-technology and Nanoscience,(2007).

[25] J. H. Bruning, "Optical lithography, 40 years and holding", Proc. of SPIE, 6520-652004, (2007).

[26] J. W. Goodman, *Speckle Phenomena in Optics: Theory and Applications*, Roberts and Company, (2006).

[27] J. C. Dainty, *Laser speckle and Related Phenomena*, Springer-Verlag, (1975).

[28] M. Bertolotti, L. Sereda, and A. Ferrari, "Application of the spectral representation of stochastic processes to the study of nonstationary light radiation: a tutorial," J. Eur. Opt. Soc. A **6**, 153–171 (1997).

[29] M. Bertolotti, A. Ferrari, and L. Sereda, "Coherence properties of nonstationary polychromatic light sources," J. Opt. Soc. Am. B **12**, 341–347 (1995).

[30] L. Sereda, M. Bertolotti, and A. Ferrari, "Coherence properties of nonstationary light wave fields," J. Opt. Soc. Am. B **15**, 695–705 (1998).

[31] H. Lajunen, J. Tervo, and P. Vahimaa, "Overall coherence and coherent-mode expansion of spectrally partially coherent pulses," J. Opt. Soc. Am. A **21**, 21172123 (2004).

[32] G. Genty, M. Surakka, J. Turunen, and Ari. T. Friberg, "Second-order coherence of supercontinuum light," Opt. Lett. **35** 3057-3059 (2010).

[33] T. Shirai, T. Setl, and A. T. Friberg, "Temporal ghost imaging with classical non-stationary pulsed light," J. Opt. Soc. Am. B **27**, 2549–2555 (2010).

[34] E. Wolf, "New spectral representation of random sources and of the partially coherent fields that they generate," Opt. Commun. **38**, 3–6 (1981).

[35] A. Starikov, "Effective number of degree of freedom of partially coherent sources," J. Opt. Soc. Am. A **72**, 1538–1544 (1982).

[36] S. A. Ponomarenko and E. Wolf, "Universal structure of field correlations within a fluctuating medium", Phys. Rev. E **65**, 016602–6 (2001).

[37] H. Lajunen, J. Tervo, J. Turunen, P. Vahimaa, and F. Wyrowski, "Spectral coherence properties of temporarily modulated stationary light sources," Opt. Express **11**, 1894–1899 (2003).

[38] F. Gori, M. Santarsiero, R. Simon, G. Piquero, R. Borghi, and G. Guattari, "Coherent-mode decomposition of partially polarized, partially coherent sources," J. Opt. Soc. Am. A **20**, 7884 (2003).

[39] F. Goria, M. Santarsieroa, R. Borghia, and S. Vicalvib, "Partially coherent sources with helicoidal modes," Journal of Modern Optics **45**, 539–554 (1998).

[40] Y. Baykal, "Average transmittance in turbulence for partially coherent sources," Opt. Commun. **231** 129–136 (2004).

[41] F. Gori, "Far-zone approximation for partially coherent sources," Opt. Lett. **30**, 2840–2842 (2005).

[42] Z. Mei and O. Korotkova, "Cosine-Gaussian Schell-model sources," Opt. Lett. **38** 2578–2580 (2013).

[43] M. Yao, O. Korotkova, C. Ding, L. Pan, "Position modulation with random pulses," Opt. Express **22**, 16197–206 (2014).

[44] S. Yang, S. A. Ponomarenko, and Z. D. Chen, "Coherent pseudo-mode decomposition of a new partially coherent source class," Opt. Lett. **40**, 3081–3084 (2015) .

[45] P. Paakkonen, J. Turunen, P. Vahimaa, A. T. Friberg, and F. Wyrowski, "Partially coherent Gaussian pulses," Opt. Commun., **204**, 53–58 (2002).

[46] S. A. Ponomarenko, G. P. Agrawal, and E. Wolf, "Energy spectrum of a nonstationary ensemble of pulses," Opt. Lett. **29**, 394–396 (2004).

[47] H. Lajunen, A. T. Friberg, and P. Ostlund, "Quasi-stationary plane-wave optical pulses and the van CittertZernike theorem in time," J. Opt. Soc. Am. A **23**, 2530–2537 (2006).

[48] H. Lajunen, P. Vahimaa, and J. Tervo, "Theory of spatially and spectrally partially coherent pulses," J. Opt. Soc. Am. A **22**, 1536–1545 (2005).

[49] J. Lancis, V. Torres-Company, E. Silvestre, and P. Andrs, "Spacetime analogy for partially coherent plane-wave-type pulses," Opt. Express **30**, 2973–2975 (2005).

[50] H. Lajunen, and T. Saastamoinen, "Non-uniformly correlated partially coherent pulses," Opt. Express **21**, 190–195 (2013).

[51] A. Starikov and E. Wolf, "Coherent-mode representation of Gaussian Schell-model sources and of their radiation fields," J. Opt. Soc. Am. A **72**, 9233–928 (1982).

[52] P. Vahimaa and J. Turunen, "Independent-elementary-pulse representation for non-stationary fields," Opt. Express **14**, 5007–5012 (2006).

[53] K. Saastamoinen, J. Turunen, P. Vahimaa, and A. T. Friberg, "Spectrally partially coherent propagation-invariant fields," Phys. Rev. A. **80**, 053804–11 (2009).

[54] J. Turunen, "Elementary-field representations in partially coherent optics," J. Modern Optics **58** 509-527 (2011).

[55] S. A. Ponomarenko, "Complex Gaussian representation of statistical pulses," Opt. Express **19**, 17086–17091 (2011).

[56] C. Ding, O. Korotkova, L. Pan, "The control of pulse profiles with tunable temporal coherence," Physics Letters A **378**, 1687–1690 (2014).

[57] C. Ding, O. Korotkova, Y. Zhanga, L. Pana, "Sinc Schell-model pulses," Opt. Commun. **339**, 115–122 (2015).

[58] G. Gbur, "Simulating fields of arbitrary spatial and temporal coherence," Opt. Express **14**, 7567–7577 (2006).

[59] B. Davis, "Measurable Coherence Theory for Statistically Periodic Fields," Phys. Rev. A. **76**, 38–43 (2007).

[60] V. Torres-Company, H. Lajunen, and A. T. Friberg, "Coherence theory of noise in ultrashort pulse trains", J. Opt. Soc. Am. B **24**, 1441–1450 (2007).

[61] A. T. Friberg, H. Lahunen, and V. Torres-Company, "Spectral elementary-coherence-function representation for partially coherent light pulses," Opt. Express **15**, 5160–5165 (2007).

[62] P. Vahimaa, and J. Tervo, "Unified measures for optical fields: degree of polarization and effective degree of coherence," J. Opt. A: Pure Appl. Opt. **6** 41–44 (2004).

[63] C. Ding, Y. Cai, O. Korotkova, Y. Zhang, and L. Pan, "Scattering-induced changes in the temporal coherence length and the pulse duration of a partially coherent plane-wave pulse," Opt. Lett. **36** 517–519 (2011).

[64] Z. Mei, O. Korotkova, and Y. Mao, "Products of Schell-model cross-spectral densities," Opt. Lett. **39**, 6879–6882 (2014).

[65] D. Marcuse, "Propagation of pulse fluctuations in single-mode fibers," Applied Optics **19**, 1856-1861 (1980).

[66] J. Capmany, D. Pastor, S. Sales, and M. Muriel, "Pulse distortion in optical fibers and waveguides with arbitrary chromatic dispersion," J. Opt. Soc. Am. B **20** 523–2533 (2003).

[67] W. Huang, S. A. Ponomarenko, M. Cada, and G. P. Agrawal, "Polarization changes of partially coherent pulses propagating in optical fibers," J. Opt. Soc. Am. A **24**, 3063–3068 (2007).

[68] C. L. Ding, L. Z. Pan, and B. D. Lu, "Changes in the spectral degree of polarization of stochastic spatially and spectrally partially coherent electromagnetic pulses in dispersive media," J. Opt. Soc. Am. B **26**, 1728–1735 (2009).

[69] P. Suret, A. Picozzi, and S. Randoux, "Wave turbulence in integrable systems: nonlinear propagation of incoherent optical waves in single-mode fibers," Opt. Express **19**, 17852–17863 (2011).

[70] Q. Lin, L. Wang, and S. Zhu, "Partially coherent light pulse and its propagation," Opt. Commun., **219**, 65–70 (2003).

[71] M. Brunel and S. Coëtlemec, "Fractional-order Fourier formulation of the propagation of partially coherent light pulses," Opt. Commun. **230**, 1–5 (2004).

[72] L. G. Wang, N. H. Liu, Q. Lin, and S. Y. Zhu, "Superluminal propagation of light pulses: A result of interference," Phys. Rev. E. **68**, 066606–10 (2003).

[73] R. W. Schoonover, B. J. Davis, R. A. Bartels, and P. S. Carney, "Propagation of spatial coherence in fast pulses," J. Opt. Soc. Am. A **26**, 1945–1953 (2009).

[74] S. A. Ponomarenko, "Degree of phase-space separability of statistical pulses," Opt. Express **20**, 2548–2555 (2012).

[75] B. Gross and J. T. Manassah, "Compression of the coherence time of incoherent signals to a few femto seconds," Opt. Lett. **16**, 1835–1837 (1991).

[76] V P. Nayyar, "Propagation of partially coherent Gaussian Schell-model sources in nonlinear media," J. Opt. Soc. Am. A **14**, 2248–2253 (1997).

[77] V. A. Aleshkevich, V. A. Vysloukh, G. D. Kozhoridze,A. N. Matveev and S. I. Terzieva, "Nonlinear propagation of partially coherent pulse in fiber waveguide and the role of higher order dispersion," Sov. J. Quantum Electron. **18**, 207–211 (1988).

[78] B. Hall, M. Lisak, D. Anderson, R. Fedele, and V. E. Semenov, "Statistical theory for incoherent light propagation in nonlinear media," Phys. Rev. E. **65**, 56602–56604 (2002).

[79] H. Lajunen, V. Torres-Company, J. Lancis, E. Silvestre, and P. Andr'es, "Pulse-by-pulse method to characterize partially coherent pulse propagation in instantaneous nonlinear media," Opt. Express **18**, 14979–14991 (2011).

[80] S. B. Cavalcanti, G. P. Agrawal and M. Yu, "Noise amplification in dispersive nonlinear media," Phys. Rev. A. , **51**, 4086–4092.

[81] V. P. Kandidov, "Monte Carlo method in nonlinear statistical optics", Sov. Phys.Usp. **39**, 1243–1272 (1996).

[82] L. Mokhtarpour, G. H. Akter, and S. A. Ponomarenko, "Partially coherent self-similar pulses in resonant linear absorbers," Opt. Express **20**, 17816–17822 (2012).

[83] L. Mokhtarpour and S. A. Ponomarenko, "Complex area correlation theorem for statistical pulses in coherent linear absorbers," Opt. Lett. **37**, 3498–3500 (2012).

[84] L. Mokhtarpour and S. A. Ponomarenko, "Ultrashort pulse coherence properties in coherent linear amplifiers," J. Opt. Soc. Am. A , **30**, 627–630 (2013).

[85] L. Mokhtarpour and S. A. Ponomarenko, "Fluctuating pulse propagation in resonant nonlinear media: self-induced transparency random phase soliton formation," Opt. Express **23**, 30270–30282 (2015).

[86] S. H. Poorvali, "Exploring soliton and similariton formation in resonant optical media", Dalhousie University, Electrical and Computer Engineering Department, (2012).

# Chapter 2

# Optical Coherence Theory

Optical fields, generated by realistic light sources, are random functions of time and position. The randomness of the field arises from either fluctuations of light sources or the medium through which the light travels. In our studies throughout the thesis, the characteristics of the medium are assumed to be fully deterministic, while optical fields are considered statistical. Neglecting the stochastic behavior of light could result in unrealistic predictions for light properties. Optical coherence theory studies stochastic behavior of light based on statistical theory using the correlation functions. The actual magnitude of stochastic pulse fields are random at any specific point in time and space. Therefore, statistical quantities such as averages and correlations are employed by the optical coherence theory to describe the random pulse magnitude and phase behavior.

The aim of this chapter is to briefly describe general concepts of statistical optics and its governing equations. In addition, several model sources of partially coherent pulses and their experimental generation methods are concisely reviewed.

## 2.1 Random Processes, Stationarity and Ergodicity

Assume $U(t)$ is an arbitrary random process where $U$ is a stochastic function of time $t$. A general description of the random process cannot be achieved without using statistical average functions. The average or expectation of the random process $U$ at a specific time $t$ can be defined as [1]

$$\langle U(t)\rangle = \lim_{N\to\infty} \frac{1}{N} \sum_{r=1}^{N} U^r, \tag{2.1}$$

where $\{U^r\}$ corresponds to a set or ensemble of all possible realizations of the random process. The angle brackets denote *ensemble averaging*. Averaging over a time interval $T$, when $T \to \infty$, is known as *time average* of the random process,

$$\bar{U} = \lim_{N\to\infty} \frac{1}{T} \int_{t+T/2}^{t-T/2} U^r(t')dt'. \tag{2.2}$$

If the probability density functional $P(U,t)$ of a random process does not depend on the time origin, or in other words, if the characteristics of fluctuations do not change over time, the process is referred to strictly stationary. More specifically, if the probability density is only a function of the time difference $\tau = t_1 - t_2$, then, the random process is referred to stationary in a wide sense. Thermal light, or the light emitted by light emitting diodes can be given as examples of statistically stationary fields [2,3].

On the other hand, a random process is referred to non-stationary if the probability density function depends on time instants $t_1$ and $t_2$. A good example of non-stationary processes are pulses generated by mode-locked lasers with random variations from pulse to pulse [4].

Another key characteristic of a random process is ergodicity. A stochastic process is called ergodic if each ensemble realization contains all of the statistical information of the whole ensemble. In ergodic processes, time averages of each realization (Eq 2.2) are equal to the ensemble average. If a random process is both stationary and ergodic, then the entire realization of the process is approximately similar and only differs in detail [1,4].

Generally, to extract information about higher-order correlations of a random process, the knowledge of higher order probability density functions is required. However, Gaussian random processes are an exception to this. Based on a Gaussian moment theorem, second-order statistical functions in a Gaussian random process include all the information about higher order correlations [1,4].

## 2.2 Correlation Functions

The lowest-order statistical properties of random optical fields are mathematically described using second-order correlation functions. These functions enable us to determine the degree of spatial and temporal coherence of random fields. Temporal coherence defines the ability of random light to interfere with a time delayed version of itself, while spatial coherence deals with spatially shifted field realizations. Throughout this thesis, we restrict ourselves to the plane-wave pulses and study temporal coherence that describes correlations of stochastic fields in time.

The mutual coherence function, being one of the most widely used statistical functions, specifies correlations of an ensemble of stochastic fields $\{U(t,z)\}$ at two time instants $t_1$

and $t_2$ in a plane $z = const$, transverse to the pulse propagation direction [1,4],

$$\Gamma(t_1,t_2,z) = \langle U^*(t_1,z)U(t_2,z)\rangle. \tag{2.3}$$

In Eq.(2.3), the asterisk represents complex conjugation and the angle brackets correspond to an average over all random field realizations $\{U(t,z)\}$. The pulse intensity, averaged over all random field realizations, is defined as

$$I(t,z) = \Gamma(t,t,z) = \langle |U(t,z)|^2\rangle. \tag{2.4}$$

The normalized form of mutual coherence function, known as the complex degree of coherence, is another widely used function describing second-order coherence properties of random fields [1,4],

$$\gamma(t_1,t_2,z) = \frac{\Gamma(t_1,t_2,z)}{\sqrt{I(t_1,z)I(t_2,z)}}. \tag{2.5}$$

The absolute value of the degree of coherence is such that $0 \leq |\gamma(t_1,t_2,z)| \leq 1$. The lower limit indicates no correlation between the fields at $(t_1,z)$ and $(t_2,z)$ positions, corresponding to an incoherent pulse. On the contrary, the upper limit refers to perfect correlation between the field realizations at specified spatio-temporal points which implies complete coherence. Any value of $|\gamma(t_1,t_2,z)|$ between zero and unity represents partially coherent fields. Most realistic optical fields belong to this class.

Using the Fourier transform technique, the space-time coherence properties of random fields can be converted to space-frequency domain as,

$$\tilde{U}(\omega,z) = \frac{1}{2\pi}\int_{-\infty}^{+\infty} U(t,z)\exp(i\omega t)dt. \tag{2.6}$$

The cross-spectral density function, which describes stochastic field $\tilde{U}$ correlations at two angular frequencies $\omega_1$ and $\omega_2$ and position $z$, is defined as [1,4],

$$W(\omega_1,\omega_2,z) = \langle \tilde{U}^*(\omega_1,z)\tilde{U}(\omega_2,z)\rangle. \tag{2.7}$$

Setting $\omega_1 = \omega_2 = \omega$ leads to the energy spectrum or spectral density function [5],

$$S(\omega,z) = W(\omega,\omega,z) = \langle |\tilde{U}(\omega,z)|^2\rangle. \tag{2.8}$$

The normalized cross-spectral density function or complex degree of spectral coherence can be defined as [1,4]

$$\mu(\omega_1,\omega_2,z) = \frac{W(\omega_1,\omega_2,z)}{\sqrt{S(\omega_1,z)S(\omega_2,z)}}. \tag{2.9}$$

The complex degree of spectral coherence satisfies $0 \leq |\mu(\omega_1, \omega_2, z)| \leq 1$ condition in which the lower limit and the upper limit correspond to spectrally incoherent or fully coherent fields, respectively. Similar to the time domain, any value between zero and unity corresponds to spectrally partially coherent fields.

For non-stationary random optical fields, the temporal coherence properties can be related to the spectral coherence using the generalized Wiener-Khinchine theorem [1, 4, 5],

$$\Gamma(t_1, t_2, z) = \int_{-\infty}^{+\infty} \int_{-\infty}^{+\infty} W(\omega_1, \omega_2, z) \exp[i(\omega_1 t_1 - \omega_2 t_2)] d\omega_1 d\omega_2 \tag{2.10}$$

Coherence time $t_c$ represents the time interval over which coherence of the optical field can be maintained. If $t < t_c$, the fluctuating field is highly correlated to its time shifted version and the pulse is rather predictable. The limits $t_c \to 0$ and $t_c \to \infty$ correspond to an uncorrelated and a highly correlated random pulse, respectively. The distance that the random pulse passes during its coherence time is defined as coherence length $l_c = ct_c$. In the frequency domain, spectral coherence width $\Omega_c$ corresponds to an optical bandwidth over which random pulses are spectrally correlated.

Temporal coherence of light can be measured using a Michelson interferometer. As can be seen in Fig.(1.1), the source pulse is divided into two pulses using the beam splitter. The split portions of the original pulse travel to the mirrors and after having been reflected back, superimpose in the observation plane. One of the mirrors is movable to impart a path difference $\Delta l = c\Delta t$ for the traveling pulse. If the path difference $\Delta l$ is small enough, interference fringes will be formed in the observation plane. Fringe formation is a sign of temporal coherence between the pulses. By moving the adjustable mirror far enough, the fringe visibility vanishes which corresponds to uncorrelated pulses. In other words, $\Delta l$ exceeds the coherence length or likewise the coherence time of light. In fact, the coherence level of a light pulse can be characterized by examining its ability to form fringes with a delayed version of itself.

## 2.3 Representation of Partially Coherent Fields

Coherent pulses are preferable in many optical applications. However, there exist some applications in which partially correlated optical pulses are more convenient to use. For instance, in optical lithography techniques, partially coherent pulses are used because the

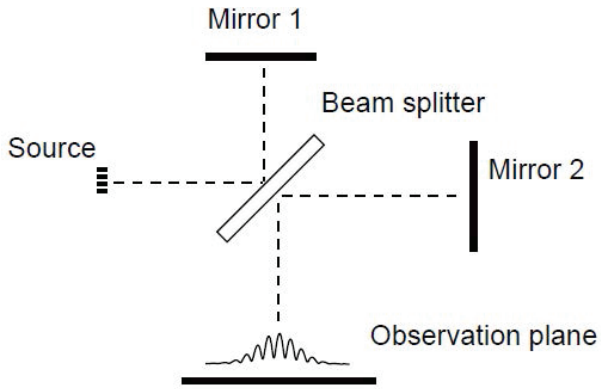


Figure 2.1: Michelson interferometer composed of source, beam splitter, two mirrors and observation plane [6]

randomness of the light improves the resolution of lithography. Therefore, it is necessary to have mathematical tools and physical devices to generate stochastic pulses with a controlled level of coherence.

In previous sections, the importance of having a convenient mathematical tool to describe coherence properties of fluctuating fields is emphasized. In order to explore the statistical properties of partially coherent pulses, we also need to employ a particular stochastic pulse model.

Gaussian Schell-model (GSM) pulses with a Gaussian distribution of intensity and complex degree of coherence are one of the most widely used generic mathematical models representing partially coherent pulses [1, 7]. There exists a limited class of partially coherent pulse models which can be analytically propagated, including GSMs. This fact makes GSMs a convenient model to be applied in propagation algorithms. Using this model enables us to produce an entire class of partially coherent pulses with the same pulse width but quite different temporal coherence properties.

GSM not only is a convenient mathematical model but also can be simply generated in laboratories. The procedure is based on chopping pulses, emitted from statistically stationary sources, using a temporal modulator. The spectrum of the stationary source and the temporal modulator profile are assumed to be Gaussian. Coherence level and temporal duration of the generated GSM pulse is determined by coherence properties of the source and modulation time, respectively [8].

The mutual coherence function of GSM pulses at the source is given by [7],

$$\Gamma_0(t_1,t_2) \propto \exp\left(-\frac{t_1^2+t_2^2}{2{t_\mathrm{p}}^2}\right) \exp\left[-\frac{(t_1-t_2)^2}{2{t_\mathrm{c}}^2}\right]. \tag{2.11}$$

The cross-spectrall density can be expressed as

$$W_0(\omega_1,\omega_2) \propto \exp\left[-\frac{(\omega_1-\omega_2)^2 t_p^2}{2}\right] \exp\left[-\frac{(\omega_1+\omega_2)^2 t_{eff}^2}{8}\right], \tag{2.12}$$

where

$$\frac{1}{t_{eff}^2} = \frac{1}{t_c^2} + \frac{1}{4t_p^2}. \tag{2.13}$$

As it was mentioned before, $t_p$ and $t_c$ are the characteristic pulse width and coherence time, respectively.

## 2.4 Coherent-Mode Representation

Representing stochastic fields as a sum of fully coherent but mutually uncorrelated fields is a convenient method to describe partially coherent fields. This method was first introduced by Wolf [9] for scalar stationary fields. Later it was extended to the electromagnetic fields [10–13], and pulses [14–16].

The coherent mode representation method has become one of the most efficient methods for computational propagation of random fields. This arises from the fact that, in this approach, each mode is fully coherent, thus it can be propagated individually using any method of coherent propagation theory. The statistical properties of the propagated stochastic field are characterized by an ensemble of such mutually uncorrelated modes.

Mercer's theorem [17] states that any Hermitian and non-negative definite, second-order correlation function can be represented as a converging series [1, 15]

$$\Gamma(t_1,t_2) = \sum_n \lambda_n \psi_n^*(t_1)\psi_n(t_2). \tag{2.14}$$

Here $\{\lambda_n\}$ and $\{\psi_n(t)\}$ are the eigenvalues and eigenfunctions of the Fredholm integral equation [15],

$$\int_{-\infty}^{\infty} \Gamma(t_1,t_2)\psi_n(t_1)dt_1 = \lambda_n \psi_n(t_2). \tag{2.15}$$

It has been shown in [15] that the eigenvalues are real and nonnegative and eigenfunctions satisfy orthonormal condition as

$$\int_{-\infty}^{\infty} \psi_n^*(t)\psi_m(t)dt = \delta_{nm}, \tag{2.16}$$

where $\delta_{nm}$ represents Kronecker's delta symbol. According to Eq.(2.14), the mutual coherence function of each mode can be represented as

$$\Gamma_n(t_1,t_2) = \lambda_n \psi_n^*(t_1)\psi_n(t_2), \tag{2.17}$$

which means that modes are completely coherent and the degree of coherence of each mode equals to unity. It can be inferred from Eqs.(2.14)-(2.17) that, each given mode is fully deterministic and its second-order coherence properties can be described by Eq.(2.17). However, as the modes are mutually uncorrelated, the total field is fluctuating and varies for each realization. Coherent modes can be defined as natural oscillations of a partially coherent source. This method found to be useful in solving different problems in statistical optics such as wave propagation problems or simulation and formation of laser resonator modes [18–21].

To determine the modes of a partially coherent pulse at the source, Eq.(2.15) should be solved for the corresponding eigenvalues and eigenfunctions of a specific pulse model which is quite challenging. However, these explorations have been successfully done in [10, 12, 15] for Gaussian Schell-model pulses and analytical expressions have been derived for their eigenvalues and eigenfunctions. This makes GSM pulses very useful in verification of numerical propagation algorithms. In the space-frequency domain, the coherent mode representation can be simply derived using Eq.(2.10).

In this chapter the general theory of statistical optics and its mathematical description were concisely reviewed. Some model sources of partially coherent pulses and their experimental realizations were discussed.

## Bibliography


[1] L. Mandel and E. Wolf, *Optical Coherence and Quantum Optics*, (Cambridge University Press, 1995).

[2] R. Loudon, *The Quantum Theory of Light*, (Oxford University Press, Oxford, 1983).

[3] S. A. Akhmanov, A. S. Chirkin, "Statistical phenomena in nonlinear optics," Radiophysics and Quantum Electronics **13**, 619–648 (1970).

[4] J. W. Goodman , *Statistical optics*, (John Willy and Sons INC, 2000).

[5] S. A. Ponomarenko, G. P. Agrawal, and E. Wolf, "Energy spectrum of a nonstationary ensemble of pulses," Opt. Lett. **29**, 394–396 (2004).

[6] C. Rydberg, "Statistical optics and optical elements for micro-technologies: partial coherence, lithography and micro-lenses," Chalmers University of Technology, Department of Micro-technology and Nanoscience, Photonics Laboratory, Goteborg, Sweden.

[7] P. Paakkonen, J. Turunen, P. Vahimaa, A. T. Friberg, and F. Wyrowski, "Partially coherent Gaussian pulses," Opt. Commun., **204**, 53–58 (2002).

[8] H. Lajunen, J. Tervo, J. Turunen, P. Vahimaa, and F. Wyrowski, "Spectral coherence properties of temporarily modulated stationary light sources," Opt. Express bf 11, 1894–1899 (2003).

[9] E. Wolf, "New spectral representation of random sources and of the partially coherent fields that they generate", Opt. Commun. **38**, 3–6 (1981).

[10] A. Starikov and E. Wolf, "Coherent-mode representation of Gaussian Schell-model sources and of their radiation fields", J. Opt. Soc. Am. A **72**, 9233–928 (1982).

[11] C. Pask, and A. Stacey, "Optical coherence and Wolfs theory for electromagnetic waves," J. Opt. Soc. Am. A **5**, 1688–1693 (1988).

[12] F. Gori, Collett-Wolf sources and multi-mode lasers, Opt. Commun. **34**, 301–305 (1980).

[13] J. Tervo, T. Setala and A. T. Friberg, " Theory of partially coherent electromagnetic fields in the space-frequency domain," J. Opt. Soc. Am. A **21**, 1084–7529 (2004).

[14] H. Lajunen and P. Vahimaa, "Theory of spatially and spectrally partially coherent pulses", J. Opt. Soc. Am. A **22**, 1536–1545 (2005).

[15] H. Lajunen, J. Tervo, and P. Vahimaa, "Overall coherence and coherent-mode expansion of spectrally partially coherent plane-wave pulses", J. Opt. Soc. Am. A **21**, 2117–2123 (2004).

[16] H. Lajunen, V. Torres-Company, J. Lancis, E. Silvestre, and P. Andr'es, "Pulse-by-pulse method to characterize partially coherent pulse propagation in instantaneous nonlinear media," Opt. Express **18**, 14979–14991 (2011).

[17] F. Riesz and B. Sz.-Nagy,*Functional Analysis* (Ungar, New York, 1978).

[18] R. Gase, "The multi-mode laser-radiation as a Gaussian-Schell model beam," Journal of Modern Optics **38**, 1107–1115 (1991).

[19] F. Gori, M. Santarsiero, R. Simon, G. Piquero, R. Borghi, and G. Guattari, "Coherent mode decomposition of partially polarized, partially coherent sources," J. Opt. Soc. Am. A **20**, 78–84 (2003).

[20] F. Gori," Mode propagation of the field generated by Collett-Wolf Schell-model sources," Opt. Commun. **46**, 149–154 (1983).

[21] A. Gamliel, "Mode analysis of spectral changes in light-propagation from sources of any state of coherence," J. Opt. Soc. Am. A **7**, 1591–1597 (1990).

# Chapter 3

# Near Resonance Pulse Propagation Theory

The classical Lorentz theory has been developed to describe linear interactions of optical fields with media. The linear term refers to the case in which the input field is weak such that atomic nonlinearities are not excited. The Lorentz model characterizes optical phenomena based on dipole oscillations of the medium that arise in response to the applied electromagnetic field. This classical theory is still applicable to describe linear resonant and near resonant interactions without need for further modifications. However, in case of intense input fields that activate atomic nonlinearities, the classical model is incapable of describing the interactions accurately. In such cases the classical model needs to be dispensed with and quantum-mechanical theories should be applied [1].

## 3.1 Two-Level Atom Model

In this thesis, we are interested in resonant and near resonant interactions which can be explored by semiclassical Maxwell-Bloch equations which are a mix of classical Maxwell and quantum mechanical Bloch equations. Bloch equations are in charge of describing the response of the resonant atoms of the medium to the driving field. At the same time Maxwell equations are employed to explore propagation effects including absorption and amplification effects. In this chapter, we briefly review the near resonance pulse propagation theory and its governing equations.

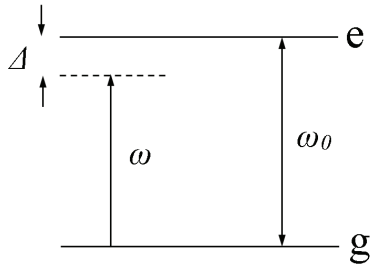


Figure 3.1: Diagram of a two-level atom model

As is known, atoms of a gaseous medium have a set of discrete energy levels, however, the medium atom response to a near resonance driving field is described based on the two-level atom theory. Although, an atom with only two energy states is too ideal to exist, most of resonant atomic interactions occur in the two atomic states. This fact validates the two-level atom approximation. In the two-level atom theory, the atoms of a medium are considered to have two energy states, ground level and excited level. Resonance frequency $\omega_0$ is characterized by the difference between this two energy states. Fig.(3.1) illustrates the diagram of the two-level atom model in which, $e$ and $g$ represent excited level and ground level, respectively. Also, $\omega$ and $\Delta = (\omega - \omega_0)$ correspond to the carrier wave frequency and detuning between the frequencies. If $\Delta = 0$ the exact resonance condition occurs such that the carrier wave frequency coincides with the atomic resonance frequency [1]. Throughout this thesis either the exact resonance $\Delta = 0$ or near resonance $\Delta << \omega_0$ conditions considered in our numerical and analytical investigations.

Material response to a resonant driving field can be described using the so-called density matrix $\rho$ with the following elements [4, 5],

$$\rho(t) = \begin{bmatrix} \rho_{gg} & \rho_{ge} \\ \rho_{eg} & \rho_{ee} \end{bmatrix} \tag{3.1}$$

The diagonal elements of the matrix $\rho_{ee}$ and $\rho_{gg}$ define the atomic level population probabilities. On the other hand, the off-diagonals $\rho_{ge}$ and $\rho_{eg}$ are known as atomic coherences.

Optical Bloch equations are expressed in terms of density matrix elements. According to probability conservation, atoms of a medium are in either ground states or excited state, $\rho_{gg} + \rho_{ee} = 1$. Density matrix elements can be converted to Bloch coefficients defined as [1, 4],

$$u = \rho_{eg} + \rho_{ge}, \tag{3.2}$$

$$v = i\,(\rho_{eg} - \rho_{ge}), \tag{3.3}$$

$$w = \rho_{ee} - \rho_{gg}, \tag{3.4}$$

where $u$, $v$ and $w$ are atomic variables corresponding to atomic dipole moment matrix elements in phase and in quadrature with the driving field and, the atomic population inversion, respectively. The population inversion has an equilibrium value $w_{eq}$, which denotes

the value of atomic inversion in the absence of input field. Population inversion, $w$, returns to its equilibrium value, $w_{eq}$, after a time duration which corresponds to atomic population decay time or energy decay time $T_{||}$.

Time evolution of atomic variables in the absence of damping is governed by Bloch equations [1]

$$\partial_t u = -\Delta v, \tag{3.5}$$

$$\partial_t v = \Delta u + \Omega w, \tag{3.6}$$

$$\partial_t w = -\Omega v. \tag{3.7}$$

Here, $\Delta = (\omega - \omega_0)$ is the detuning factor and $\Omega = 2d_{eg}\mathscr{E}/\hbar$ corresponds to a Rabi frequency associated with the field envelope $\mathscr{E}$. Optical Bloch equations cannot be described properly without considering relaxation processes. By assuming $\sigma = u - iv$ as the dipole moment variable, the final form of Bloch equations can be expressed as [1]

$$\partial_t \sigma = -\left(\frac{1}{T_\perp} + i\Delta\right)\sigma - i\Omega w, \tag{3.8}$$

$$\partial_t w = -\frac{1}{T_{||}}\left(w - w_{eq}\right) - \tfrac{i}{2}\left(\Omega^*\sigma - \Omega\sigma^*\right). \tag{3.9}$$

Here, $w_{eq}$ denotes the equilibrium value of atomic inversion in the absence of input field. $T_\perp$ and $T_{||}$ indicate atomic dipole (transverse) and atomic population (longitudinal) decay times that will be described shortly.

The wave propagation in one spatial direction can be derived using the Maxwell equations. The reduced wave equation based on the slowly varying envelope approximation (SVEA) is given by [1]

$$\partial_z \Omega = \frac{\omega N |d_{eg}|^2}{c\varepsilon_0 \hbar}\langle\sigma\rangle_\Delta. \tag{3.10}$$

In Eq.(3.10), $N$ and $d_{eg}$ are the atom density and the dipole matrix element, respectively. The angle brackets indicate an average over detuning $\Delta$, between the wave frequency $\omega$ and atomic resonance frequency $\omega_0$. Eq.(3.10), combined with Bloch Eqs.(3.8)-(3.9), known as coupled Maxwell-Bloch equations, are employed to describe resonant light-matter interactions [4].

As mentioned before, if the intensity of the input field is rather weak then no atomic population inversion takes place. Such case corresponds to the atomic linear limit in which $w = w_{eq} = \pm 1$. As a consequence of the weak pulse assumption, time evolution of dipole moment Eq.(3.8) takes on a linearized form such that [6, 7]

$$\partial_t \sigma = -\left(\frac{1}{T_\perp} + i\Delta\right)\sigma \pm i\Omega. \tag{3.11}$$

Here, $w \approx w_{eq} = +1$ indicates that all the atoms of a medium are in their excited state describing linear amplifiers. In contrast, whenever $w \approx w_{eq} = -1$, atoms are in their ground state which corresponds to linear absorbers.

As previously mentioned, classical Lorentz theory describes linear interaction of optical fields with the medium. When atoms of the medium are in their ground state, Lorentz's classical model is in a quantitative agreement with the quantum-mechanical theory. Therefore, in case of linear absorbers, the classical Lorentz harmonic oscillator model, coupled with the Maxwell equations, can be safely used to describe light-matter interactions.

### 3.2 Homogenous and Inhomogeneous Broadening and Damping Times

In this section, the decay times associated with Bloch Eqs.(3.8)-(3.9) will be briefly discussed. The decay times $T_\perp$ and $T_{||}$, describe the phase (transverse) and energy (longitudinal) relaxation, respectively. Since, atomic interaction processes could affect phase and energy relaxation rates individually, these times should be determined separately. For instance, some dissipative processes affect phase relaxation, but not atomic level populations. Generally, $T_\perp < T_{||}$ is the governing relation in real situations. The medium atom response to the driving field, in general, depends on both $T_{||}$ and $T_\perp$. The governing relation between relaxation times is [2, 4],

$$\frac{1}{T_\perp} = \frac{1}{2T_{||}} + \frac{1}{T_\perp^h}, \tag{3.12}$$

which leads to the following inequality

$$T_\perp \leq 2T_{||}. \tag{3.13}$$

Here, $T_\perp^h$ represents the homogenous broadening lifetime that will be described shortly.

The dipole oscillations of excited atoms decay after a limited time, due to a finite radiative lifetime. This phenomenon causes each atom of the medium to have a finite absorption

linewidth. There exist atomic interactions such as collisions that shorten the radiative lifetime and broaden the absorption linewidth. Collisional effects also lead to dephasing of dipole oscillations. Thus, the damping rate arising from collisions is also known as dephasing rate. Collisions affect all atoms of the medium homogenously. In other words, all atoms of the medium have identical absorption line profiles -in shape and width. The absorption line broadening associated with collisions is known as homogenous broadening with the corresponding width $\delta\nu_h$ and lifetime $T_\perp^h = 1/\delta\nu_h$ [4, 8].

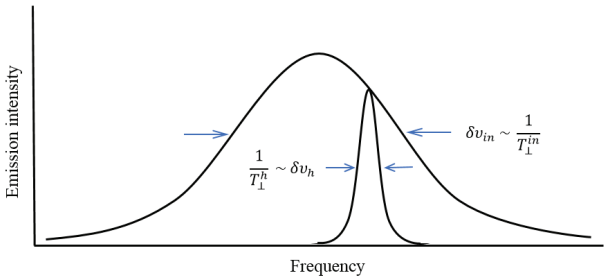


Figure 3.2: Illustation of homogenous and inhomogenous broadenings [1]

On the other hand, there exist dissipative phenomena that affect atoms of the media inhomogenously and shorten the dipole lifetime. In real systems, atoms of the medium could have various resonant frequencies. The most common reason of the distribution of resonant frequency is the Doppler effect in gases and impurities of the material in solids. In gases and atomic vapors, the Doppler effect arises from the fact that, atoms of the medium have different velocities. Hence, each atom of the medium observes the wave frequency $\omega$ in a shifted form $\omega' = \omega - kv$ according to its velocity $v$. Subsequently, atoms with various velocities have different individual detuning $\Delta$ from the resonant frequency $\omega_0$. The random distribution of detunings leads to an inhomogeneous broadening of the absorption linewidth [1]. Fig.(3.2) illustrates the concept of homogenous and inhomogeneous broadening.

Accounting for homogenous and inhomogenous broadening, leads to the following result [4]

$$\frac{1}{T_\perp} = \frac{1}{T_\perp^h} + \frac{1}{T_\perp^{in}}, \tag{3.14}$$

where $T_\perp^h$ and $T_\perp^{in}$ are homogenous and inhomogeneous broadening lifetimes, respectively. According to [4], the effective absorption lineshape of a material is affected by the ratio of homogeneous and inhomogeneous linewidths,

$$b = \sqrt{4\ ln2}\ \frac{\delta\nu_h}{\delta\nu_{in}}, \tag{3.15}$$

where, $\delta\nu_h = 1/T_\perp^h$ and $\delta\nu_{in} = 1/T_\perp^{in}$ are homogenous and inhomogeneous linewidths, respectively. Eq. (7.25) could lead to the two limiting cases. The first limit $\delta\nu_{in} >> \delta\nu_h$, is known as the inhomogeneous broadening limit. In contrast, if $\delta\nu_h >> \delta\nu_{in}$, the homogeneous broadening limit is reached such that the effective transverse decay rate is mostly influenced by collisions.

In this chapter the resonant light-matter interactions were briefly described and the two-level atom theory and semiclassical Maxwell-Bloch equations were reviewed. In addition, the relaxation processes affecting the response of the matter to the driving field were discussed.

## Bibliography


[1] L. Allen and J. H. Eberly, *Optical resonance and two-level atoms,* (Dover Publications Inc., New York, 1975).

[2] G. P. Agrawal, *Nonlinear fiber optics,* (Academic Press, 2007).

[3] P. P. Banerjee, *Nonlinear optics: Theory, Numerical Modeling and Applications* (Marcel Decker, 2004).

[4] P. W. Milonni and J. H. Eberly, *Lasers*, (Wiley, New York, 1985).

[5] R. W. Boyd, *Nonlinear Optics*, (Academic Press, 2008).

[6] S. Haghgoo and S. A. Ponomarenko, "Self-similar pulses in coherent linear amplifiers," Opt. Express **19**, 9750–9758 (2011).

[7] S. Haghgoo and S. A. Ponomarenko, "Shape-invariant pulses in resonant linear absorbers," Opt. Lett. **37**, 1328–1330 (2012).

[8] J. C. Diels and W. Rudolph, *Ultrashort Laser Pulse Phenomena*, (Academic Press, 2006)

# Chapter 4

# Partially Coherent Self-similar Pulses in Resonant Linear Absorbers

L. Mokhtarpour, G. H. Akter, and S. A. Ponomarenko

Published in: Optics Express, 30 Jul 2012, Vol. 20. No. 16, 17816
URL: http://www.opticsinfobase.org/oe/abstract.cfm?uri=oe-20-16-17816



## 4.1 Abstract

We theoretically describe several classes of ultrashort partially coherent pulses that maintain their shape on propagation in coherent linear absorbers near optical resonance.

## 4.2 Introduction

The growing interest in the ultrafast optical communication systems [1] has motivated the recent surge of activity in the field of ultrafast statistical optics [2–12]. The progress was initiated by the pioneering work [2, 3] that extended the optical coherence theory of statistically stationary fields [13] to the non-stationary case.

To date, a good deal of attention has been paid to modeling realistic partially coherent sources [4, 5], the search for an adequate definition of statistical pulse spectrum [6] and for a measurable theory of random pulses [7] as well as the advancement of various statistical representations thereof [8–10]. Propagation properties of statistical pulses–especially the ones that maintain their temporal profile on propagation–have also been explored in linear [11, 12, 14] and nonlinear [15] dispersive media far from internal resonances. Although shape-invariant propagation of fully coherent ultrashort pulses in linear amplifiers and absorbers in the vicinity of an optical resonance has been recently examined [16, 17], the influence of statistical properties on pulse evolution has not yet been explored in the resonant case.

The objective of this work is to present explicit classes of partially coherent pulses that propagate in resonant linear absorbers without changing their shape. We show how such

pulses can be constructed from the previously discovered shape-invariant modes of resonant absorbers by extending the coherent-mode representation of optical coherence theory [18] to the case of statistical pulses in a manner similar to [19].

### 4.3 Partially Coherent Self-similar Pulses in Coherent Linear Absorbers

To set the stage, we examine small-area statistical pulse propagation in a homogeneously broadened resonant absorber under exact resonance condition: the pulse carrier frequency coincides with a resonant transition frequency of the medium atoms. A dilute atomic vapor filling a high-vacuum cell can serve as a physical realization of the medium. To eliminate inhomogeneous broadening, we assume the atomic velocities to be well collimated orthogonally to the input laser beam such that no Doppler broadening takes place.

To illustrate a typical experimental situation, we consider a dilute sodium vapor with the density $N \sim 10^{11}$ cm$^{-3}$ at room temperature at the pressure of $P = 0.1$ Torr, say. One can then estimate a characteristic spectral width due to collision broadening as $\delta\nu_c \sim 10^3$ MHz [20]. Assuming further that dipole relaxation is mainly due to collisions, we can estimate a typical dipole relaxation time, $T_\perp \sim \delta\nu_c^{-1} \sim 10^{-9}$ s. It follows that the linear absorption length of this system can be estimated as $L_A = \alpha^{-1} \simeq 2$ mm, where $\alpha = NT_\perp e^2/2\varepsilon_0 mc$ is a small-signal absorption coefficient. Thus, the proposed self-similar pulses can be realized with nanosecond small-area input pulses in a few-centimeter long cell filled with the homogeneously broadened dilute vapor.

Next, we recall that the system supports a class of fully coherent shape-invariant modes; the spectral profile of each mode is given by [17]

$$\tilde{\mathscr{E}}_s(\omega,\zeta) \propto \frac{(\alpha\zeta_0/2)^s}{(1-i\omega T_\perp)^{s+1}} \exp\left[-\frac{\alpha(\zeta+\zeta_0)}{2(1-i\omega T_\perp)}\right]. \tag{4.1}$$

Here $\alpha$ is a small-signal inverse absorption length, $T_\perp$ is an individual dipole relaxation time, and $\zeta_0$ determines the spectral mode profile at the source. Introducing dimensionless variables $\Omega = \omega T_\perp$ and $Z = \alpha\zeta$ and restricting ourselves to the integer index modes ($s = n$), we can rewrite the spectral field amplitude of each shape-invariant mode in the form

$$\tilde{\mathscr{E}}_n(\Omega,Z) \propto \frac{(Z_0/2)^n}{(1-i\Omega)^{n+1}} \exp\left[-\frac{Z+Z_0}{2(1-i\Omega)}\right]. \tag{4.2}$$

Any partially coherent shape-invariant pulse can be expressed as a linear superposition

of shape-invariant modes with random coefficients as

$$\tilde{\mathscr{E}}(\Omega,Z)=\sum_{n=0}^{\infty}C_n\tilde{\mathscr{E}}_n(\Omega,Z). \tag{4.3}$$

In Eq. (4.3), the coefficients determine the statistics of the source viz.,

$$\langle C_n^* C_m\rangle=\lambda_n\delta_{mn}, \tag{4.4}$$

where $\lambda_n\geq 0$ and the angle brackets indicate ensemble averaging. The second-order statistical properties of pulses in the spectral domain are described by the cross-spectral density distribution defined as

$$W(\Omega_1,\Omega_2,Z)=\langle\tilde{\mathscr{E}}^*(\Omega_1,Z)\tilde{\mathscr{E}}(\Omega_2,Z)\rangle. \tag{4.5}$$

It follows from Eqs. (4.4) and (4.5) that the cross-spectral density can then be expressed as a Mercer-type series in the form [18]

$$W(\Omega_1,\Omega_2,Z)=\sum_{n=0}^{\infty}\lambda_n\tilde{\mathscr{E}}_n^*(\Omega_1,Z)\tilde{\mathscr{E}}_n(\Omega_2,Z). \tag{4.6}$$

Although a multitude of partially coherent shape-invariant pulses can be represented by the expansion (4.6), closed-form results can only be obtained for a few classes of pulses. In the following sections we consider two such cases.

**Pulses with the power-law distribution of modal weights**

First, assume the modal weights $\{\lambda_n\}$'s have a power distribution:

$$\lambda_n=\mathscr{A}\,\lambda^{2n}, \tag{4.7}$$

where $\mathscr{A}>0$ is a normalization constant specifying the overall intensity of a partially coherent pulse, and $\lambda\geq 0$. It follows at once from Eqs. (4.2), (4.6), and (4.7) that the spectrum of the pulse, defined as $S(\Omega,Z)\equiv W(\Omega,\Omega,Z)$ [6], is

$$S(\Omega,Z)=\frac{\mathscr{A}}{(1-\lambda^2Z_0^2/4)+\Omega^2}\exp\left[-\frac{Z+Z_0}{1+\Omega^2}\right]. \tag{4.8}$$

Equation (4.8) corresponds to a physical pulse spectrum only if the constraint $0\leq\lambda<2/Z_0$ is imposed. The latter is rather stringent as it stipulates that $\lambda$ be fairly small for sufficiently large $Z_0$. Notice also that the spectrum (4.8) has the shape reminiscent of the zero-index mode spectrum $|\tilde{\mathscr{E}}_0(\Omega,Z)|^2$ of Ref. [17], though its peak amplitude is scaled by the factor of $(1-\lambda^2Z_0^2/4)^{-1}$.

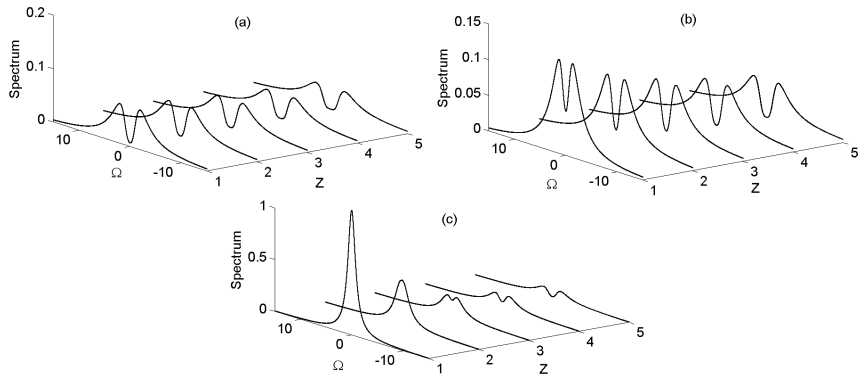


Figure 4.1: Spectral amplitude of the pulse with the power-law modal weight distribution in arbitrary units. The parameters are (a) $\lambda = 0.1$, $Z_0 = 5$; (b) $\lambda = 0.3$, $Z_0 = 3$, and (c) $\lambda = 10$, $Z_0 = 0.1$.

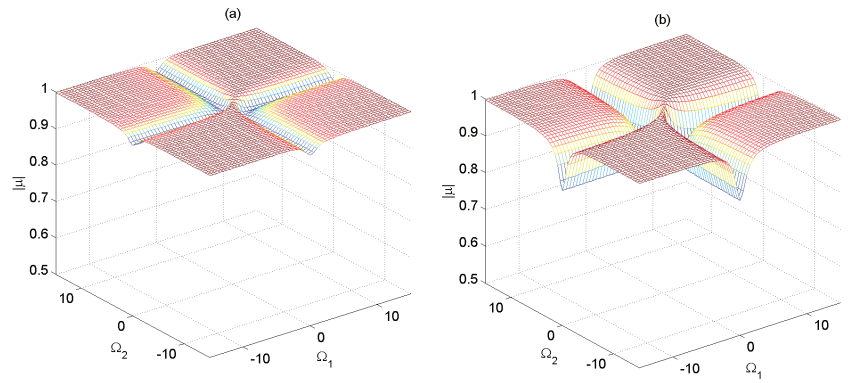


Figure 4.2: Modulus of the spectral degree of coherence. The parameters are (a) $\lambda = 0.1$, $Z_0 = 5$ and (b) $\lambda = 10$, $Z_0 = 0.1$.

Further analysis reveals that the shape of the pulse spectrum depends on the magnitude of two parameters: $\lambda$ and $Z_0$. In particular, the pulse spectrum at the source can have either a hole, or a dip, or else a peak at the center, depending on $\lambda$ and $Z_0$. The situation is illustrated in Fig. 4.1 where the pulse spectrum evolution is displayed for three sets of

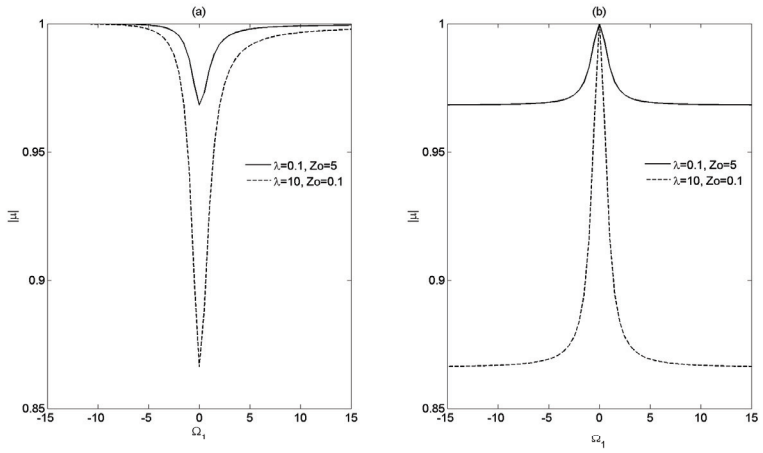


Figure 4.3: Modulus of the spectral degree of coherence as a function of $\Omega_1$ for a fixed $\Omega_2$: (a) $\Omega_2 = -15$, (b) $\Omega_2 = 0$.

parameters: (a) $\lambda = 0.1$, $Z_0 = 5$; (b) $\lambda = 0.3$, $Z_0 = 3$, and (c) $\lambda = 10$, $Z_0 = 0.1$. As is seen in Fig. 4.1 (a), the spectrum with a hole at the center propagates in a self-similar fashion from the outset. Whenever there is only a dip at the center of the incident pulse–as is shown in Fig. 4.1 (b)–the dip deepens on propagation until a hole is burnt at the center and the pulse enters its self-similar evolution stage. If, on the other hand, the spectrum has a central peak (see Fig.4.1 (c)), the latter eventually transforms into a hole with the subsequent self-similar pulse evolution.

Coherence properties of the pulse are described by the spectral degree of coherence defined as [18]

$$\mu(\Omega_1, \Omega_2, Z) = \frac{W(\Omega_1, \Omega_2, Z)}{\sqrt{S(\Omega_1, Z)}\sqrt{S(\Omega_2, Z)}}. \tag{4.9}$$

The latter can be worked out analytically, but the resulting expression is rather cumbersome. Instead, we exhibit the magnitude of the spectral degree of coherence in the source plane in Fig. 4.2 for two sets of parameters: (a) $\lambda = 0.1$, $Z_0 = 5$ and (b) $\lambda = 10$, $Z_0 = 0.1$. As is seen in the figure, the spectral coherence properties of the pulses are nonuniform and dependent on the values of parameters. To illustrate these points, we display in Fig. 4.3 $|\mu|$ as a function of $\Omega_1$, say, for fixed $\Omega_2$. It is seen in the figure that the degree of coherence can have a local maximum or minimum at the center, $\Omega_1 = 0$, depending on the position of the other spectral point. The magnitudes of the maxima and minima depend on the values of the other parameters.

**Pulses with modal weight distributions decaying faster than the power-law**

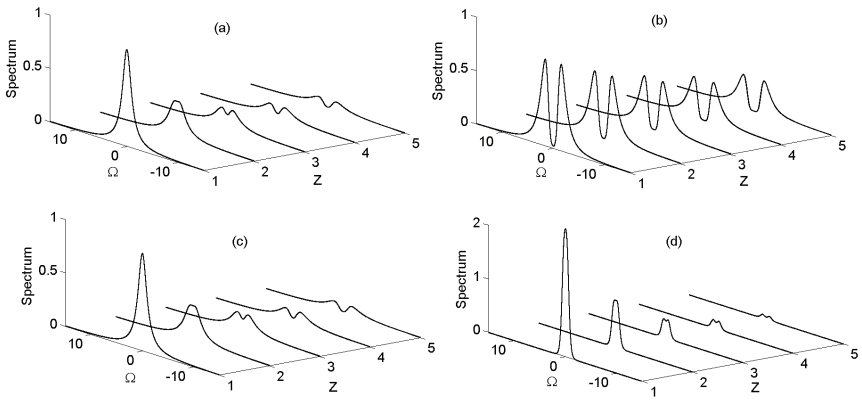


Figure 4.4: Spectral amplitude of the pulse with $\lambda_n \propto \lambda^{2n}/(n!)^2$ in arbitrary units. The parameters are (a) $\lambda = 0.9$, $Z_0 = 0.1$; (b) $\lambda = 0.9$, $Z_0 = 15$; (c) $\lambda = 2$, $Z_0 = 0.1$, and (d) $\lambda = 2$, $Z_0 = 15$.

Next, we examine the following modal weight distribution,

$$\lambda_n = \mathscr{B}\,\frac{\lambda^{2n}}{(n!)^2}, \tag{4.10}$$

$\mathscr{B}$ being a positive normalization constant. It can be inferred from Eqs. (4.2), (4.6), and (4.10) using the representation for the zero-order modified Bessel function [21],

$$I_0(x) = \sum_{n=0}^{\infty} \frac{(x/2)^{2n}}{(n!)^2}, \tag{4.11}$$

that the partially coherent pulse spectrum in the case takes the form

$$S(\Omega, Z) = \frac{\mathscr{B}}{1+\Omega^2}\, I_0\left(\frac{\lambda Z_0}{\sqrt{1+\Omega^2}}\right) \exp\left[-\frac{Z+Z_0}{1+\Omega^2}\right]. \tag{4.12}$$

We conclude by examining Eq. (4.12) that provided $\lambda < 1$, the spectral hole or dip presence at the pulse center in the source plane depends on the values of $\lambda$ and $Z_0$. However, unlike in the previously considered case, if $\lambda > 1$, there can be no spectral hole at the source.

We illustrate these observations by exhibiting the pulse spectrum of Eq. (4.12) in Fig. 4.4 for four sets of parameters: (a) $\lambda = 0.9$, $Z_0 = 0.1$; (b) $\lambda = 0.9$, $Z_0 = 15$; (c) $\lambda = 2$, $Z_0 = 0.1$, and (d) $\lambda = 2$, $Z_0 = 15$. It is seen by comparing Figs. 4.4 (a) and 4.4 (c) that for sufficiently small $Z_0 = 0.1$, there is a peak at the center in the source plane in both figures. At the same

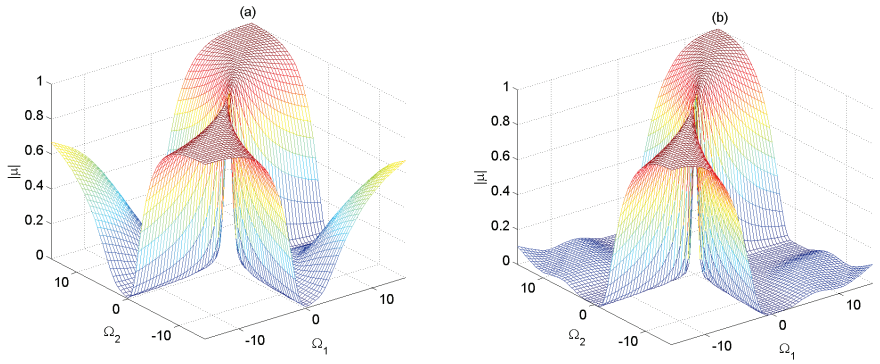


Figure 4.5: Modulus of the spectral degree of coherence. The parameters are (a) $\lambda = 0.9$, $Z_0 = 15$ and (b) $\lambda = 2$, $Z_0 = 15$.

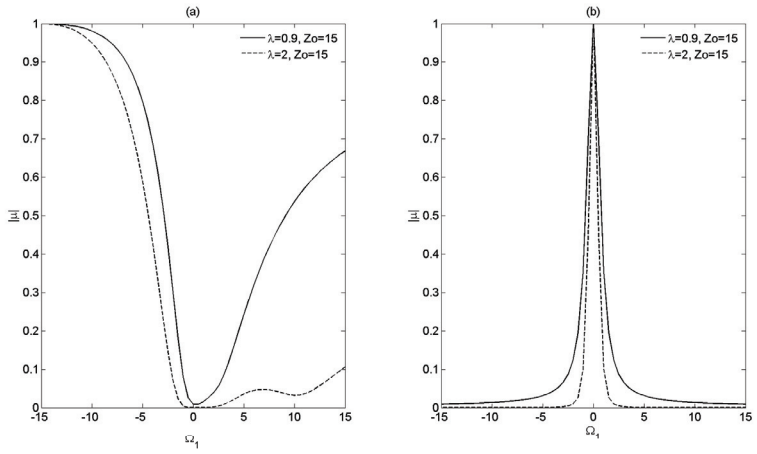


Figure 4.6: Modulus of the spectral degree of coherence as a function of $\Omega_1$ for a fixed $\Omega_2$: (a) $\Omega_2 = -15$, (b) $\Omega_2 = 0$.

time, as $Z_0$ increases to 15, say, a hole is formed at the center for $\lambda = 0.9 < 1$ as is seen in Fig. 4.4 (b). Yet, the pulse spectrum has a peak at the center for $\lambda = 2 > 1$ as shown in Fig. 4.4 (d). Our numerical simulations indicate that no matter how close the value of $\lambda$ approaches unity from the above, only a dip but not a hole can be formed at the center of the pulse spectrum.

In Fig. 4.5, we also present the corresponding spectral degree of coherence in the source plane for $Z_0 = 15$ with $\lambda = 0.9$ (left) and $\lambda = 2$ (right). Note that there is no constraint on the magnitude of $\lambda$ in Eq. (4.12) which makes this class of pulses wider than the previously considered one. On comparing Fig. 4.2 and Fig. 4.5, we observe that first, the spectral degree of coherence is rotationally symmetric in the former figure while the rotational

symmetry is broken in the latter. Second, we notice that the quantitative dependence of $|\mu|$ on the parameters is stronger for the second class of pulses than is for the first. To bring these points home, we exhibit in Fig. 4.6 the cross-sectional plot of $|\mu|$ for a couple fixed values of one of the frequencies, $\Omega_2 = -15$ in Fig. 4.6 (a) and $\Omega_2 = 0$, in Fig. 4.6 (b). On comparing Figs. 4.3 and 4.6, we can see that not only does the qualitative behavior of $|\mu|$ richer in Fig. 4.6, but pulse coherence properties can be tuned within a wider range for the second class of pulses than for the first one.

## 4.4 Conclusion

In conclusion, we have theoretically described several classes of partially coherent self-similar pulses. We found closed form expressions for two-time correlation functions fully describing second-order statistical properties of the pulses. We also explored coherence properties of the new pulses and shown that, in general, the pulse coherence properties are highly nonuniform across the their temporal profiles. The spectral profiles of the new pulses may have a spectral hole or a dip which can affect their short-distance evolution; however the long-term evolution is self-similar in either case.

## Bibliography


[1] G. P. Agrawal, *Fiber-Optic Communication Systems,* 3rd ed., (Wiley, Newy York, NY 2002).

[2] M. Bertolotti, A. Ferrari, and L. Sereda, "Coherence properties of nonstationary polychromatic light sources," J. Opt. Soc. Am. B **12**, 341–347 (1995).

[3] L. Sereda, M. Bertolotti, and A. Ferrari, "Coherence properties of nonstationary light wave fields," J. Opt. Soc. Am. B **15**, 695–705 (1998).

[4] P. Pääkkönen, J. Turunen, P. Vahimaa, A. T. Friberg, and F. Wyrowski, "Partially coherent Gaussian pulses," Opt. Commun. **204**, 53–58 (2002).

[5] H. Lajunen, J. Tervo, J. Turunen, P. Vahimaa, and F. Wyrowski, "Spectral coherence properties of temporarily modulated stationary light sources," Opt. Express **11**, 1894–1899 (2003).

[6] S. A. Ponomarenko, G. P. Agrawal, and E. Wolf, "Energy spectrum of a nonstationary ensemble of pulses," Opt. Lett. **29**, 394–396 (2004).

[7] B. Davis, "Measurable Coherence Theory for Statistically Periodic Fields," pra **76**, 043843 (2007).

[8] P. Vahimaa and J. Turunen, "Independent-elementary-pulse representation for nonstationary fields," Opt. Express **14**, 5007–5012 (2006).

[9] A. T. Friberg, H. Lahunen, and V. Torres-Company, " Spectral elementary-coherence-function representation for partially coherent light pulses," Opt. Express **15**, 5160-5165 (2007).

[10] S. A. Ponomarenko, "Complex Gaussian representation of statistical pulses," Opt. Express **19**, 17086-17091 (2011).

[11] Q. Lin, L. Wang, and S. Zhu, "Partially coherent light pulse and its propagation," Opt. Commun. **219**, 65-70 (2003).

[12] M. Brunel and S. Coëtlemec, "Fractional-order Fourier formulation of the propagation of partially coherent light pulses," Opt. Commun. **230**, 1–5 (2004).

[13] E. Wolf, *Introduction to the Theory of Coherence and Polarization,* (Cambridge University Press, 2007).

[14] S. A. Ponomarenko, "Degree of phase-space separability of statistical pulses," Opt. Express **20**, 2548–2555 (2012).

[15] H. Lajunen, V. Torres-Company, J. Lancis, E. Silvestre, and P. Andrés, "Pulse-by-pulse method to characterize partially coherent pulse propagation in instantaneous nonlinear media," Opt. Express **18**, 14979–14991 (2011).

[16] S. Haghgoo and S. A. Ponomarenko, "Self-similar pulses in coherent linearv amplifiers," Opt. Express **19**, 9750-9758 (2011).

[17] S. Haghgoo and S. A. Ponomarenko, "Shape-invariant pulses in resonant linear absorbers," Opt. Lett. **37**, 1328-1330 (2012).

[18] L. Mandel and E. Wolf, *Optical Coherence and Quantum Optics*, (Cambridge University Press, 1995).

[19] H. Lajunen, J. Tervo, and P. Vahimaa, "Overall coherence and coherent-mode expansion of spectrally partially coherent plane-wave pulses, J. Opt. Soc. Am. A **21**, 2117–2123 (2004).

[20] P. W. Milonni and J. H. Eberly, *Lasers,* (Wiley, New York, 1985).

[21] M. Abramowitz and I. A. Stegan, *Handbook of Mathematical Functions* (Dover, New York, 1972).

# Chapter 5

# Complex Area Correlation Theorem for Statistical Pulses in Coherent Linear Absorbers

L. Mokhtarpour and S. A. Ponomarenko
Published in: Optics Letters, September 1, 2012, Vol. 37. No. 17, 3498
URL: http://www.opticsinfobase.org/ol/abstract.cfm?uri=ol-37-17-3498


## 5.1 Abstract

We derive a complex area correlation theorem describing global second-order statistical properties of pulses propagating in coherent linear absorbers. We also illustrate temporal evolution of a generic partially coherent pulse in a coherent linear absorber by discussing the behavior of its temporal intensity profile and degree of coherence.

## 5.2 Introduction

As statistical properties of ultrashort pulses impose ultimate limits on the performance and accuracy of the state-of-art fiber-optical communication systems [1], there has been acute interest in exploring the evolution of statistical pulses in a variety of dispersive media that can serve as conduits for optical communications. In this context, the dynamics of partially coherent pulses in generic, weakly dispersive linear media was explored [3, 4]. More specifically, coherence and polarization properties of such pulses were discussed on their propagation in optical fibers [5, 6], and statistical properties of certain classes of partially coherent pulses propagating in linear and nonlinear dispersive media were examined and characterized in novel ways [7, 8].

More recently, the interest has arisen to statistical pulse propagation in resonant media. In particular, it was demonstrated that any asymmetric pulse with a sharp leading edge evolves toward a universal self-similar asymptotic shape on propagation in coherent linear amplifiers near optical resonance [9]. In coherent linear absorbers, on the other hand,

self-similarity can be generated only for specific–although rather wide–classes of input coherent [10] and partially coherent [11] pulses. The research to date, however, leaves unexplored the propagation properties of generic partially coherent pulses in resonant linear absorbers and amplifiers.

In this Letter, we examine global and local statistical properties of generic ultrashort pulses propagating in linear absorbers in a resonant regime. We demonstrate the existence of a novel theorem, the area correlation theorem, which governs the universal behavior of complex area correlations of any statistical pulse on propagation in a resonant linear absorber. We explain the physical significance of the theorem and relate it to the (generalized) area theorem known to determine the dynamics of coherent pulse area in such media. We also discuss the temporal intensity profile and degree of coherence evolution for Gaussian Schell-model pulses in coherent linear absorbers.

To begin, we examine small-area pulse propagation in a coherent absorber under near resonance condition: the pulse carrier frequency $\omega_c$ is tuned closely to a resonant transition frequency $\omega_0$ of the medium atoms. In the slowly-varying envelope approximation (SVEA), the pulse field $\mathscr{E}(z,t)$ and atomic dipole moment $\sigma(z,t)$ can be shown to obey the classical Maxwell-Lorentz equations (MLE) [9, 12]

$$\partial_\zeta \Omega = i\kappa \langle \sigma \rangle_\Delta, \tag{5.1}$$

and

$$\partial_\tau \sigma = -(\gamma_\perp + i\Delta)\sigma + i\Omega, \tag{5.2}$$

which are written in the transformed variables: $\zeta = z$ and $\tau = t - z/c$. Here $\Delta = \omega_c - \omega_0$ is a detuning of the pulse carrier frequency from resonance and the angle brackets with the subscript "$\Delta$" denote averaging over the frequency detuning distribution $g(\Delta)$, defined as

$$\langle \sigma \rangle_\Delta = \int_{-\infty}^{\infty} d\Delta\, \sigma(\tau, \zeta; \Delta) g(\Delta). \tag{5.3}$$

In Eqs. (5.1) and (5.2) we introduced the field envelope in frequency units, $\Omega = -e\mathscr{E}/2m\omega x_0$, where $x_0$ is an amplitude of the electron displacement from equilibrium, the inverse dipole relaxation rate $\gamma_\perp = 1/T_\perp$, where $T_\perp$ is a characteristic dipole moment relaxation time, and a coupling constant, $\kappa = Ne^2/4\varepsilon_0 mc$. The coupled MLE can be solved using a Fourier transform technique, yielding the field envelope at any propagation distance in the form

$$\mathscr{E}(\tau, \zeta) = \int_{-\infty}^{\infty} d\omega\, \tilde{\mathscr{E}}_0(\omega) \exp[-i\omega\tau - \kappa \mathscr{R}(\omega)\zeta]. \tag{5.4}$$

Here the spectral response function of the medium $\mathscr{R}$ and the spectral amplitude of the incident pulse are defined as

$$\mathscr{R}(\omega) = \left\langle \frac{1}{\gamma_\perp + i(\Delta - \omega)} \right\rangle_\Delta . \tag{5.5}$$

and

$$\tilde{\mathscr{E}}_0(\omega) = \int_{-\infty}^{\infty} \frac{dt}{2\pi} \mathscr{E}(t,0) e^{i\omega t}, \tag{5.6}$$

respectively.

Let us now consider an ensemble of statistical realizations of pulses $\{\mathscr{E}(\tau,\zeta)\}$. The second-order statistical properties of the ensemble are, in general, characterized by the two-time, two-distance correlation function, defined as

$$\Gamma(\tau_1,\zeta_1;\tau_2,\zeta_2) = \langle \mathscr{E}^*(\tau_1,\zeta_1)\mathscr{E}(\tau_2,\zeta_2)\rangle. \tag{5.7}$$

Here the angle brackets without subscripts denote pulse ensemble averaging. It follows at once from Eqs. (5.4) and (5.7) that

$$\begin{aligned}\Gamma(\tau_1,\zeta_1;\tau_2,\zeta_2) &= \int_{-\infty}^{\infty} d\omega_1 \int_{-\infty}^{\infty} d\omega_2 W_0(\omega_1,\omega_2) \\ &\times e^{i(\omega_1\tau_1 - \omega_2\tau_2)} \exp\{-\kappa[\mathscr{R}^*(\omega_1)\zeta_1 + \mathscr{R}(\omega_2)\zeta_2]\},\end{aligned} \tag{5.8}$$

where $W_0(\omega_1,\omega_2)$ is the cross-spectral density at the source given by

$$W_0(\omega_1,\omega_2) = \langle \tilde{\mathscr{E}}_0^*(\omega_1)\tilde{\mathscr{E}}_0(\omega_2)\rangle. \tag{5.9}$$

Next, we introduce a complex area of a statistical pulse by the expression

$$\mathscr{A}(\zeta) \equiv \int_{-\infty}^{\infty} d\tau \mathscr{E}(\tau,\zeta). \tag{5.10}$$

Eq. (5.10) is a generalization of the conventional real area under unchirped pulse–see c. f., [12]–to the case when a statistical pulse is chirped at the source; of course, the complex area does lose a direct geometrical interpretation as the area under the pulse temporal profile. Moreover, $\mathscr{A}$ pertains to a member of the statistical ensemble. Hence, it is a random function of the propagation distance. One can then introduce the area correlation function viz.,

$$\begin{aligned}\mathscr{C}_{\mathscr{A}}(\zeta_1,\zeta_2) &\equiv \langle \mathscr{A}^*(\zeta_1)\mathscr{A}(\zeta_2)\rangle \\ &= \int_{-\infty}^{\infty} d\tau_1 \int_{-\infty}^{\infty} d\tau_2 \Gamma(\tau_1,\zeta_1;\tau_2,\zeta_2).\end{aligned} \tag{5.11}$$

Further, on taking the double time integration on both sides of Eq. (5.8), employing the area correlation definition (5.11) and the integral representation of the delta function,

$$\delta(\omega) = \int_{-\infty}^{\infty} \frac{dt}{2\pi} e^{i\omega t}, \tag{5.12}$$

we arrive at

$$\mathscr{C}_{\mathscr{A}}(\zeta_1, \zeta_2) = \mathscr{C}_{\mathscr{A}0} \exp\{-\kappa[\mathscr{R}^*(0)\zeta_1 + \mathscr{R}(0)\zeta_2]\}, \tag{5.13}$$

where $\mathscr{C}_{\mathscr{A}0} = \mathscr{C}_{\mathscr{A}}(0,0)$. Eq. (5.13) can be transformed, with the aid of Eq. (5.5), to the final form of the correlation area theorem as

$$\mathscr{C}_{\mathscr{A}}(\zeta_1, \zeta_2) = \mathscr{C}_{\mathscr{A}0} e^{-\alpha(\zeta_1+\zeta_2)} e^{i\beta(\zeta_2-\zeta_1)}, \tag{5.14}$$

where we introduced a small-signal absorption coefficient $\alpha$ and the phase accumulation factor $\beta$ by the expressions

$$\alpha = \left\langle \frac{2\kappa\gamma_\perp}{\gamma_\perp^2 + \Delta^2} \right\rangle_\Delta, \tag{5.15}$$

and

$$\beta = \left\langle \frac{2\kappa\Delta}{\gamma_\perp^2 + \Delta^2} \right\rangle_\Delta. \tag{5.16}$$

Equation (5.14) is the key result of this Letter. It tells us that due to absorption, the area correlations of a statistical pulse exponentially decay on propagation into the coherent linear absorber, regardless of a specific temporal profile of the pulse at the source. Notice that in the same transverse plane, $\zeta_1 = \zeta_2$, the area correlation function does not pick up any additional phase on propagation–it simply exponentially decays with the propagation distance $\zeta$. We also notice that in the fully coherent limit, the area correlation function factorizes and the derived area correlation theorem reduces to

$$\mathscr{A}(\zeta) = \mathscr{A}_0 e^{-\alpha\zeta} e^{i\beta\zeta}, \tag{5.17}$$

which is a generalized area theorem for coherent pulses. The generalization entails the extension of the area concept of Ref. [12] to chirped pulses, thereby allowing for a complex area. The presence of the phase factor on the r. h. s. of Eq. (5.17) is a consequence of pulse chirping by the medium; in the form (5.14)–or (5.17) for fully coherent pulses–the classical area theorem applies to chirped small-area pulses as well.

To study local properties of statistical pulses on their propagation in resonant linear absorbers, we must specialize to a particular pulse model. In this work, we consider a

Gaussian Schell-model (GSM) statistical pulse as a rather representative case. The cross-spectral density of a GSM pulse can be expressed as [13]

$$W_0(\omega_1,\omega_2)\propto\exp\left[-\frac{(\omega_1-\omega_2)^2t_{\rm p}^2}{2}\right]\exp\left[-\frac{(\omega_1+\omega_2)^2t_{\rm eff}^2}{8}\right], \tag{5.18}$$

where

$$\frac{1}{t_{\rm eff}^2}=\frac{1}{t_{\rm c}^2}+\frac{1}{4t_{\rm p}^2}, \tag{5.19}$$

$t_{\rm p}$ and $t_{\rm c}$ being the characteristic pulse width and coherence time, respectively.

To proceed further we need to specify $g(\Delta)$. Any choice will depend on the physical nature of inhomogeneous broadening. To examine a generic case, we choose $g(\Delta)$ to be a (normalized) Lorenzian function,

$$g(\Delta)=\frac{1}{\pi}\frac{1/T_\Delta}{\Delta^2+1/T_\Delta^2}, \tag{5.20}$$

where $T_\Delta$ is a characteristic damping time associated with inhomogeneous broadening. This choice ensures that the spectral response function can be determined in the explicit form as [12]

$$\mathscr{R}_{\rm L}(\omega)=\frac{1}{1/T_{\rm eff}+i(\Delta-\omega)}. \tag{5.21}$$

Here $T_{\rm eff}^{-1}=T_\perp^{-1}+T_\Delta^{-1}$ is the effective damping time.

We numerically explore the behavior of the GSM pulse intensity profile, $I(\tau,\zeta)=\Gamma(\tau,\zeta;\tau,\zeta)$, on propagation in the absorber. To this end, we transform to dimensionless variables, $T=t/T_{\rm eff}$, $Z=\alpha\zeta$, and measure the intensity in arbitrary units (a.u). The pulse coherence state will affect its intensity evolution in the resonant absorber whenever $t_{\rm c}\sim T_{\rm eff}$. It follows from Eqs. (5.18) and (5.19) that the inverse of $min(t_{\rm c},t_{\rm p})$ plays the role of the effective input pulse bandwidth. In this connection, we can distinguish two characteristic cases: very "short", $min(t_{\rm c},t_{\rm p})\ll T_{\rm eff}$, and very "long", $min(t_{\rm c},t_{\rm p})\gg T_{\rm eff}$, pulses.

In Fig. 5.1 we present the evolution of the GSM pulse intensity profile as a function of $Z$ for (a) very long, $t_{\rm c}=T_{\rm eff}=5t_{\rm p}$, and (b) very short, $t_{\rm c}=T_{\rm eff}=t_{\rm p}/5$, pulses. It is seen in the figure that the long pulse is highly absorbed and reshaped by the absorbing medium. On the other hand, the short pulse, which has a broad spectrum as compared with the spectral amplitude $\mathscr{R}_{\rm L}(\omega)$ of the absorbing medium, its peak intensity slowly decays on propagation.

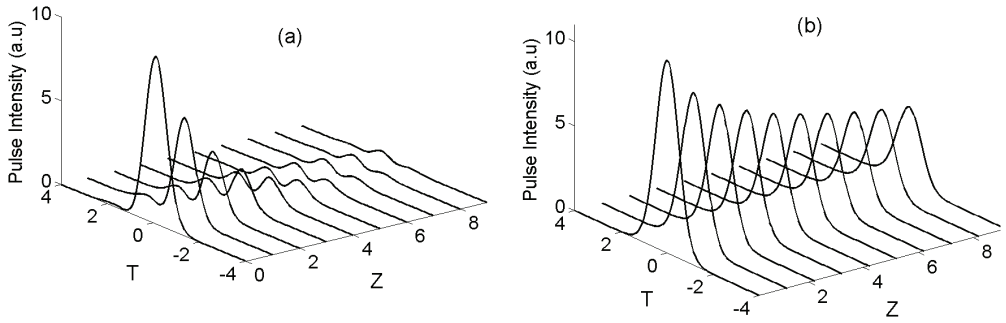


Figure 5.1: GSM pulse intensity profile. The pulse parameters are (a) $t_c = T_{eff} = 5t_p$ and (b) $t_c = T_{eff} = t_p/5$.

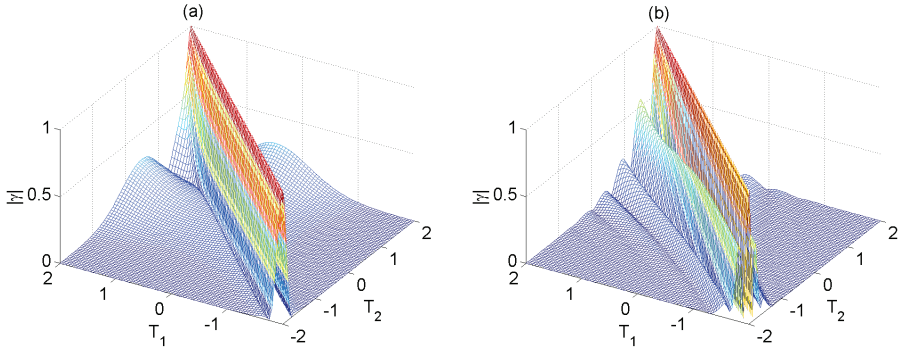


Figure 5.2: Magnitude of the temporal degree of coherence of a relatively long GSM pulse at (a) $Z = 1$ and (b) $Z = 50$. The pulse parameters are $t_c = T_{eff} = t_p/5$.

Next, we exhibit in Figs. 5.2 and 5.3 the evolution of the magnitude of the temporal degree of coherence, defined as

$$\gamma(\tau_1, \zeta; \tau_2, \zeta) \equiv \frac{\Gamma(\tau_1, \zeta; \tau_2, \zeta)}{\sqrt{I(\tau_1, \zeta) I(\tau_2, \zeta)}}, \tag{5.22}$$

for relatively long and rather short pulses, respectively. It is seen in the figures that while the degree of coherence of a short pulse is rather weakly affected by the absorbing medium, the coherence state of the long one becomes progressively more inhomogeneous across the pulse profile such that $|\gamma|$ oscillates rapidly between zero and unity. This profound coherence state evolution testifies to a strong coherent coupling of long statistical pulses with the resonant absorber atoms.

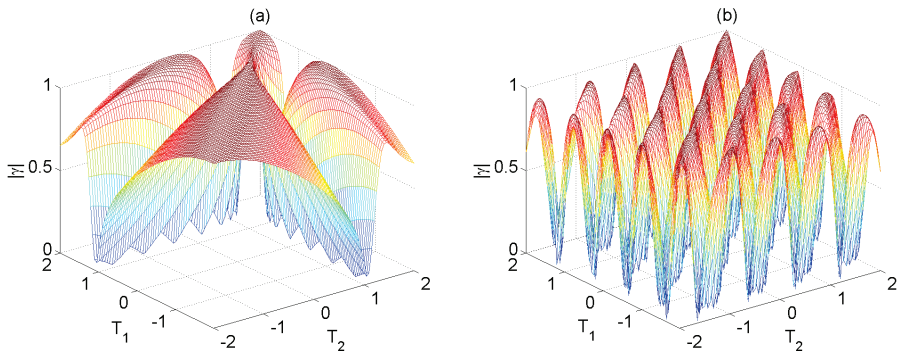


Figure 5.3: Magnitude of the temporal degree of coherence of a rather short GSM pulse at (a) $Z = 1$ and (b) $Z = 50$. The pulse parameters are $t_c = T_{eff} = 5t_p$.

## 5.3 Conclusion

In summary, we studied global and local correlation properties of statistical pulses propagating in linear absorbing media in the near resonance regime. We have derived a correlation area theorem describing the universal behavior of global correlation properties of the pulse propagating in the medium. We also examined the evolution of intensity profiles and temporal degrees of coherence of Gaussian Schell-model pulses in coherent linear absorbers. We have shown that the intensity profiles and degrees of coherence of long GSM pulses are strongly affected by the medium due to their efficient coupling to the absorbing atoms.

## Bibliography


[1] G. P. Agrawal, *Fiber-Optic Communication Systems,* 3rd ed., (Wiley, Newy York, NY 2002).

[2] M. D. Crisp, "Propagation of Small-Area Pulses of Coherent Light through a Resonant Medium," Phys. Rev. A. **6**, 1604–1611 (1972).

[3] Q. Lin, L. Wang, and S. Zhu, "Partially coherent light pulse and its propagation," Opt. Commun. **219**, 65–70 (2003).

[4] M. Brunel and S. Coëtlemec, " Fractional-order Fourier formulation of the propagation of partially coherent light pulses," Opt. Commun. **230**, 1–5 (2004).

[5] W. Huang, S. A. Ponomarenko, M. Cada, and G. P. Agrawal, "Polarization changes of partially coherent pulses propagating in optical fibers," J. Opt. Soc. Am. A **24**, 3063–3068 (2007).

[6] C. L. Ding, L. Z. Pan, and B. D. Lu, "Changes in the spectral degree of polarization of stochastic spatially and spectrally partially coherent electromagnetic pulses in dispersive media, " J. Opt. Soc. Am. B **26**, 1728-1735 (2009).

[7] S. A. Ponomarenko, "Degree of phase-space separability of statistical pulses," Opt. Express **20**, 2548–2555 (2012).

[8] H. Lajunen, V. Torres-Company, J. Lancis, E. Silvestre, and P. Andrés, "Pulse-by-pulse method to characterize partially coherent pulse propagation in instanteneous nonlonear media," Opt. Express **18**, 14979–14991 (2011).

[9] S. Haghgoo and S. A. Ponomarenko, "Self-similar pulses in coherent linear amplifiers," Opt. Express **19**, 9750-9758 (2011).

[10] S. Haghgoo and S. A. Ponomarenko, "Shape-invariant pulses in resonant linear absorbers," Opt. Lett. **37**, 1328–1330 (2012).

[11] L. Mokhtarpour, G. H. Akter, and S. A. Ponomarenko, "Partially coherent self-similar pulses in resonant linear absorbers," Opt. Express **20**, 17816–17822 (2012).

[12] L. Allen and J. H. Eberly, *Optical resonance and two-level atoms,* (Dover Publications Inc., New York, 1975).

[13] P. Paakkonen, J. Turunen, P. Vahimaa, A. T. Friberg, and F. Wyrowski, "Partially coherent Gaussan pulses," Opt. Commun., **204**, 53-58 (2002).

# Chapter 6

# Ultrashort Pulse Coherence Properties in Coherent Linear Amplifiers

L. Mokhtarpour and S. A. Ponomarenko

Published in: Journal of Optical Society of America A, April 1, 2013, Vol. 30, Issue 4, 627
URL:http://www.opticsinfobase.org/josaa/abstract.cfm.uri=josaa-30-4-627



## 6.1 Abstract

We examine coherence properties of small-area, intrinsically stationary statistical pulses propagating in amplifying media in the vicinity of an optical resonance. Any such medium acts as a coherent linear amplifier, amplifying and reshaping the pulse. We show that an initially nearly incoherent Gaussian Schell-model pulse becomes almost fully coherent and its state of coherence becomes nearly uniform across the temporal profile as the pulse propagates into the amplifying medium.

## 6.2 Introduction

The interest in statistical properties of ultrashort pulses stems, in part, from the fundamental limitations noise imposes on the performance and accuracy of the state-of-art fiber-optical communication systems [1]. To date, there has been extensive research on modeling statistical properties of intrinsically stationary [2, 3] and cyclostationary [4, 5] random pulses and pulse trains as well as on such fundamental issues as defining and measuring statistical pulse spectra [6, 7] and cross-spectral correlations [7]. Space-time correlation dynamics of statistical pulses was also addressed, both theoretically [8, 9] and experimentally [10], and several theories dealing with various representations of statistical pulses were advanced [11–13]. Further, statistical properties of pulses on their propagation in optical fibers [14, 15] and generic linear [16–18] and nonlinear [19] dispersive media far from any optical resonances were examined.

At the same time, near-resonant propagation of statistical pulses in linear media has also

been explored [20–23]. In particular, shape-invariant fully coherent pulses propagating in coherent linear amplifiers and absorbers in the resonant regime were discovered [20, 21] and the influence of statistical properties on self-similar pulse evolution was examined in resonant absorber media [22]. Moreover, global correlation properties of generic partially coherent pulses in resonant linear absorbers were examined and the general area-correlation theorem was derived [23]. To our knowledge, however, coherence properties of ultrashort statistical pulses propagating in resonant amplifying media have not yet been studied.

In this work, we explore coherence properties of small-area, intrinsically stationary statistical pulses on their propagation in coherent amplifying media. First, we show that initially symmetric pulse intensity profiles become asymmetric on propagation in the media. In particular, coherence properties of Gaussian-Schell model (GSM) pulses–which represent a rather generic model of intrinsically stationary pulses, generated, for instance, by temporal modulation of a statistically stationary source with a Gaussian spectrum [3]–become nearly uniform across the temporal profile of the pulse over sufficiently long propagation distances in the amplifier. This contrasts sharply with rapid variations of temporal coherence properties across the pulse profile for statistical pulses propagating in resonant linear absorbers [23]. We also note that coherence properties of GSM pulses remain uniform in conservative dispersive media, e.g. optical fibers [14]. Second, we demonstrate that even initially rather incoherent pulses become progressively more coherent on their propagation in amplifying media. Thus, not only do the media amplify and reshape the pulse, but they reduce the noise associated with source fluctuations. This circumstance can have important implications for short-range optical communications with ultrashort pulses.

### 6.3 Statistical Pulse Propagation in Coherent Linear Amplifiers

As the first step, we model the pulse propagation in a coherent resonant amplifier media. We describe a resonant medium using the two-level atom model. The pulse evolution in the medium can be described in the slowly-varying envelope approximation by the reduced wave equation [20, 24]

$$\partial_\zeta \Omega = i\kappa \langle \sigma \rangle_\Delta, \tag{6.1}$$

In Eq. (6.1), $\kappa = \omega N |d_{eg}|^2 / c\varepsilon_0 \hbar$ is a coupling constant, with $N$ being the atom density and $d_{eg}$ being the dipole matrix element between the ground and excited states of an atom; $\Omega = 2d_{eg}\mathscr{E}/\hbar$ is the complex pulse envelope amplitude in frequency units corresponding to

the field envelope $\mathscr{E}$. In Eq. (6.1), $\langle \ldots \rangle_\Delta$ implies averaging over a distribution of detunings $\Delta$ of the carrier wave frequency $\omega_c$ from the atomic resonance frequency $\omega_0$; as in our previous studies [23], we assume a Lorentzian detuning distribution with a characteristic decay time $T_\Delta$ associated with inhomogeneous broadening. The complex dipole envelope function $\sigma$ and one-atom inversion $w$ obey the Bloch equations in the form [24]

$$\partial_\tau \sigma = -(\gamma_\perp + i\Delta)\sigma - i\Omega w, \tag{6.2}$$

and

$$\partial_\tau w = -\gamma_\perp (w - w_{eq}) - \tfrac{i}{2}(\Omega^* \sigma - \Omega \sigma^*). \tag{6.3}$$

Here $\gamma_\perp = 1/T_\perp$ is a dipole relaxation rate, and $T_\perp$ is a dipole relaxation time. In Eqs. (6.1)-(6.3) we introduced the shifted coordinates: $\zeta = z$ and $\tau = t - z/c$.

For small-area input pulses, one can neglect any amplifier gain depletion, implying that $w$ can be well approximated by its equilibrium value $w_{eq}$ (linear amplifier) i.e.,

$$w \approx w_{eq} = 1. \tag{6.4}$$

The linearized dipole moment evolution equation then reads

$$\partial_\zeta \sigma = -(\gamma_\perp + i\Delta)\sigma - i\Omega. \tag{6.5}$$

Eqs. (6.1) and (6.5) can be solved using a Fourier transform technique resulting in

$$\mathscr{E}(\tau, \zeta) = \int_{-\infty}^{\infty} d\omega \tilde{\mathscr{E}}_0(\omega) \exp\left[-i\omega\tau + \frac{\alpha\zeta}{2(1 - i\omega T_{\text{eff}})}\right]. \tag{6.6}$$

Here $T_{\text{eff}}^{-1} = T_\perp^{-1} + T_\Delta^{-1}$ is an effective relaxation rate which fully characterizes damping in the Lorentzian detuning distribution case. Also, $\alpha = 2\kappa/\gamma_\perp$ is a small-signal amplification coefficient. The incident pulse spectrum is given by

$$\tilde{\mathscr{E}}_0(\omega) = \int_{-\infty}^{\infty} \frac{dt}{2\pi} \mathscr{E}(t, 0) e^{i\omega t}. \tag{6.7}$$

The second-order coherence properties of small-area statistical pulses in the amplifying media are specified by the two-time correlation function $\Gamma(\tau_1, \tau_2, \zeta)$, defined as

$$\Gamma(\tau_1, \tau_2, \zeta) = \langle \mathscr{E}^*(\tau_1, \zeta) \mathscr{E}(\tau_2, \zeta) \rangle, \tag{6.8}$$

where the angular brackets denote ensemble averaging. It follows from Eqs. (6.6), (6.7) and (6.8) that

$$\Gamma(\tau_1,\tau_2,\zeta)=\int_{-\infty}^{\infty}d\omega_1\int_{-\infty}^{\infty}d\omega_2\mathscr{W}_0(\omega_1,\omega_2)e^{i(\omega_1\tau_1-\omega_2\tau_2)}\times\exp\left\{\alpha\zeta\left[\frac{1}{2(1-i\omega_2T_{\rm eff})}+\frac{1}{2(1+i\omega_1T_{\rm eff})}\right]\right\}. \tag{6.9}$$

Here $\mathscr{W}_0(\omega_1,\omega_2)=\langle\tilde{\mathscr{E}}_0^*(\omega_1)\tilde{\mathscr{E}}_0(\omega_2)\rangle$ is the cross-spectral density of the pulse fields at the source; it is related to the corresponding two-time correlation function viz.,

$$\mathscr{W}_0(\omega_1,\omega_2)=\int_{-\infty}^{\infty}\int_{-\infty}^{\infty}\frac{dt_1dt_2}{(2\pi)^2}\,e^{i(\omega_2t_2-\omega_1t_1)}\Gamma_0(t_1,t_2). \tag{6.10}$$

## 6.4 Intensity and Complex Degree of Coherence Evolution for Intrinsically Statistically Stationary Pulses in Coherent Linear Amplifiers

Next, we explore the influence of the input pulse coherence on its subsequent propagation dynamics in the amplifier. To this end, we consider incident GSM pulses [2] as a rather generic statistical model of the source. The choice of the GSM model has two advantages. First, GSM pulses can be easily generated in a laboratory by "chopping" with a Gaussian temporal modulation function an output of a statistically stationary source with a Gaussian spectrum [3]. Second, being intimately related to statistically stationary sources, the generated pulses are intrinsically stationary with a Gaussian correlation function which decays very fast with the time difference. Thus, the conditions for the ergodicity hypothesis are met [25] and any time averages arising in actual experiments converge well to ensemble averages employed throughout this work.

The two-time correlation function of the GSM pulse can be written as

$$\Gamma_0(t_1,t_2)\propto\exp\left(-\frac{t_1^2+t_2^2}{2{t_{\rm p}}^2}\right)\exp\left[-\frac{(t_1-t_2)^2}{2{t_{\rm c}}^2}\right], \tag{6.11}$$

where $t_{\rm p}$ and $t_{\rm c}$ are the characteristic pulse width and coherence time, respectively. As we are interested in the coherent coupling between the near resonant pulse and medium atoms, we focus on the short pulse limit such that $t_{\rm p}\sim T_{\rm eff}$. In particular, we let $t_p=T_{\rm eff}/2$ throughout our numerical simulations, and introduce dimensionless variables, $Z=\alpha\zeta$ and $T=t/T_{\rm eff}$.

In Fig. 6.1, we display the behavior of the GSM pulse intensity profile, $I(T,Z) = \Gamma(T,T,Z)$, on propagation in the amplifier for two cases: (a) $t_c = 5t_p$, corresponding to an almost fully coherent input pulse, and (b) $t_c = t_p/5$, corresponding to a nearly incoherent input pulse. It is seen in the figure that as both pulses are amplified, their shapes become progressively more asymmetric, developing a long tail in the trailing edge. However, the amplifying medium affects the pulse with the shorter coherence time less than it does the more coherent pulse. This is because the less coherent pulse has a broader spectrum, containing a significant portion of its initial energy in the tails, outside the medium gain spectrum. Therefore, it is amplified less efficiently by the medium than is the more coherent pulse.

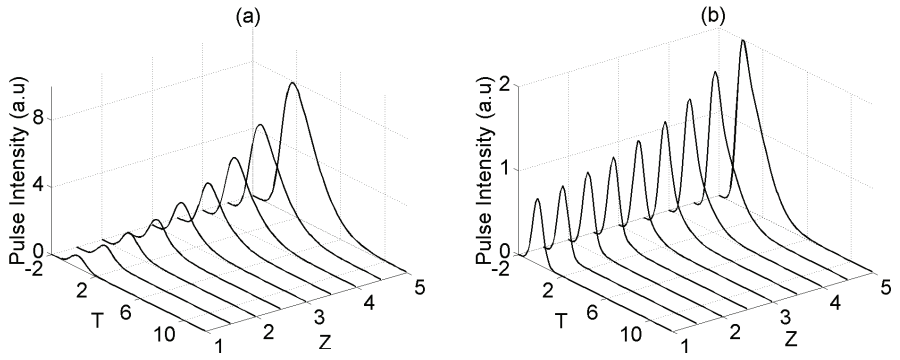


Figure 6.1: Pulse intensity profile in arbitrary units (a.u) as a function of the dimensionless propagation distance $Z$ for two partially coherent pulses: (a) $t_c = 5t_p$ and (b) $t_c = t_p/5$.

To drive this point home, we exhibit in Fig. 6.2 the energy gain factor, $G(Z) = W(Z)/W_0$, where the pulse energy $W$ is

$$W(Z) \propto \int_{-\infty}^{\infty} dT\, \Gamma(T,T,Z), \tag{6.12}$$

for both pulses as the function of the propagation distance. It is clearly seen in the figure that the more coherent pulse is able to extract much more energy from the amplifying medium over the same propagation distance than is the less coherent pulse.

Next, we examine the behavior of the complex degree of coherence $\gamma$, defined (in dimensionless variables) as [25, 26]

$$\gamma(T_1,T_2,Z) \equiv \frac{\Gamma(T_1,T_2,Z)}{\sqrt{I(T_1,Z)I(T_2,Z)}}. \tag{6.13}$$

In Fig. 6.3 we display the complex degree of coherence of the pulse with $t_c = 5t_p$ for two propagation distances, $Z = 1$ and $Z = 5$. We can see from the figure that not only does

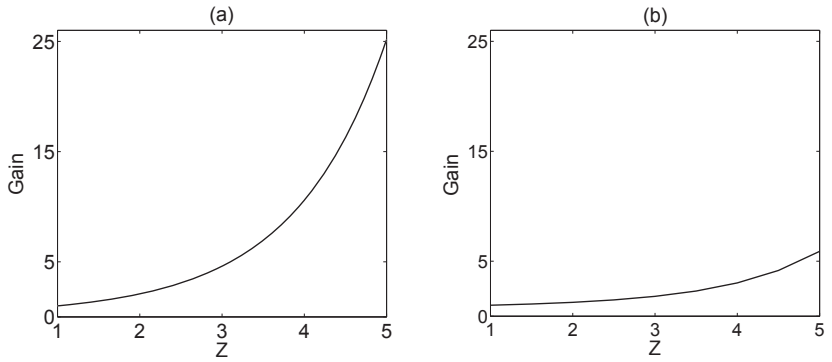


Figure 6.2: Energy gain factor as a function of the dimensionless propagation distance $Z$ for two partially coherent pulses: (a) $t_c = 5t_p$ and (b) $t_c = t_p/5$.

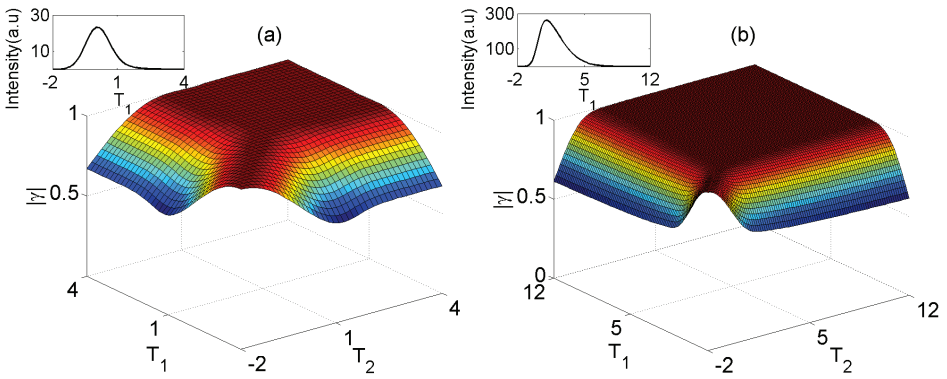


Figure 6.3: Magnitude of the complex degree of coherence of a short GSM pulse with $t_c = 5t_p$ for (a) $Z = 1$ and (b) $Z = 5$. Insets: the corresponding pulse intensity profiles.

the pulse become more coherent on propagation, but its coherence properties become more uniform as well. In the insets to Figs. 6.3 (a) and 6.3 (b), we display the corresponding pulse intensity at the same propagation distance. It is seen from Figs. 6.3 (a) and 6.3 (b) that the chosen ranges for $T_1$ and $T_2$ in both cases correspond to the time intervals within which most of the pulse energy resides at a given propagation distance. Thus, our $\gamma$ plots are representative of the whole pulse.

It is interesting to compare the behavior of the fairly coherent pulse we have just studied with that of a relatively incoherent pulse with $t_c = t_p/5$. The evolution of the complex degree of coherence for the latter is shown in Fig. 6.4. Similarly to Fig. 6.3, we display the pulse intensity in the corresponding inset which sets the $T_1$ and $T_2$ ranges. We can infer by comparing Figs. 6.3 and 6.4 that although qualitatively the behavior of $\gamma$ is the same

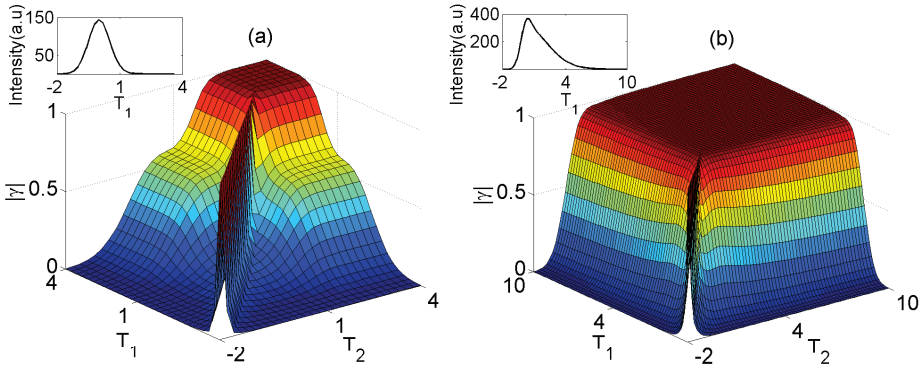


Figure 6.4: Magnitude of the temporal degree of coherence of a short GSM pulse with $t_c = t_p/5$ for (a) $Z = 1$ and (b) $Z = 5$. Insets: the corresponding pulse intensity profiles.

regardless of the initial state of pulse coherence, the coherence state of initially nearly incoherent pulses becomes nearly uniform across their temporal profile–apart from the pulse tails–and the magnitude of $\gamma$ tends to unity with the propagation distance.

## 6.5 Discussion

Finally, we mention that the small-area approximation, which is necessary for the system to be in the linear amplification regime, imposes severe constraints on the input pulse parameters and/or amplifier lengths. Hereafter we assume, for simplicity, the input pulse to be fully coherent which is fine for the order-of-magnitude estimates. First of all, the pulse area $\mathscr{A}$ at the exit of the amplifier must be much smaller than $\pi$ for nonlinear saturation effects to be negligible over the entire amplifier length [24]. Let us take $\mathscr{A} \sim 0.1$, say, implying that for the amplifier of length $L = 5L_B$, measured in Beer's absorption lengths, $L_B = \alpha^{-1}$, the input pulse area must be tiny, $\mathscr{A}_0 \sim 5 \times 10^{-4}$ where we used the area theorem for coherent amplifiers [27].

However, the very small magnitude of the input pulse area begs the question as to whether the incident pulse contains enough photons to be treated classically. To address this question, we estimate the input Gaussian pulse energy density,

$$w_0 = \tfrac{1}{2}\varepsilon_0 c \int_{-\infty}^{\infty} dt |\mathscr{E}(t,0)|^2 = \tfrac{1}{2}\varepsilon_0 c \sqrt{\pi} t_p \mathscr{E}_0^2, \tag{6.14}$$

where $\mathscr{E}_0$ is the peak amplitude of the pulse. The input area can be estimated as

$$\mathscr{A}_0 = \frac{2d_{eg}}{\hbar} \int_{-\infty}^{\infty} dt \mathscr{E}(t,0) = \frac{2d_{eg}\sqrt{2\pi} t_p \mathscr{E}_0}{\hbar}. \tag{6.15}$$

Eliminating the peak pulse amplitude from Eqs. (6.14) and (6.15), we arrive at the input energy density

$$w_0 = \frac{\varepsilon_0 c\hbar^2 \mathscr{A}_0^2}{16\sqrt{\pi} d_{\rm eg} t_{\rm p}}. \tag{6.16}$$

Assuming a picosecond laser pulse of 1 cm$^2$ cross-section and taking $d_{\rm eg} \simeq 10^{-29}$ Cm, which is appropriate for atomic vapors [24], we substitute these values into Eq. (6.16) to estimate the input pulse energy as $W_0 \sim 5 \times 10^{-13}$ J. It follows that the number of photons carried by the pulse can be estimated as $\mathscr{N}_0 = W_0/\hbar\omega_c \simeq 5 \times 10^6 \gg 1$, which is sufficiently large to treat the pulse as a classical electromagnetic field. However, this criterion can be easily violated as the amplifier length increases.

## 6.6 Conclusion

In summary, we studied partially coherent pulse propagation in resonant linear amplifiers, focusing on the change in pulse coherence properties on propagation. We have shown that regardless of the initial state of pulse coherence, it becomes progressively more coherent on propagation in the amplifying medium. Moreover, the state of coherence becomes progressively more uniform across the temporal profile as the pulse propagates into the medium. We also discussed the constraints imposed by the linear amplification regime on the input parameters of the pulse and the amplifier length.

## Bibliography


[1] G. P. Agrawal, *Fiber-Optic Communication Systems,* 3rd ed., (Wiley, New York, NY 2002).

[2] P. Paakkonen, J. Turunen, P. Vahimaa, A. T. Friberg, and F. Wyrowski, "Partially coherent Gaussian pulses," Opt. Commun., **204**, 53–58 (2002).

[3] H. Lajunen, J. Tervo, J. Turunen, P. Vahimaa, and F. Wyrowski, "Spectral coherence properties of temporarily modulated stationary light sources," Opt. Express **11**, 1894–1899 (2003).

[4] V. Torres-Company, H. Lajunen, and A. T. Friberg, "Cohrence theory of noise in ultrashort pulse trains," J. Opt. Soc. Am. B **24**, 1441–1450 (2007).

[5] C. R. Fernandez-Pousa, "Intensity spectra after first-order dispersion of composite models of scalar, cyclostationary light," J. Opt. Soc. Am. A **26** 993–1007 (2009).

[6] S. A. Ponomarenko, G. P. Agrawal and E. Wolf, "Energy spectrum of a nonstationary ensemble of pulses," Opt. Lett. **29**, 394–396 (2004).

[7] B. Davis, "Measurable Coherence Theory for Statistically Periodic Fields," Phys. Rev. A. **76**, 043843 (2007).

[8] R. W. Schoonover, B. J. Davis, and P. S. Carney, "The generalized Wolf shift for cyclostationary fields," Opt. Express , **17**, 4705–4711 (2009).

[9] R. W. Schoonover, B. J. Davis, R. A. Bartels, and P. S. Carney, "Propagation of spatial coherence in fast pulses," J. Opt. Soc. Am. A **26**, 1945–1953 (2009).

[10] R. W. Schoonover, R. Lavarello, M. L. Oezle, and P. S. Carney, "Observation of generalised Wolf shifts in short pulse spectroscopy," Applied Physics Letters, **98**, 251107–25110 (2011).

[11] P. Vahimaa and J. Turunen, "Independent-elementary-pulse representation for non-stationary fields," Opt. Express **14**, 5007–5012 (2006).

[12] A. T. Friberg, H. Lajunen, and V. Torres-Company, "Spectral elementary-coherence-function representation for partially coherent light pulses," Opt. Express **15**, 5160-5165 (2007).

[13] S. A. Ponomarenko, "Complex Gaussian representation of statistical pulses," Opt. Express **19**, 17086-17091 (2011).

[14] W. Huang, S. A. Ponomarenko, M. Cada, and G. P. Agrawal, "Polarization changes of partially coherent pulses propagating in optical fibers," J. Opt. Soc. Am. A **24**, 3063–3068 (2007).

[15] C. L. Ding, L. Z. Pan, and B. D. Lu, "Changes in the spectral degree of polarization of stochastic spatially and spectrally partially coherent electromagnetic pulses in dispersive media," J. Opt. Soc. Am. B **26**, 1728–1735 (2009).

[16] Q. Lin, L. Wang, and S. Zhu, "Partially coherent light pulse and its propagation," Opt. Commun. **219**, 65–70 (2003).

[17] M. Brunel and S. Coëtlemec, "Fractional-order Fourier formulation of the propagation of partially coherent light pulses," Opt. Commun. **230**, 1–5 (2004).

[18] S. A. Ponomarenko, "Degree of phase-space separability of statistical pulses," opex **20**, 2548–2555 (2012).

[19] H. Lajunen, V. Torres-Company, J. Lancis, E. Silvestre, and P. Andrés, "Pulse-by-pulse method to characterize partially coherent pulse propagation in instanteneous nonlinear media," Opt. Express **18**, 14979–14991 (2011).

[20] S. Haghgoo and S. A. Ponomarenko, "Self-similar pulses in coherent linear amplifiers," Opt. Express **19**, 9750–9758 (2011).

[21] S. Haghgoo and S. A. Ponomarenko, "Shape-invariant pulses in resonant linear absorbers," Opt. Lett. **37**, 1328–1330 (2012).

[22] L. Mokhtarpour, G. H. Akter, and S. A. Ponomarenko, "Partially coherent self-similar pulses in resonant linear absorbers," Opt. Express **20**, 17816–17822 (2012).

[23] L. Mokhtarpour and S. A. Ponomarenko, "Complex area correlation theorem for statistical pulses in coherent linear absorbers," Opt. Lett. **37**, 3498–3500 (2012).

[24] L. Allen and J. H. Eberly, *Optical resonance and two-level atoms,* (Dover Publications Inc., New York, 1975).

[25] L. Mandel and E. Wolf , *Optical Coherence and Quantom Optics*,(Cambridge University Press, Cambridge, 1995).

[26] H. Lajunen, J. Tervo, and P. Vahimaa, "Overall coherence and coherent-mode expansion of spectrally partially coherent plane-wave pulses," J. Opt. Soc. Am. A , **21**, 2117–2123 (2004).

[27] G. L. Lamb, Jr., "Analytical Descriptions of Ultrashort Optical Pulse Propagation in Resonant Medium," Rev. Mod. Phys., **43**, 99–124 (1971).

# Chapter 7

# Fluctuating Pulse Propagation in Resonant Nonlinear Media: Self-induced Transparency Random Phase Soliton Formation

Laleh Mokhtarpour and Sergey A. Ponomarenko
Published in: Optics Express, 11 November 2015, Vol. 23. No. 23, 30270
URL: https://www.osapublishing.org/oe/abstract.cfm?uri=oe-23-23-30270


## 7.1 Abstract

We numerically investigate partially coherent short pulse propagation in nonlinear media near optical resonance. We examine how the pulse state of coherence at the source affects the evolution of the ensemble averaged intensity, mutual coherence function, and temporal degree of coherence of the pulse ensemble. We report evidence of self-induced transparency random phase soliton formation for the relatively coherent incident pulses with sufficiently large average areas. We also show that random pulses lose their coherence on propagation in resonant media and we explain this phenomenon in qualitative terms.

## 7.2 Introduction

The invention of lasers and their wide range of applications to optical communication systems has led to a growing interest in the field of nonlinear optics, which explores modifications of optical properties of the host media upon interaction with high intensity temporal and spatio-temporal pulses [1–3]. A proper description of realistic laser pulses - with inevitable fluctuations in their amplitude, phase, and width - cannot be achieved without the aid of statistical optics. Moreover, the limitations that noise in ultrashort laser pulses imposes on the performance of optical communication systems have triggered an ever growing interest in coherence properties of ultrashort pulses [4].

Following the pioneering work of Bertolotti's group [5, 6], comprehensive research has

been carried out on various aspects of partially coherent sources [7, 8] and the pulses generated by such sources [9, 10]. Further, several theoretical approaches to the description of partially coherent pulses have been proposed to date [11, 12]. The evolution of coherence and polarization state of partially coherent pulses in generic linear [13–19] and nonlinear [20–23] dispersive media far from any internal resonances has been thoroughly examined using various mathematical techniques.

At the same time, coherence properties of generic partially coherent pulses traveling in resonant linear absorbers and amplifiers have been analyzed [24, 25] and their coherence function modifications upon propagation investigated. Furthermore, the crucial impact of the initial coherence level of random pulses on their self-similar propagation in resonant linear absorbers has been established [26]. To our knowledge, however, no study of partially coherent pulse propagation in resonant nonlinear media has yet been attempted. The subject naturally arises in the context of short intense pulse interaction with atomic vapours [27], impurity doped solids [28], or semiconductor quantum dot media [29] near resonance whenever pulse fluctuations cannot be neglected.

In this work, we fill in the gap by numerically studying short random pulse propagation in resonant nonlinear media in the two-level approximation. We examine the behaviour of the ensemble averaged intensity, mutual coherence function, and temporal degree of coherence for pulses with relatively large and relatively small average areas. We explore the influence of the coherence state at the source on ensuing pulse evolution scenarios. We reveal evidence of self-induced transparency random phase soliton formation for rather coherent large-area input pulses. We stress that although soliton formation in resonant nonlinear media has been extensively studied either in the two-level [27] or multi-level [30–32] approximation, the work in this direction has so far focused on fully temporarily coherent solitons. We also show that all pulses lose their coherence on propagation in such media, regardless of their initial state of coherence. Yet, the coherence loss rate on propagation is strongly affected by the pulse coherence level at the source: the lower the source coherence, the greater the coherence loss rate. Our results are applicable to a multitude of resonant media, including dilute atomic vapours filling the hollow-core photonic crystal fibres, impurity-doped solids, and semiconductor quantum dots in the strong quantum confinement regime.

## 7.3 Pulse Propagation in Resonant Nonlinear Media

In this work, we model resonant optical media as a collection of two-level atoms. In particular, we describe the light-matter interactions within the framework of the Maxwell-Bloch equations [27]. The fluctuating pulse evolution in the medium can then be described in the slowly-varying envelope approximation by the reduced wave equation in the transformed coordinates, $\zeta = z$ and $\tau = t - z/c$, as

$$\partial_\zeta \Omega = \frac{i}{2} \frac{\omega N |d_{eg}|^2}{c\varepsilon_0 \hbar} \overline{\sigma}_\Delta. \tag{7.1}$$

In Eq. (7.1), $\Omega = 2d_{eg}\mathscr{E}/\hbar$ is the Rabi frequency corresponding to the field envelope $\mathscr{E}$. Hereafter, we will find it convenient to express the electric field envelope in frequency units employing the Rabi frequency $\Omega$ instead of the field envelope $\mathscr{E}$.Also, $N$ is the atom density, and $d_{eg}$ is the dipole matrix element between the nondegenerate ground and excited states of an atom. Also, $\overline{\sigma}_\Delta$ denotes the dipole envelope function of an atomic dipole moment averaged over a distribution of detunings $\Delta$ of the carrier wave frequency $\omega$ from the atomic resonance frequency $\omega_0$,

$$\overline{\sigma_\Delta} = \int d\Delta g(\Delta)\sigma(\Delta). \tag{7.2}$$

Here, $g(\Delta)$ is assumed as the inhomogeneous broadening function with Gaussian distribution

$$g(\Delta) = \frac{1}{\sqrt{2\pi}\delta} \exp\left(-\frac{\Delta^2}{2\delta^2}\right), \tag{7.3}$$

in which $\delta$ represents the inhomogeneous broadening width.

Next, the Bloch equations governing the complex dipole envelope function $\sigma$ and one-atom inversion $w$ dynamics can be expressed in the form [27]

$$\partial_\tau \sigma = -(\tfrac{1}{T_\perp} + i\Delta)\sigma - i\Omega w, \tag{7.4}$$

and

$$\partial_\tau w = -\tfrac{1}{T_{||}}(w+1) - \tfrac{i}{2}(\Omega^*\sigma - \Omega\sigma^*). \tag{7.5}$$

Here, $T_\perp$ and $T_{||}$ are the dipole phase and atomic population relaxation times, respectively.

To explore the feasibility of self-induced transparency phenomena, we need to consider coherent transient regime in that the input pulse width is so short ($t_p < min(T_\perp, T_{||})$) that

atoms of the material undergo no damping during their interaction with the pulse. Therefore, the evolution of atomic variables can be studies as if no damping effect is present. In such a case the Bloch equations reduce to

$$\partial_T \sigma = -i\Delta\sigma - i\Omega w, \tag{7.6}$$

$$\partial_T w = -\tfrac{i}{2}(\Omega^*\sigma - \Omega\sigma^*). \tag{7.7}$$

Here, $Z = \alpha\zeta$ and $T = t/t_p$, $t_p$ denoting a characteristic rms width of the incident pulse, are dimensionless variables and, $\alpha = N|d_{eg}|^2\omega^2/\sqrt{2\pi}\delta\hbar\varepsilon_0 c^2$ represents the linear absorption coefficient.

To quantitatively describe the pulse evolution in the medium, we must, in general, numerically solve the Maxwell-Bloch equations, Eqs. (7.1)-(7.3), together with Eqs.(7.6)-(7.7) subject to the appropriate initial and boundary conditions. We assume that the atoms are all initially in their ground states such that $\sigma = 0$ and $w = -1$, and the source field envelope $\Omega(t,0)$ (in the frequency units) is known. However, as incident pulses have fluctuating amplitudes and phases, we can only describe the pulse evolution in terms of appropriate correlation functions.

## 7.4 Statistical Properties of Fluctuating Pulses and Statistical Ensemble Generation

Henceforth, we will be primarily interested in the second-order temporal coherence properties of fluctuating pulses, propagating in resonant nonlinear media. The latter are specified by the second-order cross-correlation function, defined as

$$\Gamma(\tau_1,\tau_2,\zeta) = \langle\Omega^*(\tau_1,\zeta)\Omega(\tau_2,\zeta)\rangle, \tag{7.8}$$

where the angle brackets denote ensemble averaging over all possible field realizations. The ensemble power distribution is then defined in terms of the average intensity as

$$I(\tau,\zeta) \equiv \Gamma(\tau,\tau,\zeta), \tag{7.9}$$

and the ensemble coherence properties are characterized by the temporal degree of coherence [33, 34]

$$\gamma(\tau_1,\tau_2,\zeta) \equiv \frac{\Gamma(\tau_1,\tau_2,\zeta)}{\sqrt{I(\tau_1,\zeta)I(\tau_2,\zeta)}}. \tag{7.10}$$

In the fully coherent limit, the degree of coherence attains its maximum, $|\gamma(\tau_1, \tau_2, \zeta)| = 1$ [33, 35, 36].

The description of fluctuating field propagation in nonlinear media directly in terms of the correlation functions runs into a formidable obstacle known as a closure problem which emerges regardless of the nonlinearity nature, see, for instance [37]. It can be shown that whenever one attempts to derive an equation of motion for the second-order correlation functions using the Maxwell-Bloch equations, the resulting equation will also involve third-order correlations. The corresponding evolution equations for the third-order correlation functions will depend on fourth-order correlations and so forth, resulting in an infinite hierarchy of the evolution equations for correlation functions of all orders. One is then forced to either neglect correlation functions higher than a certain order or make ad hoc assumptions regarding the pulse statistics that make it possible to express higher-order correlations in terms of the lower-order ones. This dilemma is known as a closure problem. In general, neither resolution of the dilemma has been shown to yield satisfactory results for realistic nonlinear media [37] unless the medium response time is much longer than a characteristic coherence time of the incident field. In the latter case, the medium averages over higher-order field fluctuations and a mean-field [38–40] or averaged-response description [41] is possible leading to a closed form evolution equation for the second-order correlation function. In the present case, the resonant medium response is noninstantaneous, but the response time can be either longer or shorter than the pulse coherence time. Thus, the closure problem cannot be easily resolved and we must resort to a different mathematical description.

To this end, we employ a wave optical Monte Carlo method which was developed in [42–44] and recently applied to random pulse propagation in nonresonant media with Kerr nonlinearities [23]. In essence, the technique entails generating an ensemble $\{\Omega(t)\}$ of random fluctuating pulses at the source with specified coherence properties and transmitting individual ensemble realizations through the resonant medium. At the end, the ensemble average is performed and the appropriate second-order correlation functions are determined. Thus, we first have to solve the Maxwell-Bloch equations Eqs.(7.1)-(7.3) and Eqs.(7.6)-(7.7) numerically for each random realization of the pulse and then average over

$L$ members of the ensemble according to

$$\Gamma_L(\tau_1,\tau_2,\zeta)=\frac{1}{L}\sum_{i=1}^{L}\Omega^*(\tau_1,\zeta)\Omega(\tau_2,\zeta), \tag{7.11}$$

to obtain the second-order cross-correlation function of the pulse ensemble. The averaged degree of coherence of the ensemble is then determined by

$$\gamma_L(\tau_1,\tau_2,\zeta)=\frac{\Gamma_L(\tau_1,\tau_2,\zeta))}{\sqrt{I_L(\tau_1,\zeta)I_L(\tau_2,\zeta)}}. \tag{7.12}$$

To construct the pulse ensemble, we begin by representing a fluctuating field in any transverse plane $\zeta\geq 0$ through the Karhunen-Loève expansion as

$$\Omega(\tau,\zeta)=\sum_n a_n\psi_n(\tau,\zeta), \tag{7.13}$$

where $\{a_n\}$ are uncorrelated random amplitudes, and $\{\psi_n(\tau,\zeta)\}$ are orthogonal coherent modes. We specify a non-Gaussian pulse ensemble statistics through

$$a_n=\sqrt{\lambda_n}\exp(i\varphi_n), \tag{7.14}$$

where $\{\varphi_n\}$ are statistically independent random phases, uniformly distributed in the interval $[-\pi,\pi]$ [23]. The statistical independence of the set $\{\varphi_n\}$ implies that

$$\langle\exp[i(\varphi_n-\varphi_m)]\rangle=\delta_{mn}, \tag{7.15}$$

Notice that the statistics (7.14), together with (7.15), imply that

$$\langle a_n^* a_m\rangle=\lambda_n\delta_{mn}. \tag{7.16}$$

Assuming the modes are normalized at the source, each $\lambda_n$ determines the power carried by the $n$th mode of the source.

It then follows at once from Eqs. (7.13) and (7.16) as well as the definition of $\Gamma$, Eq. (7.8), that [45]

$$\Gamma(\tau_1,\tau_2,\zeta)=\sum_n\lambda_n\psi_n^*(\tau_1,\zeta)\psi_n(\tau_2,\zeta). \tag{7.17}$$

Here $\lambda_n$ and $\psi_n(\tau,\zeta)$ are the eigenvalues and eigenmodes of the Fredholm integral equation,

$$\int_{-\infty}^{\infty}d\tau_1\,\Gamma(\tau_1,\tau_2,\zeta)\psi_n(\tau_1,\zeta)=\lambda_n\psi_n(\tau_2,\zeta). \tag{7.18}$$

It remains to specify the second-order correlations of the source which determine the coherent modes and their weights. To this end, we employ a generic Gaussian Schell-model (GSM) source with the cross-correlation function

$$\Gamma(t_1,t_2)=\frac{E}{\sqrt{\pi}t_{\mathrm{p}}}\exp\left[-\frac{(t_1^2+t_2^2)}{2t_{\mathrm{p}}}\right]\exp\left[-\frac{(t_1-t_2)^2}{2t_{\mathrm{c}}^2}\right], \tag{7.19}$$

where $t_{\mathrm{p}}$ and $t_{\mathrm{c}}$ are characteristic pulse width and coherence time at the source and $E$ is a total energy of the source. The coherent modes of GSM sources are analytically known [46, 47] as

$$\psi_n(t)=\frac{1}{\sqrt{2^n n!}}\left(\frac{2\pi}{d}\right)^{1/4}H_n\left(\frac{t}{\sqrt{2d}}\right)\exp\left(-\frac{t^2}{4d}\right), \tag{7.20}$$

where $H_n(t)$ is a Hermite polynomial of order $n$. The modal weights are given by

$$\lambda_n=\left(\frac{\pi}{a+b+d}\right)^{1/2}\left(\frac{b}{a+b+d}\right)^{n}. \tag{7.21}$$

The parameters $a$,$b$ and $d$ are defined as

$$a=\frac{t_{\mathrm{p}}^2t_{\mathrm{c}}^2}{2(t_{\mathrm{c}}^2+2t_{\mathrm{p}}^2)},\quad b=\frac{t_{\mathrm{p}}^4}{2(t_{\mathrm{c}}^2+2t_{\mathrm{p}}^2)}, \tag{7.22}$$

and

$$d=\sqrt{a^2+2ab}. \tag{7.23}$$

where $t_p$ and $t_c$ correspond to the characteristic width and coherence time of the pulse respectively [7, 9]. The coherence time, $t_c$ specifies a time duration over which two pulses can be added coherently. The limits $t_c=0$ and $t_c=\infty$ correspond to uncorrelated and fully correlated pulses, respectively.

In proceeding with modeling random sample pulses, we ascertain here a proper definition for the variable $a_n$ in Eq. (7.14).

As we are interested in simulating noisy laser pulses, we generate an ensemble with non-Gaussian statistics. To do so, the random phases $\varphi_n$ in Eq. (7.14), are chosen to be uniformly distributed in the interval $[-\pi,\pi]$. Here, $\varphi_n$ and $\varphi_m$ are statistically independent when $n\neq m$, so the condition in Eq. (7.13) is satisfied [45, 47]. By interpreting the modes in Eq. (7.17) as natural modes of oscillations of the source, our prescribed choice of $a_n$ generates random sample pulses, which are linear combinations of fundamental fields with random phases. It is worth mentioning that the constructed field realizations have random

fluctuations both in phase and amplitude, but that each random field realization contains the same amount of energy [23].

Propagation of GSM pulses in resonant nonlinear media can be simulated by applying the source pulse Eq. (7.13) into wave equations Eqs.(7.1)-(7.3) and Eqs.(7.6)-(7.7). As mentioned previously, each random realization will be propagated in the media individually. The process will be repeated many times for all different realizations of the field, and the resulting intensities will be averaged to produce a partially coherent pulse intensity according to Eq. (7.11).

## 7.5 Physical Model of the Source and Host Medium

We consider a GSM as a generic model of a random input pulse and proceed to generate an ensemble of source pulses according to the just outlined prescription. In Fig. 7.1, we

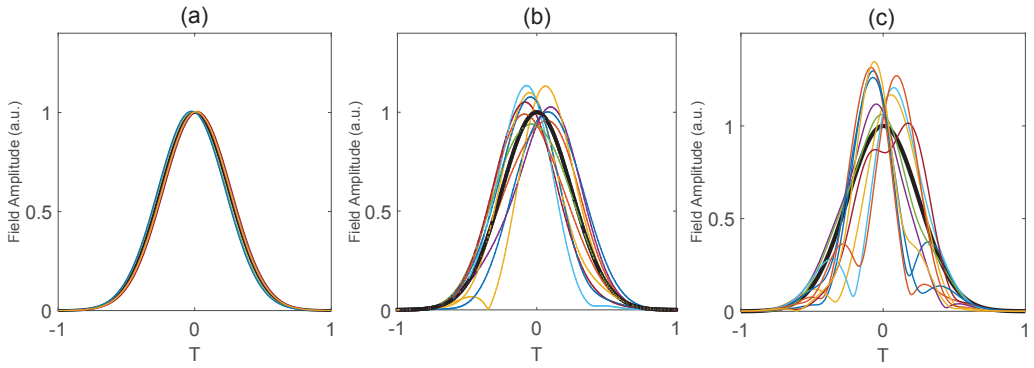


Figure 7.1: Magnitude of 10 random field realizations of the GSM pulse at the source $Z = 0$ as a function of dimensionless time $T = t/t_p$ in three cases (a) $t_c = 10t_p$, (b) $t_c = 2t_p$ and (c) $t_c = t_p$. Black thick line: ensemble average amplitude.

exhibit three short GSM pulses with different coherence level at the source: a relatively coherent input pulse with $t_c = 10t_p$, a moderately coherent pulse with $t_c = 2t_p$ and a relatively incoherent pulse with $t_c = t_p$. The magnitude of simulated sample pulses are presented in Fig. 7.1 for 10 random realizations. It can be seen in the figure that each field realization has random fluctuations which become progressively more pronounced as the pulse coherence level decreases. The averaged pulse amplitude for a large set of realizations is also displayed with thick black line. We also display the mutual coherence function profile at the source as a function of a pair of dimensionless time instances $T_1 = t_1/t_p$ and $T_2 = t_2/t_p$ in Fig. 7.2. It is seen in the figure that the relatively coherent pulse has a nearly isotropic

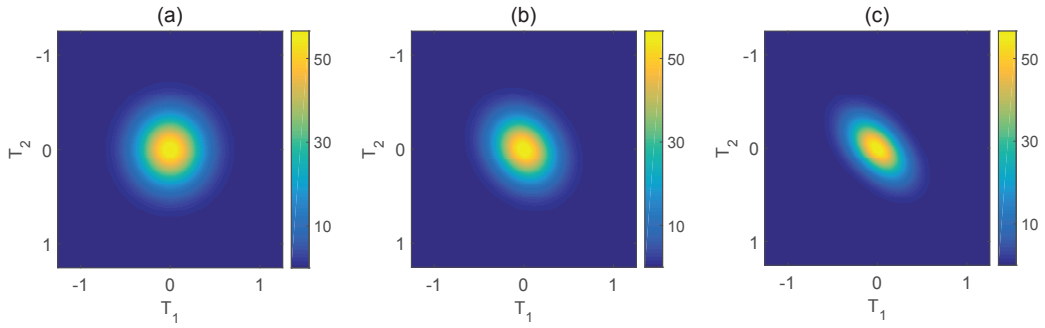


Figure 7.2: Profile of the mutual coherence function at the source, $Z = 0$ as a function of dimensionless time $T_1$ and $T_2$ in three cases : (a) $t_c = 10t_p$, (b) $t_c = 2t_p$ and (c) $t_c = t_p$.

mutual coherence function profile, while that of the relatively incoherent pulse is strongly anisotropic with a sharp peak along the diagonal $T_1 = T_2$. This behaviour naturally reflects $\delta$-function like coherence properties of such pulses.

As mentioned in the previous section, the number of modes in the Karhunen-Loève decomposition of each ensemble member is relevant to the coherence level of the source pulse. Thus, we employ a large number of modes to faithfully represent relatively incoherent pulses through Eq. (7.13) [47]. At the same time, the Monte Carlo simulation accuracy crucially depends on the number of the sample field realizations, $L$. The ensemble average represented by Eq. (7.11), converges to the time average as the sample size $L$ increases. Therefore, a high fluctuation level of relatively incoherent pulses–manifest in Fig. 7.1(c)–necessitates a high sample volume [23, 42].

The resonant host medium is modelled as a collection of two-level atoms. The two key relaxation rates–transverse and longitudinal–can be determined as follows. The total transverse relaxation rate is defined as [27]

$$\frac{1}{T_\perp} = \frac{1}{T_\perp^h} + \frac{1}{T_\perp^{in}}, \tag{7.24}$$

where $T_\perp^h$ and $T_\perp^{in}$ are homogenous and inhomogeneous broadening lifetimes, respectively. According to [48], the effective absorption line shape of the medium is affected by the ratio,

$$b = \sqrt{4\ ln2}\ \frac{\delta_h}{\delta_{in}}, \tag{7.25}$$

where $\delta_h = 1/T_\perp^h$ and $\delta_{in} = 1/T_\perp^{in}$ correspond to the homogenous and inhomogeneous linewidth, respectively. Eq.(7.25) distinguishes two limiting cases. In the first case, $\delta\nu_{in} >> \delta\nu_h$, the transverse decay rate is mainly due to inhomogeneous broadening. In contrast, if

$\delta\nu_h >> \delta\nu_{in}$, the homogeneous broadening is dominant and the transverse decay rate is mostly influenced by collisions.

The energy relaxation time $T_{||}$, defining the time interval over which the atomic populations decay, is related to $T_\perp$ according to [1,48];

$$\frac{1}{T_\perp} = \frac{1}{2T_{||}} + \frac{1}{T_\perp^h}. \tag{7.26}$$

In our simulations, we assume an inhomogeneously broadened medium such that $b \ll 1$. A dilute sodium vapour at $T = 300K$ with a density $N = 10^{11} cm^{-3}$ can serve as a physical realization of the medium. Setting $b = 0.05$ , $T_{||} = 16$ ns, a typical value for the room temperature sodium [1], and $\delta_{in} = 1GHz$, and employing Eqs.(7.24) through (7.26), we obtain $T_\perp \simeq 32$ ns.

## 7.6 Numerical Simulation Results

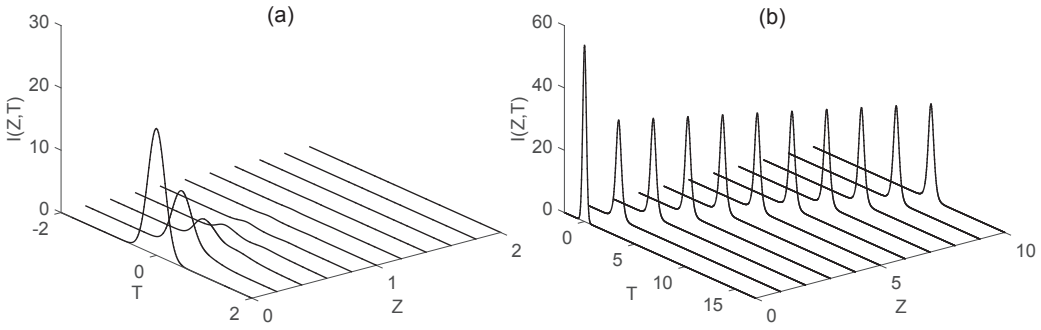


Figure 7.3: Average intensity evolution of relatively coherent pulses as a function of the propagation distance $Z$. The cases $(a)$ and $(b)$ correspond to the average input pulse areas $\mathscr{A}_0 = 0.8\pi$ and $\mathscr{A}_0 = 1.5\pi$, respectively.

We numerically study the evolution of random input pulse ensembles with the average pulse areas at the source $\mathscr{A}_0 = 0.8\pi$ and $\mathscr{A}_0 = 1.5\pi$ where the latter is defined, in dimensionless variables, as

$$\mathscr{A}(Z) \equiv \int_{-\infty}^{\infty} \sqrt{\langle I(T,Z)\rangle}\, dT; \tag{7.27}$$

$\mathscr{A}_0 \equiv \mathscr{A}(0)$. It follows at once from Eq. (7.27) that the average area reduces to the standard pulse area [27] in the fully coherent limit.

We first examine the behaviour of relatively coherent input pulses with $t_c = 10t_p$. In Fig. 7.3, we illustrate the average intensity profile evolution of two such pulses with the

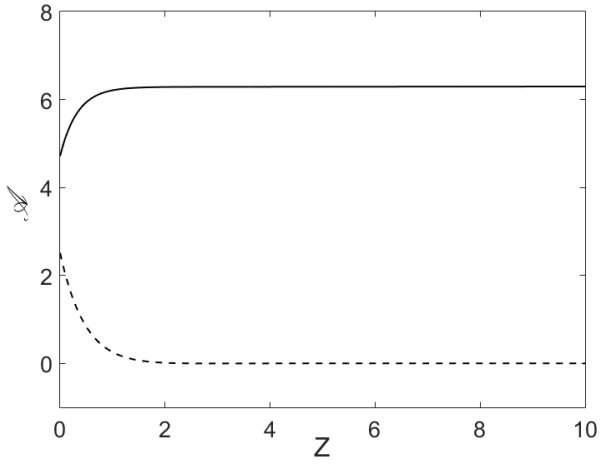


Figure 7.4: Evolution of the average pulse area as a function of the propagation distance $Z$ for relatively coherent pulses with $\mathscr{A}_0 = 0.8\pi$ (dashed ) and, $\mathscr{A}_0 = 1.5\pi$ (solid), respectively.

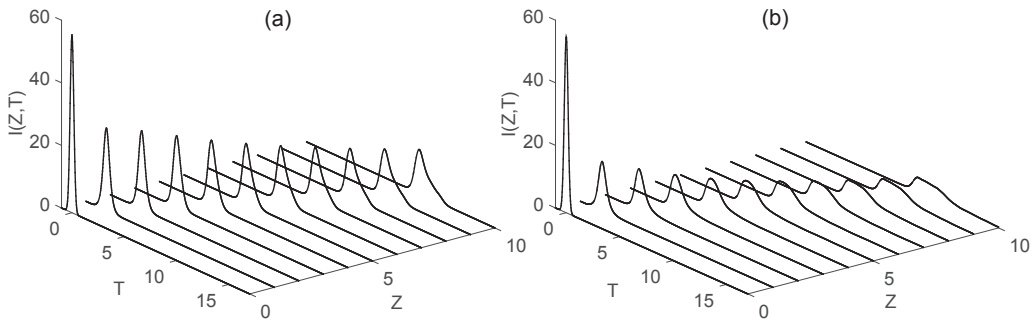


Figure 7.5: Average intensity evolution as a function of propagation distance $Z$ for input pulses with (a) $t_c = 2t_p$ and (b) $t_c = t_p$. The average pulse area at the source is $\mathscr{A}_0 = 1.5\pi$.

areas $\mathscr{A}_0 = 0.8\pi$ and $\mathscr{A}_0 = 1.5\pi$ through the inhomogeneously broadened medium, corresponding to the cases Fig. 7.3(a) and 7.3(b) in the figure. We can see in Fig. 7.3(a) that a smaller area pulse suffers strong absorption on its propagation through the medium and no soliton formation is observed. Moreover, Fig. 7.4 represents the evolution of the average pulse area as a function of the propagation distance. It is evident from the figure that the corresponding pulse area, displayed with a dashed line, rapidly reaches zero upon pulse entrance into the medium. On the other hand, we can see in Fig. 7.3(b) that a larger area pulse initially broadens, while its peak intensity decreases. The pulse is, however, ultimately converted into a stable soliton which is evident in the figure: the pulse maintains

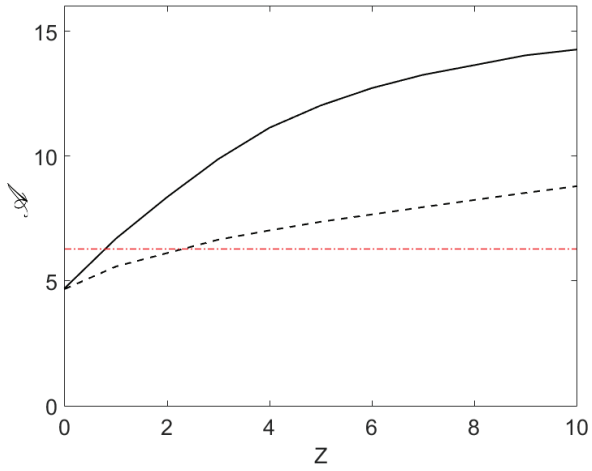


Figure 7.6: Evolution of the averaged pulse area as a function of propagation distance $Z$, corresponding to $t_c = 2t_p$ (dashed line) and, $t_c = t_p$ (solid line) with the initial area $\mathscr{A}_0 = 1.5\pi$. The red dotted-dashed line represents the $\mathscr{A} = 2\pi$ limit.

its shape, suffering no visible attenuation over sufficiently large propagation distances. We notice also that all relatively coherent pulses experience a time delay on propagation which is manifested through the pulse intensity peak shift relative to its position at the source. As is seen in Fig. 7.4, the average pulse area, plotted with a solid line, attains the asymptotic value of $2\pi$, reminiscent of the fully coherent self-induced transparency situation [27]. Thus, our results can be interpreted as the manifestation of self-induced transparency (SIT) phenomena and solitary-pulse formation in presence of small noise at the source.

To elucidate the influence of the input pulse coherence level on the SIT soliton formation, we also study the evolution of random pulses with lower levels of coherence. In Fig. 7.5, we illustrate the evolution of partially coherent ($t_c = 2t_p$) and rather incoherent ($t_c = t_p$) incident pulses with the initial area $\mathscr{A}_0 = 1.5\pi$. It can be seen in Fig. 7.5(a) that a partially coherent pulse intensity profile becomes wider and more shallow upon propagation. The pulse leading edge self-steepens, distorting its symmetry as well. The similar behaviour is exhibited by rather incoherent pulses, as is seen in Fig. 7.5(b). In this case, though, pulse broadening and peak intensity decrease are more pronounced. The average pulse area dynamics are shown in Fig. 7.6. It is seen in the figure that in both cases, the area appears to monotonously increase with the propagation distance, exceeding the value of $2\pi$. We can infer that SIT soliton formation is precluded for the incident pulses with

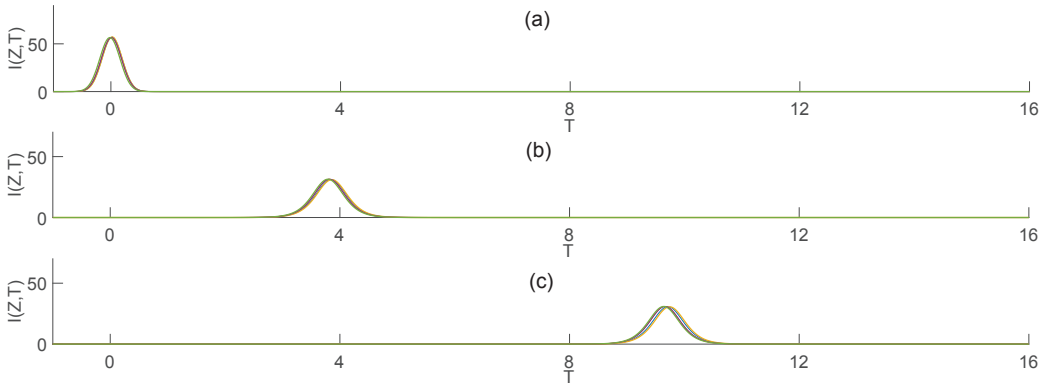


Figure 7.7: Intensity of five relatively coherent, $t_c = 10t_p$, pulse realizations with $\mathscr{A}_0 = 1.5\pi$ at three sample points in $Z$: $Z = 0$ (a), $Z = 5$ (b), and $Z = 10$ (c), respectively.

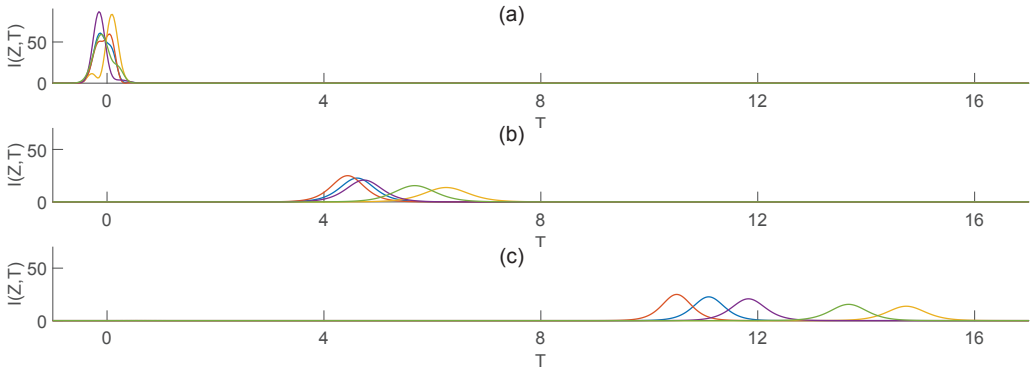


Figure 7.8: Intensity of five rather incoherent, $t_c = t_p$ pulse realizations with $\mathscr{A}_0 = 1.5\pi$ at three sample points in $Z$: $Z = 0$ (a), $Z = 5$ (b), and $Z = 10$ (c), respectively.

high enough fluctuation levels.

To explain the evolution scenario difference of more from less coherent input pulses, we recall that each statistical ensemble consists of a number of pulse realizations. As an example, in Fig. 7.7 we display the evolution of five relatively coherent random pulse realizations at three propagation distances: $Z = 0$, $Z = 5$ and $Z = 10$. As it is evident in the figure, the field realizations have almost the same initial area and, consequently nearly the same behaviour upon propagation. Thus upon averaging, such an ensemble yields a nearly coherent pulse transforming to a SIT soliton. On the contrary, in a rather incoherent pulse case, ($t_c = t_p$), the ensemble realizations, shown in Fig. 7.8, vary greatly in their initial shape and area. As a result, different realizations suffer widely different time delays upon propagation as is seen in the figure. Notice also that the realization pulse distribution in

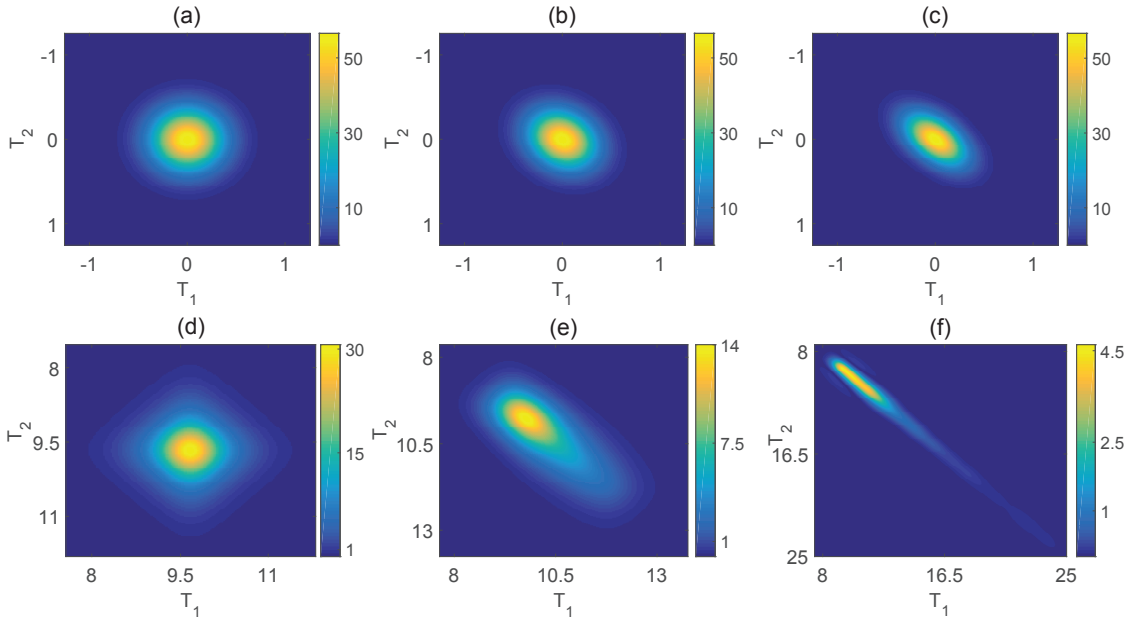


Figure 7.9: Magnitude of the mutual coherence function at $Z = 0$, (top row) and $Z = 10$, (bottom row); $t_c = 10t_p$,(a,d); $t_c = 2t_p$, (b,e); $t_c = t_p$, (c,f).

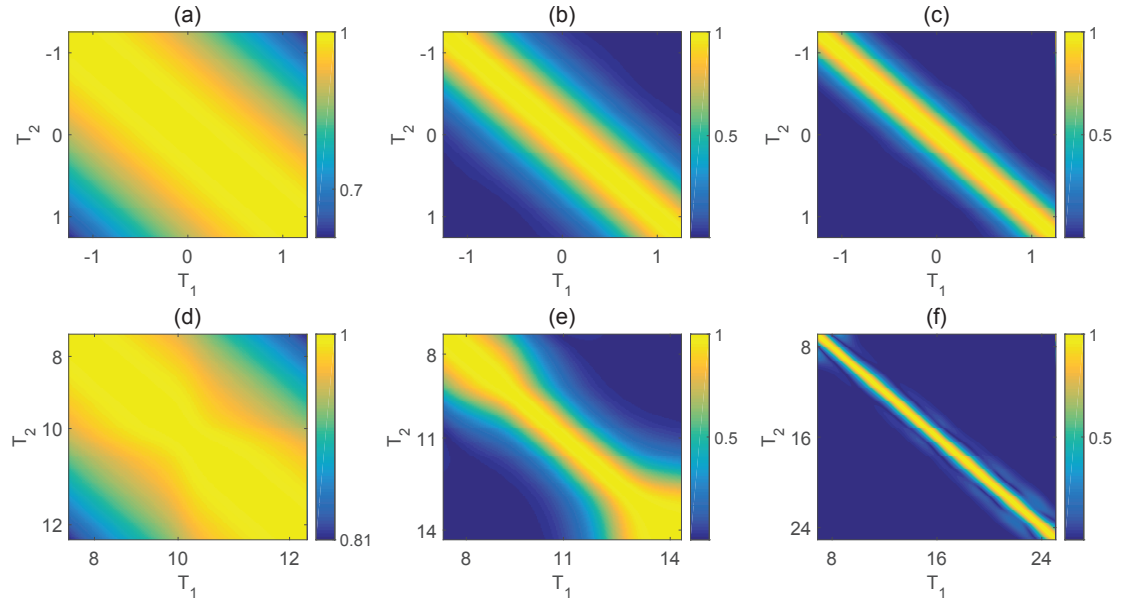


Figure 7.10: Magnitude of the complex degree of coherence function at $Z = 0$, (top row) and $Z = 10$, (bottom row); $t_c = 10t_p$,(a,d); $t_c = 2t_p$, (b,e); $t_c = t_p$, (c,f).

Fig. 7.8 explains the output pulse asymmetry manifest in Fig. 7.5. The ensemble averaging then results in a long shallow pulse, more susceptible to incoherent relaxation processes that ultimately preclude the SIT soliton formation in this case.

Let us now focus on the mutual coherence function evolution in the system. In Fig. 7.9, we represent the mutual coherence function of the three pulses–a relatively coherent, partially coherent and nearly incoherent ones–at the source $Z = 0$ and at the distance $Z = 10$ away from the source. To obtain reliable results at the output, we used $L = 2000$ sample realizations for the nearly incoherent case and $L = 1000$ for the partially coherent case. We can infer from the figure that the mutual coherence function profiles in all cases become progressively more centred along the $T_1 = T_2$ diagonal, implying pulse coherence reduction upon their propagation in the medium. Moreover, the least coherent input pulses display the fastest coherence loss rate. Such a behaviour can be explained by recalling that relatively incoherent pulses broaden faster than do relatively coherent ones. Hence, the former become long enough to be affected by incoherent relaxation processes at shorter propagation distances than are the latter. Thus, less coherent pulses lose their coherence faster than do more coherent ones. However, regardless of the initial coherence level, all random pulses become progressively less coherent on propagation in resonant media due to the their temporal broadening which makes them subject to incoherent relaxation processes. The similar trend is reflected in the temporal degree of coherence evolution, exhibited in Fig. 7.10.

## 7.7 Conclusion

In summary, we applied numerical Monte Carlo techniques to simulate partially coherent GSM pulse propagation in a resonant, inhomogeneously broadened nonlinear medium. We modeled the medium as a collection of two-level atoms. We numerically studied the dynamics of the ensemble averaged pulse intensity, the mutual coherence function, and the temporal degree of coherence as pulses of an arbitrary coherence state at the source propagate into the medium. We have elucidated conditions for self-induced transparency soliton formation in the system. Our simulation results reveal that self-induced transparency is possible provided the input pulses are sufficiently coherent and possess large enough average areas. We have also demonstrated that regardless of their initial state of coherence, random pulses lose their coherence on propagation. However, low-coherence input pulses lose their coherence at a faster rate than do their more coherent counterparts because the former broaden faster than the latter, and hence become susceptible to incoherent relaxation processes at shorter propagation distances than are the latter.

## Bibliography


[1] R. W. Boyd, *Nonlinear Optics* (Academic Press, 2008).

[2] P. P. Banerjee, *Nonlinear Optics: Theory, Numerical Modeling and Applications* (Marcel Decker, 2004).

[3] S. A. Ponomarenko and G. P. Agrawal, "Linear optical bullets," Opt. Commun. **261**, 1–4 (2006).

[4] G. P. Agrawal, *Nonlinear Fiber Optics* (Academic Press, 2007).

[5] M. Bertolotti, A. Ferrari, and L. Sereda, "Coherence properties of nonstationary polychromatic light sources," J. Opt. Soc. Am. B **12**, 341–347 (1995).

[6] L. Sereda, M. Bertolotti, and A. Ferrari, "Coherence properties of nonstationary light wave fields," J. Opt. Soc. Am. B **15**, 695–705 (1998).

[7] H. Lajunen, J. Tervo, J. Turunen, P. Vahimaa, and F. Wyrowski, "Spectral coherence properties of temporarily modulated stationary light sources," Opt. Express **11**, 1894–1899 (2003).

[8] L. Ma and S. A. Ponomarenko, "Optical coherence gratings and lattices," Opt. Lett. **39**, 6656 (2014).

[9] P. Paakkonen, J. Turunen, P. Vahimaa, A. T. Friberg, and F. Wyrowski, "Partially coherent Gaussian pulses," Opt. Commun. **204**, 53–58 (2002).

[10] S. A. Ponomarenko, G. P. Agrawal, and E. Wolf, "Energy spectrum of a nonstationary ensemble of pulses," Opt. Lett. **29**, 394–396 (2004).

[11] P. Vahimaa and J. Turunen, "Independent-elementary-pulse representation for nonstationary fields," Opt. Express **14**, 5007–5012 (2006).

[12] S. A. Ponomarenko, "Complex Gaussian representation of statistical pulses," Opt. Express **19**, 17086-17091 (2011).

[13] Q. Lin, L. Wang, and S. Zhu, "Partially coherent light pulse and its propagation," Opt. Commun. **219**, 65–70 (2003).

[14] M. Brunel and S. Coëtlemec, "Fractional-order Fourier formulation of the propagation of partially coherent light pulses," Opt. Commun. **230**, 1–5 (2004).

[15] W. Huang, S. A. Ponomarenko, M. Cada, and G. P. Agrawal, "Polarization changes of partially coherent pulses propagating in optical fibers," J. Opt. Soc. Am. A **24**, 3063–3068 (2007).

[16] R. W. Schoonover, B. J. Davis, R. A. Bartels, and P. S. Carney, "Propagation of spatial coherence in fast pulses," J. Opt. Soc. Am. A **26**, 1945–1953 (2009).

[17] C. L. Ding, L. Z. Pan, and B. D. Lu, "Changes in the spectral degree of polarization of stochastic spatially and spectrally partially coherent electromagntic pulses in dispersive media," J. Opt. Soc. Am. B **26**, 1728–1735 (2009).

[18] S. A. Ponomarenko, "Degree of phase-space separability of statistical pulses," Opt. Express **20**, 2548–2555 (2012).

[19] S. A. Ponomarenko, "Self-imaging of partially coherent light in graded-index media," Opt. Lett. **40**, 566 (2015).

[20] B. Gross and J. T. Manassah, "Compression of the coherence time of incoherent signals to a few femto seconds," Opt. Lett. **16**, 1835–1837 (1991).

[21] V. A. Aleshkevich, V. A. Vysloukh, G. D. Kozhoridze,A. N. Matveev and S. I. Terzieva, "Nonlinear propagation of partially coherent pulse in fiber waveguide and the role of higher order dispersion," Sov. J. Quantum Electron. **18**, 207–211 (1988).

[22] S. B. Cavalcanti, G. P. Agrawal and M. Yu, " Noise amplification in dispersive nonlinear media," Phys. Rev. A. **51**, 4086–4092 (1995).

[23] H. Lajunen, V. Torres-Company, J. Lancis, E. Silvestre, and P. Andrés, "Pulse-by-pulse method to characterize partially coherent pulse propagation in instantaneous nonlinear media," Opt. Express **18**, 14979–14991 (2011).

[24] L. Mokhtarpour and S. A. Ponomarenko, "Complex area correlation theorem for statistical pulses in coherent linear absorbers," Opt. Lett. **37**, 3498–3500 (2012).

[25] L. Mokhtarpour and S. A. Ponomarenko, "Ultrashort pulse coherence properties in coherent linear amplifiers," J. Opt. Soc. Am. A **30**, 627–630 (2013).

[26] L. Mokhtarpour, G. H. Akter, and S. A. Ponomarenko, "Partially coherent self-similar pulses in resonant linear absorbers," Opt. Express **20**, 17816–17822 (2012).

[27] L. Allen and J. H. Eberly, *Optical Resonance and Two-level Atoms* (Dover, 1975).

[28] J. C. Diels and W. Rudolph, *Ultrashort Laser Pulse Phenomena* (Academic Press, 2006)

[29] L. Banyai and S. W. Koch, *Semiconductor Quantum Dots* (World Scientific, 1993).

[30] Y. Wu and L. Deng, "Ultraslow bright and dark optical solitons in a cold three-state system," Opt. Lett. **29**, 2064–2066 (2004).

[31] C. Hang and G. Huang, "Giant Kerr nonlinearity and weak-light superluminal optical solitons in a four-state atomic system with gain doublet," Opt. Express **18**, 2952-2966 (2010).

[32] W-X. Yang, Ai-Xi Chen, L-G. Si, K. Jiang, X. Yang, and R-K. Lee, "Three coupled ultraslow solitons in a five-level tripod system," Phys. Rev. A. **81** 023814 (2010).

[33] L. Mandel and E. Wolf, *Optical Coherence and Quantum Optics* (Cambridge University, 1997).

[34] S. A. Ponomarenko and E. Wolf, "Coherence properties of light in Young's interference pattern formed with partially coherent light,"Opt. Commun. **170**, 1–8 (1999).

[35] S. A. Ponomarenko, H. Roychoudhury, and E. Wolf, "Physical significance of complete spatial coherence of optical fields," Phys. Lett. A, **345**, 10–12 (2005).

[36] S. A. Ponomarenko and E. Wolf, "The spectral degree of coherence of fully spatially coherent electromagnetic beams," Opt. Commun. **227**, 73–74 (2003).

[37] A. S. Monin and A. M. Yaglom, *Statistical Fluid Mechanics: Mechanics of Turbulence*, Vols. 1& 2, (Dover, 2007).

[38] G. A. Pasmanik, "Self-interaction of incoherent light beams," Sov. Phys. JETP, **39**, 234–238 (1974).

[39] M. Mitchell, M. Segev, T. H. Coskun, and D. N. Christodoulides, "Theory of Self-Trapped Spatially Incoherent Light Beams," Phys. Rev. Lett. **79**, 4990–4993 (1997).

[40] D. N. Christodoulides, E. D. Eugenieva, T. H. Coskun, M. Segev, and M. Mitchell, "Equivalence of three approaches describing partially incoherent wave propagation in inertial nonlinear media," Phys. Rev. E. **63**, 035601(R) (2001).

[41] S. A. Ponomarenko, N. M. Litchinitser, and G. P. Agrawal, "Theory of incoherent solitons: Beyond the mean-field approximation," Phys. Rev. E. **70**, 015603(R) (2004).

[42] V. P. Kandidov, "Monte Carlo method in nonlinear statistical optics", Sov. Phys.Usp. **39**, 1243–1272 (1996).

[43] X. Xiao and D. Voelz, "Wave optics simulation approach for partial spatially coherent beams," Opt. Express **16**, 6986–6992 (2006).

[44] S. A. Parhl, D. G. Fischer and D. D. Duncan, "Monte Carlo Green's function for the propagation of partially coherent light," J. Opt. Soc. Am. A **260**, 1533–1543 (2009).

[45] E. Wolf,"New spectral representation of random sources and of the partially coherent fields that they generate," Opt. Commun. **38**, 3–6 (1981).

[46] F. Gori, "Collett-Wolf sources and multimode lasers," Opt. Commun. **34**, 301–305 (1980).

[47] A. Starikov and E. Wolf, "Coherent-mode representation of Gaussian Schell-model sources and of their radiation fields," J. Opt. Soc. Am. A **72**, 9233–928 (1982).

[48] P. W. Milonni and J. H. Eberly, *Lasers* (Wiley, 1985).

# Chapter 8

# Discussion

## 8.1 Conclusion

In this thesis, our aim was to focus on the stochastic nature of pulses to achieve a more realistic description of ultrashort optical pulses affected by noise. In order to simulate ultrashort pulses, various stochastic pulse models were applied. The effects of pulse amplitude and phase fluctuations on its propagation in various linear and nonlinear media were studied based on optical coherence theory.

The response of the medium atoms to the applied stochastic pulses was investigated for the particular resonant case in which the pulse frequency nearly coincides with the atom resonance frequency. Analytical and numerical propagation methods were applied to explore evolutions of ultrashort stochastic pulses in the vicinity of optical resonance.

Our studies on resonant interactions of stochastic pulses and matter are divided into four distinct phases. A general description of each phase and its main results are given in the following.

**Phase1.** Partially Coherent Self-Similar Pulses in Resonant Linear Absorbers.

In this phase of our research, propagation of small-area partially coherent pulses in resonant linear absorber media was investigated and the exact resonant condition was considered. A physical realization of linear absorber media could be a dilute atomic vapor which fills a high-vacuum cell.

Our main objective of this phase was to demonstrate a special class of partially coherent pulses that maintain their shape upon propagation in resonant absorber media. It was shown that such pulses can be represented as a sum of shape-invariant modes with stochastic coefficients.

The spectral shape of partially coherent pulses is mainly affected by two factors, the modal weight distribution of random coefficients and the spectral mode profile at the source. It was shown that these factors could lead to formation of a dip, a hole or a peak at the center of input pulse profiles. In order to investigate the crucial effects of the above-mentioned

factors on the pulse evolution behavior, two classes of partially coherent pulses with different modal weigh factors were generated:

1. Pulses with the power-law distribution of modal weights;

2. Pulses with higher decay rate of modal weight distributions compared to power-law.

In each case, partially coherent pulses with different source mode profiles were transmitted through the resonant linear absorber media. It has been illustrated that, although varying the two mentioned factors lead to formation of hole or dip at the source pulse profile, in the long-term limit a self-similar evolution of the pulses would be achieved in both cases.

Moreover, evolution of statistical properties of partially coherent pulses upon propagation was investigated using the magnitude of their spectral degree of coherence function. Non-uniform behavior of the degree of coherence for different classes of input pulses revealed that variation of the mentioned parameters results in various spectral coherence properties of the pulses.

**Phase2.** Complex Area Correlation Theorem for Statistical Pulses in Coherent Linear Absorbers.

In this phase, propagation of partially coherent small-area pulses in resonant linear absorbers was investigated. Gaussian Schell Model (GSM) pulses were employed as a generic model to simulate stochastic pulses at the source. To study the impact of statistical properties of the source pulses on their behavior upon propagation, two partially coherent pulses with different levels of coherence -more and less coherent- were generated. Second-order coherence functions, including the pulse intensity and magnitude of the degree of coherence, were used to investigate evolution of the statistical properties of pulses.

Comparison of the intensity profiles of the two partially coherent pulses as a function of propagation distance indicated that although the intensities of both pulses were attenuated upon propagation, the more coherent pulse is strongly absorbed and reshaped by the medium. The low attenuation rate of less coherent pulses is due to their broad spectrum. Specifically, most of their energy remains in their tails which lie outside the absorption spectrum of the medium and the pulse spectra are only partially absorbed.

Additionally, variations of the degree of coherence of partially coherent pulses at various propagation distances were studied. It was shown that the degree of coherence of pulses becomes more inhomogenous across the pulse profile which is more pronounced in

longer pulses.

Exploring the behavior of the intensity and the degree of coherence of partially coherent pulses led to the conclusion that longer pulses are stronger coupled with the atoms of the absorbing medium than are shorter pulses.

**Phase3.** Ultrashort Pulse Coherence Properties in Coherent Linear Amplifiers.

In this phase of our research, coherence properties of small-area intrinsically stationary pulses were examined upon propagation in resonant linear amplifying media. The generic GSM pulses with different levels of coherence- nearly incoherent and almost fully coherent- were employed to simulate various stochastic pulse models at the source.

It was shown that the intensities of both pulses were amplified and their shape gradually became asymmetric upon propagation in resonant amplifying media. However, comparison of the more and less coherent pulses led to the conclusion that the more coherent pulses are more significantly affected by the amplifying media than are less coherent pulses.

Moreover, variation of the energy gain factor of pulses upon propagation in the amplifying media was presented. The higher slope of the gain factor of the more coherent pulse confirms the fact that such pulses extract much more energy from the atoms of the media than do less coherent pulses.

Furthermore, the evolution of the complex degree of coherence of the two sample stochastic pulses was studied and it was shown that in both cases the degree of coherence of pulses increased and their temporal profile became more uniform upon propagation in the linear amplifying medium.

**Phase 4.** Fluctuating Pulse Propagation in Resonant Nonlinear Media: Self-induced Transparency Random Phase Soliton Formation.

In this part, a numerical investigation of propagation of an ensemble of ultrashort stochastic pulses in a resonant nonlinear medium was performed. The Monte Carlo method was employed to generate realizations of partially coherent pulses with controllable temporal coherence and simulate their propagation in resonant nonlinear media. The incident random pulses were simulated by an uncorrelated superposition of fully coherent modes with non-Gaussian statistical coefficients.

It has been concluded that the behavior of the averaged intensities and degree of coherence of pulses upon propagation were significantly affected by the initial coherence state and area of the source pulses.

The formation of self-induced transparency solitons and self-similar evolution of stochastic pulses for inhomogeneously broadened nonlinear media were also studied. To provide a better overview of the potential application of this phase of our research, dilute atomic vapors and semiconductor quantum dots were suggested as physical realization of such resonant media.

## 8.2 Future work

In this research, a comprehensive study of stochastic pulse propagation in resonant media has been carried out with the aid of analytical and numerical methods. However, it is reasonable to believe that an experimental implementation of the proposed simulations could support our investigations and is recommended as a future research step.

Exploring alternative stochastic pulse models for achieving a better simulation of particular laser pulses seems valuable as future work.

# Appendix A

## Simulation Codes for Simulating Propagation of Partially Coherent Self-similar Pulses in Resonant Linear Absorbers

```
%=========================================================================
%Pulses with the power-law distribution of modal weights:
%=========================================================================

%evaluating spectral degree of coherence, cross-spectral
%density and spectrum::
clear
clc
lambda=0.1;%0.3%10 %---Modal weight
zo=5;%3%0.1 %-- Spectral mode profile at the source
ww1=0; %--Dimensionless frequency variable
ww2=0;
zz1=0; %---Dimensionless space variable

 for z1=0:1:0;
      zz1=zz1+1;
      ww1=0;
     for w11=-15:0.5:15;
         ww1=ww1+1;
         ww2=0;
         for w21=-15:0.5:15;
             ww2=ww2+1;
             cross=0;
             for n=0:50;
                 pulse1=((zo/2)^n)*(1/((1+1i*w11)^(n+1)))*...
                 (exp(-0.5*(z1+zo)/(1+1i*w11))); %--spectral pulse ...
                    profile
```

```
                pulse2=((zo/2)^n)*(1/((1-1i*w21)^(n+1)))...
                *(exp(-0.5*(z1+zo)/(1-1i*w21)));

                cross= cross+((lambda^(2*n))*(pulse1)*(pulse2));...
                    %--evaluating cross-spectral density
            end
            spectrum1=(1/(1-(0.25*((lambda^2)*(zo^2)))+w11^2))*...
            (exp(-(z1+zo)/(1+(w11^2))));%--evaluating pulse spectrum

            spectrum2=(1/(1-(0.25*((lambda^2)*(zo^2)))+w21^2))*...
                (exp(-(z1+zo)/(1+(w21^2))));

            mu(ww1,ww2)=abs(cross/(((spectrum1)^0.5)*((spectrum2)^0.5)));...
                %--evaluating spectral degree of coherence
        end
    end
end

w11=-15:0.5:15;
w21=-15:0.5:15;

figure(1)
mesh(w11,w21,mu) % plot spectral degree of coherence
  title('(a)');
  xlabel('\Omega1');
  ylabel('\Omega2');
  zlabel('|\mu|');

%-------------------------------------------------------------------------
%Evaluating pulse spectrum over Z:
clear
clc
lambda=0.3;%0.1%10
zo=3;%5%0.1
zz1=0;
for z1=0:1:10;
    zz1=zz1+1;
    ww1=0;
    for w1=-15:0.001:15;
```

```
        ww1=ww1+1;
%         H1=lambda*zo/(sqrt(1+(w1^2)));
        spectrum(zz1,ww1)= (1/(1-(0.25*((lambda^2)*(zo^2)))+w1^2))...
            *(exp(-(z1+zo)/(1+(w1^2))));%--evaluating pulse spectrum

    end
end
w1=-15:0.001:15;
Z1=1:5;

figure(2), %plot the pulse spectrum
 mesh(Z1,w1,spectrum(1:5,:)',...
     'MeshStyle', 'col','EdgeColor', 'black');
 hidden off;
 grid off;
 hold on
 title('(a)');
 xlabel('Z');
 ylabel('\Omega');
 zlabel('Spectrum');

%=========================================================================
%Pulses with modal weight distributions decaying faster than power-law
%=========================================================================

%Evaluating spectral degree of coherence, spectrum and cross-spectral
%density::

clear
clc
lambda=0.9;%2
zo=15;%0.1
ww1=0;
ww2=0;
zz1=0;
 for z1=0:1:0;
      zz1=zz1+1;
      ww1=0;
     for w11=-15:0.5:15;
```

```
            ww1=ww1+1;
            ww2=0;
            for w21=-15:0.5:15;
                ww2=ww2+1;
                cross=0;
                for n=0:100;
                    pulse1=((zo/2)^n)*(1/((1+1i*w11)^(n+1)))*...
                        (exp(-0.5*(z1+zo)/(1+1i*w11)));

                    pulse2=((zo/2)^n)*(1/((1-1i*w21)^(n+1)))*...
                        (exp(-0.5*(z1+zo)/(1-1i*w21)));

                    cross= cross+((lambda^(2*n))*(1/((factorial(n))^2))*...
                        (pulse1)*(pulse2));
                end
                H11=lambda*zo/(sqrt(1+(w11^2)));
                spectrum1=(1/(1+(w11)^2))*(besseli(0,H11))*...
                    (exp(-(z1+zo)/(1+(w11^2))));

                H21=lambda*zo/(sqrt(1+(w21^2)));
                spectrum2=(1/(1+(w21)^2))*(besseli(0,H21))*...
                    (exp(-(z1+zo)/(1+(w21^2))));

                mu(ww1,ww2)=abs(cross/(((spectrum1)^0.5)*((spectrum2)^0.5)));
            end
        end
     end
w11=-15:0.5:15;
w21=-15:0.5:15;

figure(3)
mesh(w11,w21,mu) %--plot spectral degree of coherence
  title('(a)');
  xlabel('\Omega_1');
  ylabel('\Omega_2');
  zlabel('|\mu|');
```

```
%-------------------------------------------------------------------------
%Evaluating pulse spectrum over Z:
clear
clc
lambda=0.9;%2
zo=15;%0.1
zz1=0;
for z1=0:1:10;
    zz1=zz1+1;
    ww1=0;
    for w1=-15:0.001:15;
        ww1=ww1+1;
        H1=lambda*zo/(sqrt(1+(w1^2)));
        spectrum(zz1,ww1)=(1/(1+(w1^2)))*(besseli(0,H1))*...
            (exp(-(z1+zo)/(1+(w1^2))));
    end
end
w1=-15:0.001:15;
Z1=1:5;

figure(4), %plot the pulse spectrum
 mesh(Z1,w1,spectrum(1:5,:)',...
     'MeshStyle', 'col','EdgeColor', 'black');
 hidden off;
 grid off;
 hold on
 title('(a)');
 xlabel('Z');
 ylabel('\Omega');
 zlabel('Spectrum');
```

# Appendix B

## Numerical Codes for Simulating Propagation of Partially Coherent Pulses in Resonant Linear Absorbers and Amplifers

```
%=========================================================================
%partially coherent pulses propagating in linear absorbers and ...
   amplifiers
%=========================================================================
clear
tic
clc
Tp=0.5; %--pulse width
Teff=0.0995; %--effective pulse width (less coherent case)
%Teff=0.995; %--effective pulse width (more coherent case)
coeff=-1;   %--absorber coefficient
%coeff=+1;  %--amplifier coefficient

de=0.25; %--step size of the integral
s=47;
det=0.2; %--time step
tt1=-20; %--time margin
tt2=20;

zzz=5; %--space margin
nz=5;
nnz=1;
tcc=0;
kk=tt1:det:tt2; %--dimensionless time variable
k=length(kk);
coh=zeros(k,k);%--mutual coherence function
I=zeros(k,1);  %--pulse intensity
gamma=zeros(k,k); %--complex degree of coherence
```

```
z=0;

for zz=nnz:1:nz;
    z=z+1;
m1=0;
for t1=tt1:det:tt2;
    m1=m1+1;
    m2=0;
    for t2=tt1:det:tt2;
        m2=m2+1;
         d12=0;
         for i= -1*s:de:s-de;
            for j= -1*s:de:s-de;
              f1= i+0.5*de;
              f2= j+0.5*de;
              d12=d12+de^2*(exp(-0.5*(Tp^2)*((f1- ...
                  f2)^2)-0.125*(Teff^2)*((f1 + ...
                  f2)^2)))*(exp(coeff*0.5*zzz*((1/(1- 1i * ...
                  f2))+(1/(1+ 1i * f1)))))*(exp (1i*(f1*t1 - f2*t2)));
            end
         end
         coh(m1,m2,z)=d12; %--evaluating mutual coherence function
    end
end
end

m1=0;
z=0;
for zz=nnz:1:nz;
    z=z+1;
m1=0;
for t1=tt1:det:tt2;
    m1=m1+1;
 I(m1,1,z)=coh(m1,m1,z); %--evaluating pulse intensity
end
end

z=0;
for zz=nnz:1:nz;
```

```
    z=z+1;
m1=0;
m2=0;
for t1=tt1:det:tt2;
    m1=m1+1;
    m2=0;
    for t2=tt1:det:tt2;
        m2=m2+1;
        gamma(m1,m2,z)=(coh(m1,m2,z))/(I(m1,1,z)*I(m2,1,z))^0.5; ...
           %--evaluating complex degree of coherence
    end
end
end

t1=tt1:det:tt2;
t2=tt1:det:tt2;

figure(1) %--plot comlex degree of coherence
surf(t1,t2,gamma(:,:,1))
title('(a)');
 xlabel('T_2');
 ylabel('T_1');
 zlabel('|\gamma|');

figure(2) %--plot pulse intensity over Z
mesh(z,t1,I,...
     'MeshStyle', 'col','EdgeColor', 'black');
 hidden off;
 grid off;
 title('(a)');
 xlabel('Z');
 ylabel('T');
 zlabel('Pulse Intensity (a.u)');
```

# Appendix C

## Numerical Codes for Simulating Propagation of Fluctuating Pulses in Resonant Nonlinear Media

```
%=========================================================================
%partially coherent pulse propagation in resonant nonlinear medium
%=========================================================================
clear
clc
tic
%-----------------------
NN=0:40; %-- number of modes
tp=0.25; %-- pulse width
tc=1*tp; %-- coherence time (less coherent case)
%tc=10*tp; %-- coherence time (more coherent case)
%-----------------------
dt=0.025; %--time step
t=(-2:dt:25)'; %-- dimensionless time vector
nt=length(t);
%-----------------------
z=10;
nz=400;
dz=z/nz;   %--space step size
zz=0:dz:z; %-- dimensionless space vector
nplot=10;  %-- number of plots in Z
n1=round(nz/nplot);
%-------------------------------------------------------------------------
N=0:50;
H=hermit(t/(sqrt(2*d)),N);%--generating hermit function
%-------------------------------------------------------------------------
L=2000; %--number of random realizations
zv=(0:nplot)*(z/nplot);
```

```
%--initializing variables
Ut=zeros(length(t),length(zv));
Vt=zeros(length(t),length(zv));
Wt=zeros(length(t),length(zv));
Gt=zeros(length(t),length(t),length(zv));
omegan=zeros(length(t),length(NN));
%-------------------------------------------------------------------------

fp=sqrt((1/(tp^2))+ (2/(tc^2)));
fc=(tc*fp)/tp;
a=1/(2*fp^2); %--modal weight coefficients
b=1/(2*fc^2);
d=sqrt(a^2+2*a*b);
phi=((2*pi*rand(L,length(NN)))-pi); %-- random phase generation

for jn=1:length(NN)
    n=NN(jn);

lambda=sqrt(pi/(a+b+d))*((b/(a+b+d))^n ) ;%-- modal weight generation
a_big=0.75*10.0266; %-- initial pulse coefficient
teta= a_big*(inv(sqrt((2^n)*(factorial(n)))))* ((2*d/pi)^0.25 ...
   )*H(:,jn).*exp(- (t.^2)/(4*d));
omegan(:,jn)=sqrt(lambda)*teta;
end

%-- Monte Carlo method
parfor jL=1:L
jL
omega0=zeros(length(t),1);
omegan;
phi;
for jN=1:length(NN)%-- generating the source pulse
omega0=omega0+omegan(:,jN)*exp(1i*phi(jL,jN));
end
area_omega0=abs(sum(omega0)*dt)%-- pulse area at the source

omega=zeros(length(t),length(zv)); %-- random pulse
Gamma=zeros(length(t),length(t),length(zv)); %-- mutual coherence
```

```
sigma=zeros(length(t),length(zv)); %-- dipole moment variable
sigma1=zeros(length(t),length(zv));
w=zeros(length(t),length(zv)); %--inversion variable

%-- setting initial conditions
omega(:,1)=omega0;
Gamma(:,:,1)=omega0*(omega0');
sigma(1,:)=0;
w(1,:)=-1;

y1=bloch(omega(:,1),nt,dt);
sigma(:,1)=y1(:,1);
w(:,1)=y1(:,2);

%-- transmitting pulse realizations through resonant nonlinear media
for ii=1:nplot
    ii;
    y2=maxwell(omega(:,ii),sigma(:,ii),dt,dz,n1);
    omega(:,ii+1)=y2(:,1);
    sigma(:,ii+1)=y2(:,2);
    w(:,ii+1)=y2(:,3);
    sigma1(:,ii+1)=y2(:,4);
    Gamma(:,:,ii+1)=omega(:,ii+1)*(omega(:,ii+1)');
end

%-- generating an ensemble of realizations
Ut=Ut+real(sigma);
Vt=Vt+(-imag(sigma));
Wt=Wt+w;
Gt=Gt+Gamma;
%--------------------------------------------------------------------------
end
Gt;
%--performing ensemble averaging
G=(1/L)*Gt;
U=(1/L)*Ut;
V=(1/L)*Vt;
W=(1/L)*Wt;
%--------------------------------------------------------------------------
```

```
I=zeros(length(t),length(zv));%-- pulse intensity
MU=zeros(length(t),length(t),length(zv)); %-- degree of coherence
for rz=1:length(zv)

        I(:,rz)=diag(G(:,:,rz));
        MU(:,:,rz)=abs(G(:,:,rz)./sqrt(I(:,rz)*I(:,rz)'));
end
%-------------------------------------------------------------------------
area_I=zeros(1,length(zv));%--pulse area over Z

for rz=1:length(zv)
   area_I(rz)=sum(sqrt(I(:,rz))*dt);
end
%-------------------------------------------------------------------------

figure(1) %-- plot the pulse intensity over Z
mesh(zv,t,I, ...
     'MeshStyle', 'col', 'EdgeColor', 'black');
set(gca,'YDir','reverse');
hidden off;
title('(a)','fontsize',24)
xlabel ('Z','fontsize',20);
ylabel('T','fontsize',20)
zlabel ('I(Z,T)','fontsize',20)

figure(2) %-- plot the pulse area
plot(zv,area_I,'--k','linewidth',1.5)
xlabel('Z','fontsize',20)
ylabel('A(Z)','fontsize',20)
legend('t_c= t_p')
hold on
zzz=0:0.1:10;
ccc=2*pi*ones(1,length(zzz));
plot(zzz,ccc,'*r')

figure(3) %-- plot the complex degree of coherence
subplot(1,3,1),imagesc(t1,t1,MU(:,:,1))
title('(a)','fontsize',24)
```

```
xlabel('T_1','fontsize',20)
ylabel('T_2','fontsize',20)
subplot(1,3,2),imagesc(t1,t1,MU(:,:,5))
title('(b)','fontsize',24)
xlabel('T_1','fontsize',20)
ylabel('T_2','fontsize',20)
subplot(1,3,3),imagesc(t1,t1,MU(:,:,10))
title('(c)','fontsize',24)
xlabel('T_1','fontsize',20)
ylabel('T_2','fontsize',20)
disp(toc/60)


%=========================================================================
%evaluating the Hermit function for each mode
%=========================================================================

function HH=hermit(t,N)

HH = zeros ( length(t), length(N) );

  HH(:,1) = 1.0; %--for N=0
  HH(:,2) = 2.0 *t; %--for N=1

  for jh = 2 : (length(N)-1)
    HH(:,jh+1) = 2.0 *t.* HH(:,jh) - 2.0 * ( jh - 1 ) * HH(:,jh-1);
  end


%=========================================================================
% Solving Bloch equations, See Ref[86]
%=========================================================================

function y=bloch(omega,nt,dt)

dΔ=0.2;%-- step size of Delta
DELTA=-50:dΔ:50; %-- detuning variable
sigma=zeros(size(omega));
w=zeros(size(omega));
```

```
average1=zeros(size(omega));
y=zeros(length(sigma),3);
gΔ=zeros(length(DELTA),1); %-- inhomogenous broadening function
sigmaΔ=zeros(length(sigma),length(DELTA));
InhomLngth=15;
sigma(1)=0;
w(1)=-1;
y(1,1)=sigma(1);
y(1,2)=w(1);

for m=1:length(DELTA)
        gΔ(m)=exp(-((DELTA(m).^2)/(2*(InhomLngth^2))));

     for i=1:nt-1 %-- numerical Rung Kutta method
          k1=derivatives(omega(i),sigma(i),w(i),DELTA(m));
          sigma1=sigma(i)+dt*k1(1)/2;
          w1=w(i)+dt*k1(2)/2;
          k2=derivatives(omega(i),sigma1,w1,DELTA(m));
          sigma1=sigma(i)+dt*k2(1)/2;
          w1=w(i)+dt*k2(2)/2;
          k3=derivatives(omega(i),sigma1,w1,DELTA(m));
          sigma1=sigma(i)+dt*k3(1);
          w1=w(i)+dt*k3(2);
          k4=derivatives(omega(i),sigma1,w1,DELTA(m));
          nextstep=(dt*(k1+2*k2+2*k3+k4))/6;
          sigma(i+1)=sigma(i)+nextstep(1);
          w(i+1)=w(i)+nextstep(2);
     end

     sigmaΔ(:,m)=sigma;

     %--averageing dipole moment over a distribution of detunings(Δ)
     average1=average1+gΔ(m)*sigmaΔ(:,m)*dΔ;
end

y(:,1)=average1;
y(:,2)=w;
y(:,3)=sigma;
```

```
%=========================================================================
% Bloch differential equations: neglecting damping effects, See Ref[86]
%=========================================================================
function dy=derivatives(omega,sigma,w,DELTA)

dy(1)=-1i*DELTA*sigma-1i*omega*w;
dy(2)=real(omega)*imag(sigma)-imag(omega)*(real(sigma));



%=========================================================================
%Solving Maxwell equation, See Ref[86]
%=========================================================================

function y=maxwell(omega,sigma,dt,dz,n1)

nt=length(omega);
r1=dz/1;

for iz=1:n1
    y=omega+1i*(r1*sigma);
    omega=y;
    y1=bloch(omega,nt,dt);
    sigma=y1(:,1);
    w=y1(:,2);
    sigma1=y1(:,3);
end

y(:,1)=omega;
y(:,2)=sigma;
y(:,3)=w;
y(:,4)=sigma1;
```

# Appendix D

## Copyright Permissions

From: Laleh Mokhtarpour [laleh.mkht@dal.ca]
Sent: Wed 2015-11-11 5:26 PM
To: copyright@osa.org;
Subject: Copyright Permission

Dear Optical Society of America,
I am the first author of the following journals, while I was working toward my PhD degree. Now, I am preparing my PhD thesis for submission to the Faculty of Graduate Studies at Dalhousie University, Halifax, Nova Scotia, Canada. I am seeking your permission to include a manuscript version of the following paper(s) as a chapter in the thesis:

1. L. Mokhtarpour, G. H. Akter, and S. A. Ponomarenko, Partially coherent self-similar pulses in resonant linear absorbers, Opt. Express 20, 1781617822 (2012).

2. L. Mokhtarpour and S. A. Ponomarenko, Complex area correlation theorem for statistical pulses in coherent linear absorbers, Opt. Lett. 37, 34983500 (2012).

3. L. Mokhtarpour and S. A. Ponomarenko, Ultrashort pulse coherence properties in coherent linear amplifiers, J. Opt. Soc. Am. A , 30, 627630 (2013).

4. L. Mokhtarpour and S. A. Ponomarenko, Fluctuating pulse propagation in resonant nonlinear media: self-induced transparency random phase soliton formation, Opt. Express 23, 3027030282 (2015).

Full publication details and a copy of this permission letter will be included in the thesis.

Best Regards,
Laleh Mokhtarpour.

From: pubscopyright [copyright@osa.org]
Sent: Thu 2015-11-12 4:37 PM
To: Laleh Mokhtarpour;
Subject: RE: Copyright Permission

Dear Laleh Mokhtarpour,

Thank you for contacting The Optical Society.
Because you are the author of the source paper from which you wish to reproduce material, OSA considers your requested use of its copyrighted materials to be permissible within the author rights granted in the Copyright Transfer Agreement submitted by the requester on acceptance for publication of his/her manuscript. It is requested that a complete citation of the original material be included in any publication. This permission assumes that the material was not reproduced from another source when published in the original publication.
Please let me know if you have any questions.

Kind Regards,
Susannah Lehman

Susannah Lehman
November 12, 2015
Authorized Agent, The Optical Society

## Bibliography


[1] M. Born and E. Wolf, *Principles of Optics*, 7th ed. (Cambridge University Press, 1999).

[2] M. E. Fermann, A. Galvanauskas, and G. Sucha, *Ultrafast Lasers, Technology and Applications*, (Marcel Dekker, New York, 2003).

[3] H. G. Weber and M. Nakazawa, *Ultra High Speed Optical Transmission Technology*, (Springer Verlag, New York, 2007).

[4] L. Allen and J. H. Eberly, *Optical Resonance and Two-level Atoms,* (Dover Publications Inc., New York, 1975).

[5] J. C. Diels and W. Rudolph, *Ultrashort Laser Pulse Phenomena*, 2nd ed. (Academic Press, 2006).

[6] P. W. Milonni and J. H. Eberly, *Lasers*, (Wiley, New York, 1985).

[7] L. Mandel and E. Wolf, *Optical Coherence and Quantum Optics*, (Cambridge University Press, 1995).

[8] J. W. Goodman , *Statistical Optics*, (John Willy and Sons INC, 2000).

[9] G. P. Agrawal, *Fiber-Optic Communication Systems,* 3rd., (Wiley, New York, NY 2002).

[10] V. V. Tuchin, *Handbook of Coherent Domain Optical methods: Biomedical Diagnostics, Environmental and Material Science* V2, Kluver Academic Publishers (2004).

[11] J. W. Goodman, *Speckle Phenomena in Optics: Theory and Applications*, Roberts and Company, (2006).

[12] J. C. Dainty, *Laser speckle and Related Phenomena*, Springer-Verlag, (1975).

[13] G. P. Agrawal, *Nonlinear fiber optics,* (Academic Press, 2007).

[14] P. P. Banerjee, *Nonlinear optics: Theory, Numerical Modeling and Applications* (Marcel Decker, 2004).

[15] R. W. Boyd, *Nonlinear Optics*, (Academic Press, 2008).

[16] R. Loudon, *The Quantum Theory of Light*, (Oxford University Press, Oxford, 1983).

[17] F. Riesz and B. Sz.-Nagy, *Functional Analysis* (Ungar, New York, 1978).

[18] E. Wolf, *Introduction to the Theory of Coherence and Polarization,* (Cambridge University Press, 2007).

[19] L. Banyai and S. W. Koch, *Semiconductor Quantum Dots* (World Scientific, 1993).

[20] A. S. Monin and A. M. Yaglom, *Statistical Fluid Mechanics: Mechanics of Turbulence*, Vols. 1& 2, (Dover, 2007).

[21] T. Brabec and F. Krausz, "Intense few-cycle laser fields: Frontiers of nonlinear optics," Rev. Mod. Phys. **72**, 545–591 (2000).

[22] T. H. Maimann, "Stimulated optical radiation in ruby," Nature **187**, 493–494 (1960).

[23] F. P. Schfer, F. P. W. Schmidt, and J. Volze, "Organic dye solution laser", Appl. Phys. Lett. **9**, 306–309 (1966).

[24] R. Ell, U. Morgner, F. X. Kartner, J. G. Fujimoto, E. P. Ippen, V. Scheuer, G. Angelow, and T. Tschudi, "Generation of 5-fs pulses and octave-spanning spectra directly from a Ti:sapphire laser", Opt. Lett. **26**, 373–375 (2001).

[25] G. Steinmeyer, D. H. Sutter, L. Gallmann, N. Matuschek, and U. Keller, "Frontiers in ultrashort pulse generation: pushing the limits in linear and nonlinear optics," Science **286**, 1507–1512 (1999).

[26] H. Hentschel, R. Kienberger, Ch. Spielmann, G. A. Reider, N. Milosevic, T. Brabec, P. Corkum, U. Heinzmann, M. Drescher, and F. Krausz, "Attosecond metrology," Nature **414**, 509–513 (2001).

[27] P. H. Bucksbaum, "The future of attosecond spectroscopy," Science **317**, 766–769 (2007).

[28] W. H. Carter and B. E. A. Saleh, "Applications of coherence and statistical optics, J.Opt.Soc.Am.A 7, 934–1012 (1984).

[29] A. F. Fercher, W. Drexler, C. K. Hitzenberger, and T. Lasser, "Optical coherence tomography - principles and applications," Rep. Prog. Phys. 66, 239303 (2003).

[30] V. Torres Company, "Coherence in ultrashort pulses and applications in temporal optics", Universitat de Valncia, Department d'ptica (2009).

[31] J. Tervo, T. Setala and A. T. Friberg, "Theory of partially coherent electromagnetic fields in the space-frequency domain," J. Opt. Soc. Am. A **21**, 1084–7529 (2004).

[32] J. Tervo, T. Setala and A. T. Friberg, "Degree of coherence for electromagnetic fields," Opt. Express **11**, 1137–1143 (2003).

[33] C. Rydberg, "Statistical optics and optical elements for micro-technologies: partial coherence, lithography and micro-lenses", Chalmers University of Technology Department of Micro-technology and Nanoscience,(2007).

[34] J. H. Bruning, "Optical lithography, 40 years and holding", Proc. of SPIE, 6520-652004, (2007).

[35] M. Bertolotti, L. Sereda, and A. Ferrari, "Application of the spectral representation of stochastic processes to the study of nonstationary light radiation: a tutorial," J. Eur. Opt. Soc. A **6**, 153–171 (1997).

[36] M. Bertolotti, A. Ferrari, and L. Sereda, "Coherence properties of nonstationary polychromatic light sources," J. Opt. Soc. Am. B **12**, 341–347 (1995).

[37] L. Sereda, M. Bertolotti, and A. Ferrari, "Coherence properties of nonstationary light wave fields," J. Opt. Soc. Am. B **15**, 695–705 (1998).

[38] H. Lajunen, J. Tervo, and P. Vahimaa, "Overall coherence and coherent-mode expansion of spectrally partially coherent plane-wave pulses," J. Opt. Soc. Am. A **21**, 21172123 (2004).

[39] G. Genty, M. Surakka, J. Turunen, and Ari. T. Friberg, "Second-order coherence of supercontinuum light," Opt. Lett. **35** 3057-3059 (2010).

[40] T. Shirai, T. Setl, and A. T. Friberg, "Temporal ghost imaging with classical non-stationary pulsed light," J. Opt. Soc. Am. B **27**, 2549–2555 (2010).

[41] E. Wolf, "New spectral representation of random sources and of the partially coherent fields that they generate," Opt. Commun. **38**, 3–6 (1981).

[42] A. Starikov, "Effective number of degree of freedom of partially coherent sources," J. Opt. Soc. Am. A **72**, 1538–1544 (1982).

[43] S. A. Ponomarenko and E. Wolf, "Universal structure of field correlations within a fluctuating medium", Phys. Rev. E **65**, 016602–6 (2001).

[44] H. Lajunen, J. Tervo, J. Turunen, P. Vahimaa, and F. Wyrowski, "Spectral coherence properties of temporarily modulated stationary light sources," Opt. Express **11**, 1894–1899 (2003).

[45] F. Gori, M. Santarsiero, R. Simon, G. Piquero, R. Borghi, and G. Guattari, "Coherent-mode decomposition of partially polarized, partially coherent sources," J. Opt. Soc. Am. A **20**, 7884 (2003).

[46] F. Goria, M. Santarsieroa, R. Borghia, and S. Vicalvib, "Partially coherent sources with helicoidal modes," Journal of Modern Optics **45**, 539–554 (1998).

[47] Y. Baykal, "Average transmittance in turbulence for partially coherent sources," Opt. Commun. **231** 129–136 (2004).

[48] F. Gori, "Far-zone approximation for partially coherent sources," Opt. Lett. **30**, 2840–2842 (2005).

[49] Z. Mei and O. Korotkova, "Cosine-Gaussian Schell-model sources," Opt. Lett. **38** 2578–2580 (2013).

[50] M. Yao, O. Korotkova, C. Ding, L. Pan, "Position modulation with random pulses," Opt. Express **22**, 16197–206 (2014).

[51] S. Yang, S. A. Ponomarenko, and Z. D. Chen, "Coherent pseudo-mode decomposition of a new partially coherent source class," Opt. Lett. **40**, 3081–3084 (2015) .

[52] P. Paakkonen, J. Turunen, P. Vahimaa, A. T. Friberg, and F. Wyrowski, "Partially coherent Gaussian pulses," Opt. Commun., **204**, 53–58 (2002).

[53] S. A. Ponomarenko, G. P. Agrawal, and E. Wolf, "Energy spectrum of a nonstationary ensemble of pulses," Opt. Lett. **29**, 394–396 (2004).

[54] H. Lajunen, A. T. Friberg, and P. Ostlund, "Quasi-stationary plane-wave optical pulses and the van CittertZernike theorem in time," J. Opt. Soc. Am. A **23**, 2530–2537 (2006).

[55] H. Lajunen, P. Vahimaa, and J. Tervo, "Theory of spatially and spectrally partially coherent pulses," J. Opt. Soc. Am. A **22**, 1536–1545 (2005).

[56] J. Lancis, V. Torres-Company, E. Silvestre, and P. Andrs, "Spacetime analogy for partially coherent plane-wave-type pulses," Opt. Express **30**, 2973–2975 (2005).

[57] H. Lajunen, and T. Saastamoinen, "Non-uniformly correlated partially coherent pulses," Opt. Express **21**, 190–195 (2013).

[58] A. Starikov and E. Wolf, "Coherent-mode representation of Gaussian Schell-model sources and of their radiation fields," J. Opt. Soc. Am. A **72**, 9233–928 (1982).

[59] P. Vahimaa and J. Turunen, "Independent-elementary-pulse representation for non-stationary fields," Opt. Express **14**, 5007–5012 (2006).

[60] K. Saastamoinen, J. Turunen, P. Vahimaa, and A. T. Friberg, "Spectrally partially coherent propagation-invariant fields," Phys. Rev. A. **80**, 053804–11 (2009).

[61] J. Turunen, "Elementary-field representations in partially coherent optics," J. Modern Optics **58** 509-527 (2011).

[62] S. A. Ponomarenko, "Complex Gaussian representation of statistical pulses," Opt. Express **19**, 17086–17091 (2011).

[63] C. Ding, O. Korotkova, L. Pan, "The control of pulse profiles with tunable temporal coherence," Physics Letters A **378**, 1687–1690 (2014).

[64] C. Ding, O. Korotkova, Y. Zhanga, L. Pana, "Sinc Schell-model pulses," Opt. Commun. **339**, 115–122 (2015).

[65] G. Gbur, "Simulating fields of arbitrary spatial and temporal coherence," Opt. Express **14**, 7567–7577 (2006).

[66] B. Davis, "Measurable Coherence Theory for Statistically Periodic Fields," Phys. Rev. A. **76**, 38–43 (2007).

[67] V. Torres-Company, H. Lajunen, and A. T. Friberg, "Coherence theory of noise in ultrashort pulse trains", J. Opt. Soc. Am. B **24**, 1441–1450 (2007).

[68] A. T. Friberg, H. Lahunen, and V. Torres-Company, "Spectral elementary-coherence-function representation for partially coherent light pulses," Opt. Express **15**, 5160–5165 (2007).

[69] P. Vahimaa, and J. Tervo, "Unified measures for optical fields: degree of polarization and effective degree of coherence," J. Opt. A: Pure Appl. Opt. **6** 41–44 (2004).

[70] C. Ding, Y. Cai, O. Korotkova, Y. Zhang, and L. Pan, "Scattering-induced changes in the temporal coherence length and the pulse duration of a partially coherent plane-wave pulse," Opt. Lett. **36** 517–519 (2011).

[71] Z. Mei, O. Korotkova, and Y. Mao, "Products of Schell-model cross-spectral densities," Opt. Lett. **39**, 6879–6882 (2014).

[72] D. Marcuse, "Propagation of pulse fluctuations in single-mode fibers," Applied Optics **19**, 1856-1861 (1980).

[73] J. Capmany, D. Pastor, S. Sales, and M. Muriel, "Pulse distortion in optical fibers and waveguides with arbitrary chromatic dispersion," J. Opt. Soc. Am. B **20** 523–2533 (2003).

[74] W. Huang, S. A. Ponomarenko, M. Cada, and G. P. Agrawal, "Polarization changes of partially coherent pulses propagating in optical fibers," J. Opt. Soc. Am. A **24**, 3063–3068 (2007).

[75] C. L. Ding, L. Z. Pan, and B. D. Lu, "Changes in the spectral degree of polarization of stochastic spatially and spectrally partially coherent electromagnetic pulses in dispersive media," J. Opt. Soc. Am. B **26**, 1728–1735 (2009).

[76] P. Suret, A. Picozzi, and S. Randoux, "Wave turbulence in integrable systems: nonlinear propagation of incoherent optical waves in single-mode fibers," Opt. Express **19**, 17852–17863 (2011).

[77] Q. Lin, L. Wang, and S. Zhu, "Partially coherent light pulse and its propagation," Opt. Commun., **219**, 65–70 (2003).

[78] M. Brunel and S. Coëtlemec, "Fractional-order Fourier formulation of the propagation of partially coherent light pulses," Opt. Commun. **230**, 1–5 (2004).

[79] L. G. Wang, N. H. Liu, Q. Lin, and S. Y. Zhu, "Superluminal propagation of light pulses: A result of interference," Phys. Rev. E. **68**, 066606–10 (2003).

[80] R. W. Schoonover, B. J. Davis, R. A. Bartels, and P. S. Carney, "Propagation of spatial coherence in fast pulses," J. Opt. Soc. Am. A **26**, 1945–1953 (2009).

[81] S. A. Ponomarenko, "Degree of phase-space separability of statistical pulses," Opt. Express **20**, 2548–2555 (2012).

[82] B. Gross and J. T. Manassah, "Compression of the coherence time of incoherent signals to a few femto seconds," Opt. Lett. **16**, 1835–1837 (1991).

[83] V P. Nayyar, "Propagation of partially coherent Gaussian Schell-model sources in nonlinear media," J. Opt. Soc. Am. A **14**, 2248–2253 (1997).

[84] V. A. Aleshkevich, V. A. Vysloukh, G. D. Kozhoridze,A. N. Matveev and S. I. Terzieva, "Nonlinear propagation of partially coherent pulse in fiber waveguide and the role of higher order dispersion," Sov. J. Quantum Electron. **18**, 207–211 (1988).

[85] B. Hall, M. Lisak, D. Anderson, R. Fedele, and V. E. Semenov, "Statistical theory for incoherent light propagation in nonlinear media," Phys. Rev. E. **65**, 56602–56604 (2002).

[86] S. H. Poorvali, "Exploring soliton and similariton formation in resonant optical media", Dalhousie University, Electrical and Computer Engineering Department, (2012).

[87] H. Lajunen, V. Torres-Company, J. Lancis, E. Silvestre, and P. Andr'es, "Pulse-by-pulse method to characterize partially coherent pulse propagation in instantaneous nonlinear media," Opt. Express **18**, 14979–14991 (2011).

[88] S. B. Cavalcanti, G. P. Agrawal and M. Yu, "Noise amplification in dispersive nonlinear media," Phys. Rev. A. , **51**, 4086–4092.

[89] V. P. Kandidov, "Monte Carlo method in nonlinear statistical optics", Sov. Phys.Usp. **39**, 1243–1272 (1996).

[90] S. A. Akhmanov, A. S. Chirkin, "Statistical phenomena in nonlinear optics," Radiophysics and Quantum Electronics **13**, 619–648 (1970).

[91] C. Rydberg, "Statistical optics and optical elements for micro-technologies: partial coherence, lithography and micro-lenses," Chalmers University of Technology, Department of Micro-technology and Nanoscience.

[92] C. Pask, and A. Stacey, "Optical coherence and Wolfs theory for electromagnetic waves," J. Opt. Soc. Am. A **5**, 1688–1693 (1988).

[93] F. Gori, Collett-Wolf sources and multi-mode lasers, Opt. Commun. **34**, 301–305 (1980).

[94] R. Gase, "The multi-mode laser-radiation as a Gaussian-Schell model beam," Journal of Modern Optics **38**, 1107–1115 (1991).

[95] F. Gori," Mode propagation of the field generated by Collett-Wolf Schell-model sources," Opt. Commun. **46**, 149–154 (1983).

[96] A. Gamliel, "Mode analysis of spectral changes in light-propagation from sources of any state of coherence," J. Opt. Soc. Am. A **7**, 1591–1597 (1990).

[97] S. Haghgoo and S. A. Ponomarenko, "Self-similar pulses in coherent linear amplifiers," Opt. Express **19**, 9750–9758 (2011).

[98] S. Haghgoo and S. A. Ponomarenko, "Shape-invariant pulses in resonant linear absorbers," Opt. Lett. **37**, 1328–1330 (2012).

[99] M. D. Crisp, "Propagation of Small-Area Pulses of Coherent Light through a Resonant Medium," Phys. Rev. A. **6**, 1604–1611 (1972).

[100] C. R. Fernandez-Pousa, "Intensity spectra after first-order dispersion of composite models of scalar, cyclostationary light," J. Opt. Soc. Am. A **26** 993–1007 (2009).

[101] R. W. Schoonover, B. J. Davis, and P. S. Carney, "The generalized Wolf shift for cyclostationary fields," Opt. Express , **17**, 4705–4711 (2009).

[102] R. W. Schoonover, R. Lavarello, M. L. Oezle, and P. S. Carney, "Observation of generalized Wolf shifts in short pulse spectroscopy," Applied Physics Letters, **98**, 251107–25110 (2011).

[103] G. L. Lamb, Jr., "Analytical descriptions of ultrashort optical pulse propagation in resonant medium," Rev. Mod. Phys., **43**, 99–124 (1971).

[104] S. A. Ponomarenko and G. P. Agrawal, "Linear optical bullets," Opt. Commun. **261**, 1–4 (2006).

[105] L. Ma and S. A. Ponomarenko, "Optical coherence gratings and lattices," Opt. Lett. **39**, 6656 (2014).

[106] S. A. Ponomarenko, "Self-imaging of partially coherent light in graded-index media," Opt. Lett. **40**, 566 (2015).

[107] Y. Wu and L. Deng, "Ultraslow bright and dark optical solitons in a cold three-state system," Opt. Lett. **29**, 2064–2066 (2004).

[108] C. Hang and G. Huang, "Giant Kerr nonlinearity and weak-light superluminal optical solitons in a four-state atomic system with gain doublet," Opt. Express **18**, 2952-2966 (2010).

[109] W-X. Yang, Ai-Xi Chen, L-G. Si, K. Jiang, X. Yang, and R-K. Lee, "Three coupled ultraslow solitons in a five-level tripod system," Phys. Rev. A. **81** 023814 (2010).

[110] S. A. Ponomarenko and E. Wolf, "Coherence properties of light in Young's interference pattern formed with partially coherent light,"Opt. Commun. **170**, 1–8 (1999).

[111] S. A. Ponomarenko, H. Roychoudhury, and E. Wolf, "Physical significance of complete spatial coherence of optical fields," Phys. Lett. A, **345**, 10–12 (2005).

[112] S. A. Ponomarenko and E. Wolf, "The spectral degree of coherence of fully spatially coherent electromagnetic beams," Opt. Commun. **227**, 73–74 (2003).

[113] G. A. Pasmanik, "Self-interaction of incoherent light beams," Sov. Phys. JETP, **39**, 234–238 (1974).

[114] M. Mitchell, M. Segev, T. H. Coskun, and D. N. Christodoulides, "Theory of Self-Trapped Spatially Incoherent Light Beams," Phys. Rev. Lett. **79**, 4990–4993 (1997).

[115] D. N. Christodoulides, E. D. Eugenieva, T. H. Coskun, M. Segev, and M. Mitchell, "Equivalence of three approaches describing partially incoherent wave propagation in inertial nonlinear media," Phys. Rev. E. **63**, 035601(R) (2001).

[116] S. A. Ponomarenko, N. M. Litchinitser, and G. P. Agrawal, "Theory of incoherent solitons: Beyond the mean-field approximation," Phys. Rev. E. **70**, 015603(R) (2004).

[117] X. Xiao and D. Voelz, "Wave optics simulation approach for partial spatially coherent beams," Opt. Express **16**, 6986–6992 (2006).

[118] S. A. Parhl, D. G. Fischer and D. D. Duncan, "Monte Carlo Green's function for the propagation of partially coherent light," J. Opt. Soc. Am. A **260**, 1533–1543 (2009).

[119] L. Mokhtarpour, G. H. Akter, and S. A. Ponomarenko, "Partially coherent self-similar pulses in resonant linear absorbers," Opt. Express **20**, 17816–17822 (2012).

[120] L. Mokhtarpour and S. A. Ponomarenko, "Complex area correlation theorem for statistical pulses in coherent linear absorbers," Opt. Lett. **37**, 3498–3500 (2012).

[121] L. Mokhtarpour and S. A. Ponomarenko, "Ultrashort pulse coherence properties in coherent linear amplifiers," J. Opt. Soc. Am. A , **30**, 627–630 (2013).

[122] L. Mokhtarpour and S. A. Ponomarenko, "Fluctuating pulse propagation in resonant nonlinear media: self-induced transparency random phase soliton formation," Opt. Express **23**, 30270–30282 (2015).